

Tainá Medeiros Suizu

Morfodinâmica e hidro-geomorfologia do médio Rio Araguaia: investigação dos padrões
e dos controles físicos e sua relevância para a análise ambiental

Goiânia
2023



UNIVERSIDADE FEDERAL DE GOIÁS
GERÊNCIA DE CURSOS E PROGRAMAS INTERDISCIPLINARES

TERMO DE CIÊNCIA E DE AUTORIZAÇÃO (TECA) PARA DISPONIBILIZAR VERSÕES ELETRÔNICAS DE TESES

E DISSERTAÇÕES NA BIBLIOTECA DIGITAL DA UFG

Na qualidade de titular dos direitos de autor, autorizo a Universidade Federal de Goiás (UFG) a disponibilizar, gratuitamente, por meio da Biblioteca Digital de Teses e Dissertações (BDTD/UFG), regulamentada pela Resolução CEPEC nº 832/2007, sem resarcimento dos direitos autorais, de acordo com a [Lei 9.610/98](#), o documento conforme permissões assinaladas abaixo, para fins de leitura, impressão e/ou download, a título de divulgação da produção científica brasileira, a partir desta data.

O conteúdo das Teses e Dissertações disponibilizado na BDTD/UFG é de responsabilidade exclusiva do autor. Ao encaminhar o produto final, o autor(a) e o(a) orientador(a) firmam o compromisso de que o trabalho não contém nenhuma violação de quaisquer direitos autorais ou outro direito de terceiros.

1. Identificação do material bibliográfico

[] Dissertação [X] Tese

2. Nome completo do autor

Taina Medeiros Suizu

3. Título do trabalho

Morfodinâmica e hidro-geomorfologia do médio Rio Araguaia: investigação dos padrões e dos controles físicos e sua relevância para a análise ambiental

4. Informações de acesso ao documento (este campo deve ser preenchido pelo orientador)

Concorda com a liberação total do documento [] SIM [X] NÃO¹

[1] Neste caso o documento será embargado por até um ano a partir da data de defesa. Após esse período, a possível disponibilização ocorrerá apenas mediante:

- a) consulta ao(a) autor(a) e ao(a) orientador(a);
 - b) novo Termo de Ciência e de Autorização (TECA) assinado e inserido no arquivo da tese ou dissertação.
- O documento não será disponibilizado durante o período de embargo.
- Casos de embargo:
- Solicitação de registro de patente;
 - Submissão de artigo em revista científica;
 - Publicação como capítulo de livro;
 - Publicação da dissertação/tese em livro.

Obs. Este termo deverá ser assinado no SEI pelo orientador e pelo autor.



Documento assinado eletronicamente por **Taina Medeiros Suizu, Discente**, em 18/09/2023, às 09:34, conforme horário oficial de Brasília, com fundamento no § 3º do art. 4º do [Decreto nº 10.543, de 13 de novembro de 2020](#).



Documento assinado eletronicamente por **Edgardo Manuel Latrubesse, Professor do Magistério Superior-Visitante**, em 19/09/2023, às 19:12, conforme horário oficial de Brasília, com fundamento no § 3º do art. 4º do [Decreto nº 10.543, de 13 de novembro de 2020](#).



A autenticidade deste documento pode ser conferida no site https://sei.ufg.br/sei/controlador_externo.php?acao=documento_conferir&id_orgao_acesso_externo=0, informando o código verificador **3922089** e o código CRC **2F99F4DD**.

Tainá Medeiros Suizu

Morfodinâmica e hidro-geomorfologia do médio Rio Araguaia: investigação dos padrões e dos controles físicos e sua relevância para a análise ambiental

Tese de Doutorado apresentada ao Programa de Pós-Graduação em Ciências Ambientais (CIAMB) da Universidade Federal de Goiás, como requisito para obtenção do título de Doutora em Ciências Ambientais.

Área de concentração: Estrutura e Dinâmica Ambiental

Orientador: Prof. Dr. Edgardo Manuel Latrubesse

Coorientador: Prof. Dr. Maximiliano Bayer

Goiânia

2023

Ficha de identificação da obra elaborada pelo autor, através do
Programa de Geração Automática do Sistema de Bibliotecas da UFG.

Suizu, Tainá Medeiros
Morfodinâmica e hidro-geomorfologia do médio Rio Araguaia
[manuscrito] : investigação dos padrões e dos controles físicos e sua
relevância para a análise ambiental / Tainá Medeiros Suizu. - 2023.
109 f.: il.

Orientador: Prof. Dr. Edgardo Manuel Latrubesse; co-orientador
Dr. Maximiliano Bayer.

Tese (Doutorado) - Universidade Federal de Goiás, Pró-reitoria de
Pós-graduação (PRPG), Programa de Pós-Graduação em Ciências
Ambientais, Goiânia, 2023.

Bibliografia.

Inclui mapas, gráfico, tabelas.

1. Rio Araguaia. 2. Bioma Cerrado. 3. Resposta geomórfica. 4.
Segmentação fluvial. 5. Abordagem hidrogeomórfica. I. Latrubesse,
Edgardo Manuel, orient. II. Título.



UNIVERSIDADE FEDERAL DE GOIÁS

GERÊNCIA DE CURSOS E PROGRAMAS INTERDISCIPLINARES

ATA DE DEFESA DE TESE

Ata Nº 019/2023 da sessão de Defesa de Tese de **Taina Medeiros Suizu**, que confere o título de **Doutora em Ciências Ambientais**, na área de concentração em **Estrutura e Dinâmica Ambiental**.

Aos vinte e cinco dias do mês de agosto do ano de 2023, a partir das 09horas, na plataforma Google Meet: <https://meet.google.com/jed-dnva-juc>, cuja participação ocorreu através de videoconferência, realizou-se a sessão pública de Defesa de Tese intitulada "**Morfodinâmica e hidrogeomorfologia do médio Rio Araguaia: investigação dos padrões e dos controles físicos e sua relevância para a análise ambiental**". Os trabalhos foram instalados pelo Orientador, Professor Doutor **Edgardo Manuel Latrubesse (PRPG/UFG)** com a participação dos demais membros da Banca Examinadora: Professor Doutor **Márcio Henrique de Campos Zancopé (IESA/UFG)**, membro titular externo; Professor Doutor **Naziano Pantoja Filizola Junior (UFAM)**, membro titular externo; Professora Doutora **Karla Maria Silva de Faria (IESA/UFG)**, membro titular interno; Professor Doutor **Manuel Eduardo Ferreira (IESA/UFG)**, membro titular interno. Durante a arguição os membros da banca **não sugeriram** alteração do título do trabalho. A Banca Examinadora reuniu-se em sessão secreta a fim de concluir o julgamento da Tese tendo sido a candidata **aprovada** pelos seus membros. Proclamados os resultados pelo Professor Doutor **Edgardo Manuel Latrubesse**, Presidente da Banca Examinadora, foram encerrados os trabalhos e, para constar, lavrou-se a presente ata que é assinada pelos Membros da Banca Examinadora, aos **vinte e cinco dias do mês de agosto do ano de 2023**.



Documento assinado eletronicamente por **Edgardo Manuel Latrubesse, Professor do Magistério Superior-Visitante**, em 25/08/2023, às 12:15, conforme horário oficial de Brasília, com fundamento no § 3º do art. 4º do [Decreto nº 10.543, de 13 de novembro de 2020](#).



Documento assinado eletronicamente por **Karla Maria Silva De Faria, Professora do Magistério Superior**, em 25/08/2023, às 12:27, conforme horário oficial de Brasília, com fundamento no § 3º do art. 4º do [Decreto nº 10.543, de 13 de novembro de 2020](#).



Documento assinado eletronicamente por **Márcio Henrique De Campos Zancopé, Professor do Magistério Superior**, em 28/08/2023, às 11:20, conforme horário oficial de Brasília, com fundamento no § 3º do art. 4º do [Decreto nº 10.543, de 13 de novembro de 2020](#).



Documento assinado eletronicamente por **Taina Medeiros Suizu, Discente**, em 14/09/2023, às 13:50, conforme horário oficial de Brasília, com fundamento no § 3º do art. 4º do [Decreto nº 10.543, de 13 de novembro de 2020](#).



Documento assinado eletronicamente por **Manuel Eduardo Ferreira, Professor do Magistério Superior**, em 14/09/2023, às 16:30, conforme horário oficial de Brasília, com fundamento no § 3º do art. 4º do [Decreto nº 10.543, de 13 de novembro de 2020](#).



Documento assinado eletronicamente por **NAZIANO PANTOJA FILIZOLA JÚNIOR, Usuário Externo**, em 19/09/2023, às 13:23, conforme horário oficial de Brasília, com fundamento no § 3º do art. 4º do [Decreto nº 10.543, de 13 de novembro de 2020](#).



A autenticidade deste documento pode ser conferida no site https://sei.ufg.br/sei/controlador_externo.php?acao=documento_conferir&id_orgao_acesso_externo=0, informando o código verificador **3922075** e o código CRC **F5E653D7**.

Aos meus familiares, exemplos de resiliência e perseverança.

Em especial, aos meus pais, Nelson e Suely, em reconhecimento à batalha incansável de vocês para que eu chegassem até aqui.

O amor incondicional e os seus valores de humildade e respeito são as raízes que sustentam a busca pelos meus sonhos.

AGRADECIMENTOS

A Deus, por estar sempre ao meu lado, guiando os meus passos ao longo da jornada.

Ao meu querido irmão Danilo, “o amigo: um ser que a vida não explica [...] e o espelho da minha alma multiplica” – Vinícius de Moraes.

Ao meu marido Leandro, minha metade, pelo seu contínuo apoio e encorajamento. O seu amor é uma força estabilizadora em minha vida.

Ao Prof. Edgardo Latrubesse, pela sua generosidade em compartilhar o seu conhecimento. Me sinto afortunada por ter um orientador tão comprometido com o meu crescimento profissional e minha pesquisa. Com sorte, deixo a UFG tendo absorvido uma pequena fração de toda a sua vasta experiência na Geomorfologia.

Ao Prof. Maximiliano Bayer, por contribuir na minha formação com os seus ensinamentos durante os trabalhos de campo.

Ao Prof. Gerald Nanson, por ter me incentivado na realização do doutorado. Um pesquisador exímio com um coração altruísta, que transforma vidas por simplesmente acreditar no ser humano.

Aos professores Dr. Manuel Eduardo Ferreira, Dra. Karla Maria Silva de Faria, Dr. Márcio Henrique de Campos Zancopé e Dr. Naziano Pantoja Filizola Junior pelas valiosas discussões e contribuições a esta pesquisa na ocasião da defesa.

Aos colegas do CIAMB, em especial à turma 2019/01, pelo suporte recíproco e companheirismo.

À Coordenação de Aperfeiçoamento de Pessoal de Nível Superior – Brasil (CAPES) - Código de Financiamento 001 e ao Conselho Nacional de Desenvolvimento Científico e Tecnológico (CNPq) - processo 422559/2021-0, pelo apoio financeiro concedido para o desenvolvimento desta pesquisa.

RESUMO

O Rio Araguaia representa o último e mais importante rio de fluxo livre localizado no ecótono Cerrado-Amazônia. A crescente influência humana sobre esse sistema fluvial constitui uma ameaça iminente aos valiosos serviços ecossistêmicos por ele fornecidos. Assim, torna-se imprescindível a produção do conhecimento sobre a estrutura física e a função desse rio, que é base para a ocorrência de porção significativa da biodiversidade do bioma. A presente tese contribui para os campos da Geomorfologia e Hidrologia de grandes rios tropicais, trazendo novas descobertas que enriquecem o corpo de pesquisa existente sobre o sistema Araguaia. No primeiro artigo, realizamos uma avaliação das mudanças na morfologia bidimensional do médio-curso superior entre 2001 e 2018, ampliando a série temporal dos dados sobre a evolução das macroformas para um período de 53 anos. Verificamos que a atual fase de transição do rio, marcada pela contração da zona ativa do canal e pela perda parcial das características de entrelaçamento, devido ao aumento da representatividade das ilhas, provavelmente está relacionada às mudanças no regime hidrossedimentar ocorridas nas últimas duas décadas. Com base em um conjunto de variáveis geomorfológicas do canal e da planície de inundação, no segundo artigo foi desenvolvida uma metodologia para subdividir o médio Araguaia em 19 trechos distintos (R1-R19), os quais foram estatisticamente agrupados em cinco grandes segmentos fluviais (SI-SV). Constatou-se que as mudanças no gradiente do vale exercem uma influência significativa na morfologia de SI, SIII e SIV, enquanto a entrada de afluentes importantes e a natureza do vale constituem os principais fatores de controle do estilo fluvial em SII e SV, respectivamente. Essa caracterização planialtimétrica em larga escala do médio curso do rio complementa estudos geomorfológicos anteriores, fornecendo *insights* sobre a diversidade morfológica e a sensibilidade de cada segmento às mudanças ambientais. No terceiro artigo, apresentamos uma nova abordagem para as classificações existentes na literatura dos eventos de inundação no médio Araguaia. As inundações de pequena escala (tipos B e D2) demonstram padrões de atenuação distintos associados à ocorrência de anos mais secos (D2). A atenuação das inundações de escala intermediária (Tipos C e D1) e grande escala (tipo A) é influenciada pela magnitude das vazões máximas na estação fluviométrica a montante, sem significância estatística para a influência dos afluentes nas mudanças do pico. As propriedades do hidrograma de inundação mostraram responder à organização geomorfológica regional do sistema. Ao considerar os segmentos propostos no segundo artigo, observamos que a natureza do vale desempenha um papel central na transmissão eficiente das inundações em SI, SIV e SV. A ampla e complexa planície de inundação em SII influencia significativamente a capacidade

de armazenamento, permitindo a dissipação gradual do excesso de água das inundações e a atenuação dos picos. O desvio de água para o antigo sistema (Rio Javaés) exibiu padrões únicos de transferência em diferentes condições de fluxo, resultando em perdas e ganhos anuais globais em SIII. As metodologias e os conhecimentos disciplinares gerados nesta tese poderão subsidiar futuros trabalhos e investigações interdisciplinares no contexto das ciências ambientais.

Palavras-chave: Grandes rios tropicais. Bioma Cerrado. Resposta geomórfica. Segmentação fluvial. Abordagem hidrogeomórfica. Gestão fluvial.

ABSTRACT

The Araguaia River represents the last and most important free-flowing river located in the Cerrado-Amazon ecotone. The increasing human influence on this river system poses an imminent threat to the valuable ecosystem services it provides. Therefore, it is essential to produce knowledge about the physical structure and functioning of this river, which serves as a basis for a significant portion of the biome's biodiversity. This thesis contributes to the fields of Geomorphology and Hydrology of large tropical rivers, bringing new discoveries that enrich the existing body of research on the Araguaia system. In the first paper, we conducted an assessment of the planform morphology changes in the upper-middle course between 2001 and 2018, expanding the temporal data series on the evolution of macroforms to a 53-year period. We found that the current transition phase of the river, characterized by the contraction of the channel's active zone and the partial loss of braiding due to a higher representativeness of the islands, is likely related to changes in the hydro-sedimentary regime over the last two decades. Based on a set of channel and floodplain geomorphological variables, in the second paper we developed a methodology to subdivide the middle Araguaia into 19 distinct reaches (R1-R19), which were further clustered into five major segments (SI-SV). We found that changes in valley gradient have a significant influence on the morphology of SI, SIII, and SIV, while the inflow of important tributaries and the nature of the valley floor are the main controlling factors for the fluvial style in SII and SV, respectively. This large-scale planimetric characterization of the river's middle course complements previous geomorphic studies, providing insights into the morphological diversity and sensitivity of each segment to environmental changes. In the third paper, we present a new approach to the existing classifications in the literature of flood events in the middle Araguaia. Small-scale floods (types B and D2) exhibit distinct attenuation patterns associated with the occurrence of drier years (D2). The attenuation of intermediate-scale floods (types C and D1) and large-scale floods (type A) is influenced by the magnitude of maximum flows at the upstream river gauge station, with no statistical significance for the influence of tributaries on peak changes. Flood hydrograph properties were found to respond to the regional geomorphological organization of the system. When considering the segments proposed in the second paper, we observed that the nature of the valley floor plays a central role in the efficient transport of floods in SI, SIV, and SV. The wide and complex floodplain in SII significantly influences the storage capacity, allowing for gradual dissipation of floodwater excess and peak attenuation. Water diversion to the old system (Rio Javaés) exhibited unique transfer patterns under different flow conditions, resulting in overall annual losses and gains in SIII. The

methodologies and disciplinary knowledge produced in this thesis can support future interdisciplinary work and investigations in the context of environmental sciences.

Keywords: Large tropical rivers. Cerrado biome. Geomorphic response. Fluvial segmentation. Hydrogeomorphic approach. River management.

SUMÁRIO

1 INTRODUÇÃO	11
2 DESENVOLVIMENTO.....	22
2.1 Artigo 1 – Resposta da morfologia do médio-curso superior do Rio Araguaia às mudanças no regime hidrossedimentar no período 2001-2018	22
2.1.1 <i>Introdução</i>	23
2.1.2 <i>Área de Estudo</i>	24
2.1.3 <i>Materiais e Métodos</i>	26
2.1.4 <i>Resultados</i>	28
2.1.5 <i>Discussão</i>	34
2.1.6 <i>Conclusões</i>	39
2.2 Artigo 2 – Geomorphic diversity of the middle Araguaia River, Brazil: a segment-scale classification to support river management.....	43
2.2.1 <i>Introduction</i>	43
2.2.2 <i>Study Area</i>	46
2.2.3 <i>Materials and Methods</i>	49
2.2.3.1 Definition of river reaches.....	50
2.2.3.2 River classification into major geomorphic segments	52
2.2.3.3 Planform dynamics in the river segments	53
2.2.4 <i>Results and Discussion</i>	54
2.2.4.1 Spatial patterns of morphological variability at the reach scale.....	54
2.2.4.2 Characterization of the middle Araguaia River segments.....	58
2.2.5 <i>Conclusions</i>	64
2.3 Artigo 3 – The role of geomorphology on flood propagation in a large tropical river: the peculiar case of the Araguaia River, Brazil	70
2.3.1 <i>Introduction</i>	70
2.3.2 <i>Study area</i>	72
2.3.3 <i>Data and methods</i>	73
2.3.3.1 Hydrological data	73
2.3.3.2 Flood type classification.....	75
2.3.3.3 Geomorphic and flood metrics	77
2.3.3.4 Statistical analysis	79
2.3.4 <i>Results</i>	79
2.3.4.1 The flood types in the middle Araguaia River	79
2.3.4.2 Propagation of flood waves along the middle Araguaia River	82
2.3.4.3 Impact of tributaries on mainstem flood attenuation	84
2.3.4.4 Influence of geomorphic variables on the floods	88
2.3.5 <i>Discussion: linking flood hydrology in the middle Araguaia River with its major geomorphic segments.....</i>	95
2.3.6 <i>Conclusions</i>	99
3 CONCLUSÃO E RECOMENDAÇÕES	105

1 INTRODUÇÃO

O Programa de Pós-Graduação em Ciências Ambientais (CIAMB) da Universidade Federal de Goiás (UFG), estrategicamente localizado e inspirado pela tradição de pesquisa de seus docentes, é reconhecido por sua identidade de pesquisa interdisciplinar, desempenhando um papel fundamental na compreensão integrada dos aspectos econômicos, sociais e físico-naturais do Bioma Cerrado. Além disso, o programa busca ativamente soluções para a conservação e gestão dos recursos naturais e sociais, com ênfase nesse importante bioma (UFG, [s. d.]).

No âmbito das pesquisas desenvolvidas no CIAMB, merecem destaque aquelas relacionadas à hidrogeomorfologia do sistema Araguaia, que abrange aproximadamente 77% de sua área total de drenagem ($\sim 385.000 \text{ km}^2$) no Cerrado. Iniciadas ao final da década de 1990, essas pesquisas contribuíram significativamente para elucidar aspectos do sistema até então desconhecidos no cenário acadêmico mundial. Dentre os aspectos abordados, podemos mencionar a compreensão da geomorfologia geral da bacia hidrográfica (LATRUBESSE; STEVAUX, 2002), a investigação da história quaternária e do caráter avulsivo do sistema (VALENTE; LATRUBESSE, 2012), a análise da hidrologia do canal principal (AQUINO; STEVAUX; LATRUBESSE, 2005) e de seus tributários (AQUINO et al., 2009), a caracterização das grandes unidades morfosedimentares que compõem sua planície aluvial (BAYER, 2002, 2010), a avaliação da transmissão das ondas de inundação e seu impacto no complexo sistema lacustre da planície (AQUINO; LATRUBESSE; SOUZA FILHO, 2008; LININGER; LATRUBESSE, 2016; MORAIS et al., 2005), a investigação da influência da geomorfologia nas unidades vegetacionais da paisagem fluvial (MORAIS; AQUINO; LATRUBESSE, 2008; VALENTE; LATRUBESSE; FERREIRA, 2013), bem como as respostas hidrológicas (COE et al., 2011) e morfosedimentares (LATRUBESSE et al., 2009) do sistema diante do desmatamento na bacia hidrográfica.

O objetivo central desta tese é enriquecer a compreensão sobre a hidrogeomorfologia do Araguaia, trazendo novas descobertas que complementam os esforços de pesquisa anteriores dedicados a esse sistema. Para alcançar este objetivo, nossas contribuições abrangem três áreas-chave: em primeiro lugar, ampliamos a escala temporal das caracterizações morfológicas (Artigo 1). Em segundo lugar, propomos uma abordagem sistemática para a definição dos segmentos fluviais do Rio Araguaia (Artigo 2). Por fim, aprofundamos os conhecimentos sobre

a hidrologia de inundação desse rio, baseando-nos em uma perspectiva geomorfológica (Artigo 3).

Latrubesse et al. (2009) realizaram uma análise morfosedimentar integrada ao longo de 570 km do médio curso do Rio Araguaia. Os resultados revelaram que, em resposta ao acelerado desmatamento na bacia hidrográfica a partir da década de 1970, ocorreu um aumento significativo no balanço positivo de sedimentação na planície aluvial, um incremento no transporte de sedimentos de fundo e uma transformação na morfologia do canal entre os anos de 1965 e 1998. A relevância dessas descobertas no contexto da pressão antrópica atual sobre o sistema fluvial (LATRUBESSE et al., 2019) nos levou a formular a hipótese de que as respostas morfosedimentares do Rio Araguaia, observadas no estudo anterior, tenham se intensificado nas últimas duas décadas.

Assim, o primeiro artigo da tese, intitulado "Resposta da morfologia do médio-curso superior do Rio Araguaia às mudanças no regime hidrossedimentar no período 2001-2018" (SUIZU et al., 2022), teve como objetivo avaliar as mudanças na morfologia bidimensional do médio-curso superior do Rio Araguaia ao longo do período de 2001 a 2018, utilizando imagens multitemporais de sensoriamento remoto e aplicando novos parâmetros morfométricos. Ao realizar essa análise, fornecemos informações sobre as tendências atuais da dinâmica morfológica da zona ativa do canal e sua possível relação com as alterações no regime hidrológico.

Ao apresentar sua análise geomorfológica detalhada, Latrubesse et al. (2009) subdividiram o rio em dez compartimentos geomorfológicos. Embora essa primeira subdivisão do médio-curso superior tenha sido de grande importância para identificar áreas mais ou menos suscetíveis ao armazenamento de sedimentos e mudanças no canal, até o presente estudo não havia na literatura um estudo geomórfico abrangente que capturasse a diversidade longitudinal de todo o médio curso desse grande sistema fluvial. Além disso, Valente e Latrubesse (2012) já haviam destacado o caráter avulsivo do sistema, que culminou no abandono em curso de parte da antiga faixa fluvial do médio Araguaia (Rio Javaés). As implicações desse desvio em larga escala sobre o estilo fluvial e os ajustes do canal a jusante também não haviam sido investigadas, o que nos conduziu a postular a hipótese de que existe uma pronunciada variabilidade longitudinal do continuum fluvial fortemente influenciada pela história avulsiva desse rio durante o Pleistoceno tardio-Holoceno.

Diante dessa conjuntura, no segundo artigo da tese, intitulado "*Geomorphic diversity of the middle Araguaia River, Brazil: A segment-scale classification to support river management*" (SUIZU; LATRUBESSE; BAYER, 2023), caracterizamos a geodiversidade do

médio Araguaia com base em uma abordagem sistemática de identificação de segmentos geomórficos. Os objetivos específicos desse estudo foram: (i) obter unidades de trecho do rio (river reaches) e avaliar suas tendências longitudinais por meio da aplicação de métricas de canal e planície de inundação; (ii) realizar uma análise de agrupamento (cluster analysis) para classificar de forma objetiva os trechos do rio com atributos morfológicos relativamente uniformes em grandes segmentos fluviais; e (iii) identificar os principais fatores de controle do estilo fluvial em cada uma das classes de segmento.

Em seus estudos sobre a hidrologia do sistema, Aquino, Latrubesse e Souza Filho (2008) já haviam demonstrado que as variações longitudinais nos estilos fluviais do Rio Araguaia desempenhavam um papel importante no controle da dinâmica das inundações. Esses autores identificaram uma transmissão atípica das inundações ao longo de um trecho de aproximadamente 430 km no médio-curso superior, no qual as estações fluviométricas a jusante registraram vazões de pico menores em relação às estações a montante, mesmo diante do aumento da área de drenagem e da entrada tributária, um fenômeno conhecido como atenuação do pico de vazão. Essa redução no fluxo foi atribuída ao armazenamento de água na planície aluvial e, secundariamente, à perda de vazão para o Rio Javaés. O grau de redução das vazões máximas, à medida que as enchentes avançam, ainda levou os autores a categorizar os eventos de inundação em três tipos (A, B e C). Posteriormente, Lininger e Latrubesse (2016) realizaram novas contribuições à compreensão da atenuação do pico de vazão no médio-curso superior do Rio Araguaia, utilizando um balanço hídrico simplificado e investigando a conectividade e as variações sazonais na área dos lagos da planície de inundação. Além disso, Lininger (2013) introduziu duas novas categorias de tipos de enchentes (D1 e D2), complementando as categorias anteriormente definidas por Aquino, Latrubesse e Souza Filho (2008).

No terceiro artigo da tese, intitulado "*The role of geomorphology on flood propagation in a large tropical river: the peculiar case of the Araguaia River, Brazil*", apresentamos uma abordagem inovadora ao integrar e aprimorar os métodos anteriores de classificação dos tipos de inundação no médio Araguaia. Ampliamos o período de análise (1975-2014) e monitoramos o comportamento de todos os eventos de inundação ao longo de todo o curso médio do rio. Buscamos também uma distinção mais sistemática dos atributos-chave e dos fatores de controle de cada tipo de inundação, examinando diferentes propriedades do hidrograma de inundação, realizando análises estatísticas e fornecendo insights sobre a influência dos afluentes na atenuação dos picos de vazão. Além disso, investigamos a hipótese de que a propagação das ondas de inundação a jusante é condicionada pelos distintos segmentos geomórficos definidos em nosso estudo anterior (Artigo 2). Ao concentrarmos nossos esforços na interface dinâmica

entre hidrologia e geomorfologia, aprimoramos significativamente nossa compreensão das funções fluviais que operam no sistema.

As pesquisas realizadas nas últimas duas décadas, assim como os resultados apresentados nesta tese, destacam a singularidade do Rio Araguaia em relação a outros grandes rios tropicais do mundo e sua imensa importância como um sistema ambiental. A ascensão do Brasil como principal exportador mundial de soja e carne bovina resultou na devastação de extensas áreas de vegetação no Cerrado. Com quase metade de sua área original já ocupada por atividades agropecuárias (LAPOLA et al., 2014), as planícies do Rio Araguaia e do Bananal representam a última fronteira ambiental desse bioma (LATRUBESSE et al., 2009; LATRUBESSE et al., 2019). Nenhum outro bioma no mundo foi destruído com tamanha rapidez na história humana. Em resposta a essa devastação generalizada, Latrubesse et al. (2009) identificaram duas características peculiares do Rio Araguaia: (i) sua alta sensibilidade geomórfica às perturbações antrópicas; e (ii) o curto período de reação (aproximadamente uma década) após a perturbação, similar ao observado em bacias hidrográficas de pequeno e médio porte.

Uma outra característica única do Rio Araguaia, em comparação com outros grandes rios aluviais da América do Sul, como o Rio Paraná e muitos dos rios amazônicos, é a sua alta proporção de carga arenosa transportada, representando até ~57% do total de carga de sedimentos, em contraste com a carga em suspensão que corresponde, em média, a 43-49% do total (AQUINO; LATRUBESSE; BAYER, 2009). Além disso, a forma como as ondas de inundação se propagam pelo médio curso torna este rio distinto em relação a outros sistemas aluviais axiais, especialmente na região tropical da América do Sul (LININGER; LATRUBESSE, 2016).

Os mecanismos geomórficos que atenuam os picos de inundação, como as características geomorfológicas lacustres da planície aluvial e sua conexão com o canal principal, desempenham um papel fundamental na manutenção ecológica do corredor fluvial (AQUINO; LATRUBESSE; SOUZA FILHO, 2008; LININGER; LATRUBESSE, 2016; MORAIS et al., 2005). Nesse viés, pesquisas anteriores destacaram o impacto significativo do ciclo anual de inundação no médio Araguaia em vários aspectos ecológicos, incluindo a organização espacial das formações vegetais (MORAIS; AQUINO; LATRUBESSE, 2008; KURZATKOWSKI; LEUSCHNER; HOMEIER, 2015), concentrações de nutrientes e comunidades fitoplanctônicas (NABOUT; NOGUEIRA; OLIVEIRA, 2006), estrutura da comunidade de peixes (TEJERINA-GARRO; FORTIN; RODRÍGUEZ, 1998), habitats de

nidificação de tartarugas gigantes do Rio Amazonas (FERREIRA; CASTRO, 2005) e estrutura genética de populações de roedores (ROCHA et al., 2014).

Apesar de sua imensa importância para a conservação de espécies e fornecimento de serviços ecossistêmicos, a Bacia do Araguaia emerge como um sistema ambiental do Cerrado que enfrenta forte pressão das atividades antrópicas. De acordo com dados de 2019, aproximadamente 49% da área da bacia é ocupada por pastagens e monoculturas (ASSIS, 2022). Além disso, estima-se a ocorrência de cerca de 14.472,03 km² de desmatamento acumulado e o registro de 114.326 focos de queimadas e incêndios florestais entre os anos de 2012 e 2020 (ASSIS; FARIA; BAYER, 2021). No alto e médio-curso superior do Araguaia, aproximadamente 38,5% de sua área total permanece preservada, e 61,5% de sua extensão sofreu algum tipo de perturbação ambiental, incluindo 44,6% da vegetação ribeirinha (FERREIRA et al., 2008).

Concomitantemente à fragmentação da paisagem, a expansão da fronteira agrícola, iniciada na década de 1970, não foi acompanhada por práticas adequadas de conservação dos solos arenosos que caracterizam a alta bacia, resultando em sua degradação com a formação generalizada de feições erosivas lineares (CASTRO et al., 1999; MARINHO; CASTRO; CAMPOS, 2006; NUNES, 2015). Como consequência do desmatamento massivo e da erosão dos solos, foram observadas profundas alterações na carga sedimentar e no padrão de canal do Rio Araguaia (LATRUBESSE et al., 2009).

Além do impacto direto do desmatamento na erosão e transporte de sedimentos, as ações antrópicas na bacia hidrográfica também provocaram alterações na hidrologia do sistema. Nesse contexto, Coe et al. (2011) observaram um aumento de 25% na vazão do Rio Araguaia na estação Aruanã entre as décadas de 1970 e 1990, sendo que dois terços dessa mudança hidrológica foram atribuídos às mudanças no uso e cobertura da terra na bacia hidrográfica, e não às mudanças climáticas, uma vez que as alterações na precipitação foram de apenas 2,5% no mesmo período.

Ressalta-se que os modelos de cenários futuros da mudança climática antropogênica revelam modificações diretas no regime de precipitação e em outros aspectos do ciclo hidrológico na região dos trópicos (IPCC, 2018; WOHL et al., 2012). As projeções para o Tocantins-Araguaia sugerem reduções na vazão durante a estação seca (HO; THOMPSON; BRIERLEY, 2016), e os modelos de séries temporais de vazão em estações fluviométricas distribuídas ao longo da Bacia do Araguaia mostram que, com exceção da alta bacia, há uma tendência generalizada de redução nas vazões no período 1965–2019 (LIMA; CRIBARI-NETO; LIMA-JUNIOR, 2022).

O uso excessivo de água para fins de irrigação exerce uma pressão adicional sobre os recursos hídricos. Para o ano de 2020, Guimarães e Landau (2020) identificaram 738 pivôs centrais em funcionamento na Bacia do Araguaia, abrangendo uma área total potencialmente irrigada de 82.414,7 hectares. É importante ressaltar que o número de pivôs de irrigação em operação ilegal no Cerrado é desconhecido, mas sabe-se que somente no estado de Goiás, mais de 2.600 pivôs estão operando sem as devidas licenças ambientais (LATRUBESSE et al., 2019). A extração direta de água dos canais também é uma prática comum. O Projeto de Irrigação de Luiz Alves do Araguaia (PILAA) beneficia-se da captação de água do curso principal e, atualmente, abrange uma área irrigada de aproximadamente três mil hectares. O governo estadual tem como objetivo ampliar esse projeto a fim de alcançar uma extensão de quase sete mil hectares destinados a atender às demandas hídricas dos produtores da região (CODEVASF, 2022).

Há ainda o interesse na exploração do potencial hidrelétrico da Bacia do Araguaia. Na sub-bacia do Tocantins, já existem grandes barragens, como as de Tucuruí, Estreito e Serra da Mesa, e estão planejadas mais 90 barragens nessa mesma sub-bacia (LATRUBESSE et al., 2019). O Rio Araguaia, que atualmente possui nove pequenas usinas hidrelétricas a montante, é o único grande sistema no Cerrado de fluxo livre de barramentos a jusante. No entanto, com as propostas de construção de 70 barragens, incluindo quatro de grande porte no canal principal do rio, a sua preservação enfrenta sérios desafios (LATRUBESSE et al., 2019).

Latrubesse et al. (2019) realizaram importantes considerações sobre as ameaças ambientais aos recursos hídricos do Cerrado derivadas das atividades e práticas correntes no bioma. Essas ameaças podem resultar em alterações significativas no funcionamento do sistema físico, como mudanças no regime hidrológico, na morfodinâmica, nos fluxos de sedimentos, nos padrões de conectividade e na extensão da planície de inundação. Tais alterações representam um risco iminente para a perda irreversível dos valiosos serviços ecossistêmicos fornecidos pelo Rio Araguaia (vide Tabela 1 em Latrubesse et al., 2019 para maiores detalhamentos desses impactos), sendo imprescindível a implementação, de forma efetiva e integrada, de iniciativas como o Corredor Araguaia-Bananal, o Corredor de Biodiversidade do Araguaia e o Arco das Nascentes.

Além dos avanços teórico-metodológicos nos campos da Hidrologia e Geomorfologia de grandes rios tropicais, os resultados disciplinares desta tese têm o potencial de integrar futuras investigações na interface com outros ramos do conhecimento, como ecologia, sedimentologia e engenharia. Essa abordagem interdisciplinar será fundamental para aprimorar

projetos de manejo sustentável e subsidiar políticas públicas eficazes diante dos desafios ambientais complexos e multifacetados apresentados por esse imponente sistema fluvial.

REFERÊNCIAS

- AQUINO, S.; LATRUBESSE, E. M.; BAYER, M. Assessment of wash load transport in the Araguaia River (Aruanã gauge station), central Brazil. **Latin American Journal of Sedimentology and Basin Analysis**, vol. 16, no. 2, p. 119–128, 2009.
- AQUINO, S.; LATRUBESSE, E. M.; SOUZA FILHO, E. E. Relações entre o regime hidrológico e os ecossistemas aquáticos da planície aluvial do rio Araguaia. **Acta Scientiarum - Biological Sciences**, vol. 30, no. 4, p. 361–369, 2008. <https://doi.org/10.4025/actascibiolsci.v30i4.5866>.
- AQUINO, S.; LATRUBESSE, E. M.; SOUZA FILHO, E. E. Caracterização hidrológica e geomorfológica dos afluentes da Bacia do Rio Araguaia. **Revista Brasileira de Geomorfologia**, vol. 10, no. 1, p. 43–54, 2009. DOI 10.20502/RBG.V10I1.116.
- AQUINO, S.; STEVAUX, J. C.; LATRUBESSE, E. M. Regime Hidrológico E Aspectos Do Comportamento Morfohidráulico Do Rio Araguaia. **Revista Brasileira de Geomorfologia**, vol. 6, no. 2, p. 29–41, 2005. <https://doi.org/10.20502/rbg.v6i2.49>.
- ASSIS. P. C. **Análise ambiental integrada da paisagem na bacia hidrográfica do Rio Araguaia**. 2022. 116 f. Universidade Federal de Goiás (UFG), 2022.
- ASSIS, P. C.; FARIA, K. M. S.; BAYER, M. Unidades de Conservação e sua efetividade na proteção dos recursos hídricos na Bacia do Rio Araguaia. **Sociedade & Natureza**, vol. 34, no. 1, p. 1–13, 2021. <https://doi.org/10.14393/sn-v34-2022-60335>.
- BAYER, M. **Diagnóstico dos processos de erosão/assoreamento na planície aluvial do rio Araguaia: entre Barra do Garças e Cocalinho**. 2002. Universidade Federal de Goiás (UFG), 2002.
- BAYER, M. **Dinâmica do transporte , composição e estratigrafia dos sedimentos da planície aluvial do rio Araguaia . Dinâmica do transporte , composição e estratigrafia dos sedimentos da planície aluvial do rio Araguaia**. 2010. 1–83 f. Universidade Federal de Goiás (UFG), 2010.
- CASTRO, S. S. de.; CAMPOS, A. B de; OLIVEIRA, C. J.; SILVA, A. A. The Upper Araguaia Basin and the Effects of Human-induced Erosion. In: Boletim Goiano de Geografia 1999, Anais [...]. DOI: 10.5216/bgg.v19i1.15342.
- COE, M. T.; LATRUBESSE, E. M.; FERREIRA, M. E.; AMSLER, M. L. The effects of deforestation and climate variability on the streamflow of the Araguaia River, Brazil. **Biogeochemistry**, vol. 105, no. 1, p. 119–131, 2011. <https://doi.org/10.1007/s10533-011-9582-2>.
- COMPANHIA DE DESENVOLVIMENTO DOS VALES DO SÃO FRANCISCO E DO PARNAÍBA - CODEVASF. Codevasf anuncia investimentos federais no Projeto de Irrigação de Luiz Alves do Araguaia, em Goiás. 2022. Available at: <https://www.codevasf.gov.br/noticias/2020/codevasf-anuncia-investimentos-federais-no-projeto-de-irrigacao-de-luiz-alves-do-araguaia-em-goias>. Accessed on: 12 Jul. 2023.
- FERREIRA, M. E.; FERREIRA, L. G.; LATRUBESSE, E. M.; MIZIARA, F. High resolution

remote sensing based quantification of the remnant vegetation cover in the Araguaia river basin, central Brazil. **International Geoscience and Remote Sensing Symposium (IGARSS)**, vol. 4, no. 1, p. 2008–2010, 2008.
<https://doi.org/10.1109/IGARSS.2008.4779828>.

FERREIRA, P. D.; CASTRO, P. de T. A. Nest placement of the giant amazon river turtle, *Podocnemis expansa*, in the Araguaia river, Goiás State, Brazil. **Ambio**, vol. 34, no. 3, p. 212–217, 2005. <https://doi.org/10.1579/0044-7447-34.3.212>.

GUIMARÃES, D. P.; LANDAU, E. C. Georreferenciamento dos pivôs centrais de irrigação no Brasil: Ano-base 2020. **Boletim de Pesquisa e Desenvolvimento**, no. 222, p. 64, 2020.

HO, J. T.; THOMPSON, J. R.; BRIERLEY, C. Projections of hydrology in the Tocantins-Araguaia Basin, Brazil: uncertainty assessment using the CMIP5 ensemble. **Hydrological Sciences Journal**, vol. 61, no. 3, p. 551–567, 2016. DOI 10.1080/02626667.2015.1057513.

INTERGOVERNMENTAL PANEL ON CLIMATE CHANGE – IPCC. **Global Warming of 1.5°C**. New York: Cambridge University Press, 2018.

KURZATKOWSKI, D.; LEUSCHNER, C.; HOMEIER, J. Effects of flooding on trees in the semi-deciduous transition forests of the Araguaia floodplain, Brazil. **Acta Oecologica**, vol. 69, p. 21–30, 2015. <https://doi.org/10.1016/j.actao.2015.08.002>.

LAPOLA, D. M.; MARTINELLI, L. A.; PERES, C. A.; OMETTO, J. P. H. B.; FERREIRA, M. E.; NOBRE, C. A.; AGUIAR, A. P. D.; BUSTAMANTE, M. M. C.; CARDOSO, M. F.; COSTA, M. H.; JOLY, C. A.; LEITE, C. C.; MOUTINHO, P.; SAMPAIO, G.; STRASSBURG, B. B. N.; VIEIRA, I. C. G. Pervasive transition of the Brazilian land-use system. **Nature Climate Change**, vol. 4, no. 1, p. 27–35, 2014. DOI 10.1038/nclimate2056.

LATRUBESSE, E. M.; AMSLER, M. L.; MORAIS, R. P.; AQUINO, S. The geomorphologic response of a large pristine alluvial river to tremendous deforestation in the South American tropics: The case of the Araguaia River. **Geomorphology**, vol. 113, no. 3–4, p. 239–252, 2009. DOI 10.1016/j.geomorph.2009.03.014.

LATRUBESSE, E. M.; ARIMA, E.; FERREIRA, M. E.; NOGUEIRA, S. H.; WITTMANN, F.; DIAS, M. S.; DAGOSTA, F. C. P.; BAYER, M. Fostering water resource governance and conservation in the Brazilian Cerrado biome. **Conservation Science and Practice**, vol. 1, no. 9, p. 1–8, 2019. <https://doi.org/10.1111/csp2.77>.

LATRUBESSE, E. M.; STEVAUX, J. C. Geomorphology and environmental aspects of the Araguaia fluvial basin, Brazil. **Zeitschrift für Geomorphologie**, vol. 129, p. 109–127, 2002.

LIMA, L. B.; CRIBARI-NETO, F.; LIMA-JUNIOR, D. P. Dynamic quantile regression for trend analysis of streamflow time series. **River Research and Applications**, vol. 38, no. 6, p. 1051–1060, 2022. <https://doi.org/10.1002/rra.3983>.

LININGER, K. B.; LATRUBESSE, E. M. Flooding hydrology and peak discharge attenuation along the middle Araguaia River in central Brazil. **Catena**, vol. 143, p. 90–101, 2016. DOI 10.1016/j.catena.2016.03.043.

LININGER, K. B. **The hydro-geomorphology of the middle Araguaia River: floodplain dynamics of the largest fluvial system draining the Brazilian Cerrado.** 2013. 150 f. The University of Texas at Austin, 2013.

MARINHO, G. V.; CASTRO, S. S.; CAMPOS, A. B. Hydrology and gully processes in the upper Araguaia River basin, Central Brazil. **Zeitschrift fur Geomorphologie, Supplementband**, vol. 145, p. 119–145, 2006.

MORAIS, R. P.; AQUINO, S.; LATRUBESSE, E. M. Controles hidrogeomorfológicos nas unidades vegetacionais da planície aluvial do rio Araguaia, Brasil. **Acta Scientiarum - Biological Sciences**, vol. 30, no. 4, p. 411–421, 2008.
<https://doi.org/10.4025/actascibiolsci.v30i4.5871>.

MORAIS, R. P.; GONÇALVES OLIVEIRA, L.; LATRUBESSE, E. M.; DIÓGENES PINHEIRO, R. C. Morfometria de sistemas lacustres da planície aluvial do médio rio Araguaia. **Acta Scientiarum. Biological Sciences**, vol. 27, no. 3, p. 203–213, 2005.
<https://doi.org/10.4025/actascibiolsci.v27i3.1278>.

NABOUT, J. C.; NOGUEIRA, I. S.; OLIVEIRA, L. G. Phytoplankton community of floodplain lakes of the Araguaia River, Brazil, in the rainy and dry seasons. **Journal of Plankton Research**, vol. 28, no. 2, p. 181–193, 2006. <https://doi.org/10.1093/plankt/fbi111>.

NUNES, E. D. **Modelagem de processos erosivos hídricos lineares no município de Mineiros - GO.** 2015. 242 f. Universidade Federal de Goiás (UFG), 2015.

ROCHA, R. G.; FERREIRA, E.; FONSECA, C.; JUSTINO, J.; LEITE, Y. L. R.; COSTA, L. P. Seasonal flooding regime and ecological traits influence genetic structure of two small rodents. **Ecology and Evolution**, vol. 4, no. 24, p. 4598–4608, 2014.
<https://doi.org/10.1002/ece3.1336>.

SUIZU, T. M.; LATRUBESSE, E. M.; BAYER, M. Geomorphic diversity of the middle Araguaia River, Brazil: A segment-scale classification to support river management. **Journal of South American Earth Sciences**, vol. 121, 2023.
<https://doi.org/10.1016/j.jsames.2022.104166>.

SUIZU, T. M.; LATRUBESSE, E. M.; STEVAUX, J. C.; BAYER, M. Resposta da morfologia do médio-curso superior do Rio Araguaia às mudanças no regime hidrossedimentar no período 2001-2018. **Revista Brasileira de Geomorfologia**, vol. 23, no. 2, p. 1420–1434, 2022. <https://doi.org/10.20502/rbg.v23i2.2088>.

TEJERINA-GARRO, F. L.; FORTIN, R.; RODRÍGUEZ, M. A. Fish community structure in relation to environmental variation in floodplain lakes of the Araguaia River, Amazon Basin. **Environmental Biology of Fishes**, vol. 51, p. 399–410, 1998.

UFG - UNIVERSIDADE FEDERAL DE GOIÁS. Apresentação: Programa de Pós-Graduação em Ciências Ambientais (CIAMB). [s. d.]. Available at: <https://ciamb.prpg.ufg.br/p/6684-apresentacao>. Accessed on: 30 Jun. 2023.

VALENTE, C. R.; LATRUBESSE, E. M. Fluvial archive of peculiar avulsive fluvial patterns in the largest Quaternary intracratonic basin of tropical South America: The Bananal Basin,

Central-Brazil. **Palaeogeography, Palaeoclimatology, Palaeoecology**, vol. 356–357, p. 62–74, 2012. DOI 10.1016/j.palaeo.2011.10.002.

VALENTE, C. R.; LATRUBESSE, E. M.; FERREIRA, L. G. Relationships among vegetation, geomorphology and hydrology in the Bananal Island tropical wetlands, Araguaia River basin, Central Brazil. **Journal of South American Earth Sciences**, vol. 46, p. 150–160, 2013. DOI 10.1016/j.jsames.2012.12.003.

WOHL, E.; BARROS, A.; BRUNSELL, N.; CHAPPELL, N. A.; COE, M.; GIAMBELLUCA, T.; GOLDSMITH, S.; HARMON, R.; HENDRICKX, J. M. H.; JUVIK, J.; McDONNELL, J.; OGDEN, F. The hydrology of the humid tropics. **Nature Climate Change**, vol. 2, no. 9, p. 655–662, 2012. DOI 10.1038/nclimate1556.

2 DESENVOLVIMENTO

2.1 Artigo 1 – Resposta da morfologia do médio-curso superior do Rio Araguaia às mudanças no regime hidrossedimentar no período 2001-2018¹

Resumo: O Rio Araguaia se caracteriza pela rápida resposta geomórfica à degradação pelas atividades antrópicas em sua bacia hidrográfica. A morfologia bidimensional do médio-curso superior do Rio Araguaia foi avaliada durante o período 2001-2018, ampliando para 53 anos a série temporal preexistente na bibliografia da análise quali-quantitativa das macroformas desse rio e de suas respostas às mudanças no uso e cobertura da terra. Com base no processamento de imagens multitemporais de sensoriamento remoto, realizou-se a quantificação dos parâmetros morfométricos de ilhas e barras arenosas e a estimativa areal dos processos erosivos e deposicionais no sistema fluvial atual. Entre 1965 e 1998, o rio alterou parcialmente o seu padrão anabanching, ampliando a tendência ao entrelaçamento. No período 2001-2018, foram identificadas mudanças na morfologia que denotam a uma fase transicional de contração da zona ativa do canal e perda parcial das características de entrelaçamento devido à ampliação da representatividade das ilhas. Tal conjuntura responde às alterações no regime hidrossedimentar nas últimas duas décadas. Diante do avanço da fronteira agrícola e das propostas de construção de quatro grandes barragens ao longo de seu curso, o atual estado de ajuste do sistema canal-planície aluvial deve ser considerado no manejo deste grande rio do Cerrado.

Palavras-chave: Rios multicanais; Resposta geomórfica; Morfometria do canal; Bioma Cerrado.

Abstract: The Araguaia River is characterized by a rapid geomorphic response to the degradation of the basin induced by land-use changes. The planform geometry in the upper middle-course of the Araguaia River was assessed over the 2001-2018 period. Thus, we extended to 53 years the pre-existing published time series data on the river's morphology and its response to land use changes. Based on the analysis of multi-temporal remotely sensing images we quantified the morphometric parameters on islands and sandy bars and estimated

¹Artigo publicado: SUIZU, T. M.; LATRUBESSE, E. M.; STEVAUX, J. C.; BAYER, M. Resposta da morfologia do médio-curso superior do Rio Araguaia às mudanças no regime hidrossedimentar no período 2001-2018. *Revista Brasileira de Geomorfologia*, vol. 23, no. 2, p. 1420–1434, 2022. <https://doi.org/10.20502/rbg.v23i2.2088>.

erosive and depositional areas in the actual river system. From 1965 to 1998, the river partially changed its anabranching pattern, increasing the tendency toward braiding. The morphological changes from 2001 to 2018 reveal a new transitional phase of contraction of the channel's active zone and a partial loss of braiding due to higher representativeness of the islands. This scenario responds to changes in the hydro-sedimentary regime over the last two decades. Given the expansion of the agricultural frontier and the proposals for the construction of four large dams along its main stem, the current state of adjustment of the channel-floodplain system must be considered in the management plans of this large river of the Cerrado biome.

Keywords: Anabranching rivers; Geomorphic response; Channel morphometry; Cerrado biome.

2.1.1 *Introdução*

O Rio Araguaia é o principal sistema fluvial do Brasil Central. A sua bacia hidrográfica, com 377.000 km², está majoritariamente inserida no Cerrado. Esse bioma, considerado a savana tropical mais diversa do globo com um elevado grau de endemismo, contém a Planície do Bananal, uma das mais importantes áreas úmidas da América do Sul (COLLI; VIEIRA; DIANESE, 2020; LENTHALL; BRIDGEWATER; FURLEY, 1999; VALENTE; LATRUBESSE, 2012).

A ascensão do Brasil como maior exportador de soja e carne bovina no mercado mundial levou à eliminação de extensas áreas de vegetação do Cerrado, estimulada pela demanda global, tecnologias agronômicas e políticas governamentais favoráveis (BRANNSTROM et al., 2008). Com a ocupação de ~50% de sua extensão original por atividades agropecuárias (LAPOLA et al., 2014), a planície do Rio Araguaia e a Planície do Bananal, detentoras de grande diversidade fitofisionômica em razão da constante disponibilidade hídrica (FURLEY, 1999), atuam como a última fronteira ambiental do bioma (LATRUBESSE et al., 2009; LATRUBESSE et al., 2019).

Em resposta ao acelerado desmatamento na bacia hidrográfica a partir da década de 1970, o Rio Araguaia tem apresentado mudanças geomorfológicas, hidrológicas e sedimentares (LATRUBESSE et al., 2009; COE et al., 2011). Com base na análise morfosedimentar integrada (descrições morfométricas, balanço entre os processos erosivos e deposicionais em área e volume, e estimativas do transporte sedimentar), Latrubesse et al. (2009) verificaram, ao longo de 570 km do médio curso do Rio Araguaia, um aumento substancial no balanço positivo de sedimentação na planície aluvial, o incremento do transporte de sedimentos de fundo e a metamorfose na morfologia do canal entre os anos 1965 e 1998.

O estudo de Latrubblesse et al. (2009) revelou: (i) a elevada sensibilidade geomórfica do Rio Araguaia às perturbações antrópicas e; (ii) o reduzido período de reação (da ordem de uma década) após a perturbação, de modo bastante similar ao esperado para bacias hidrográficas de pequeno e médio porte. A relevância dessas constatações diante do atual quadro de modificações antropogênicas (expansão da agricultura e captação de água para irrigação) e das ações adicionais propostas (construção de barragens) para o sistema fluvial (LATRUBESSE et al., 2019) resulta na necessidade da produção de novos dados documentando as respostas morfossedimentares do Rio Araguaia nas últimas duas décadas.

Assim, o presente estudo objetiva avaliar as mudanças na morfologia bidimensional do médio-curso superior do Rio Araguaia ao longo do período 2001-2018 com base no uso de imagens multitemporais de sensoriamento remoto e na aplicação de parâmetros morfométricos. A execução dessa proposição permite ampliar a escala temporal das caracterizações morfológicas conduzidas por Latrubblesse et al. (2009), e fornece subsídios à gestão ambiental desse sistema fluvial de grande importância para o Cerrado.

2.1.2 Área de Estudo

A área sob investigação compreende um segmento de 132,8 km no médio-curso superior do Rio Araguaia (Figura 1A). Diversas razões justificam a seleção desse segmento fluvial. A partir dos anos 2000, pesquisas (AQUINO; LATRUBESSE; BAYER, 2009; BAYER, 2002, 2010; COE et al., 2011; LININGER; LATRUBESSE, 2016; MORAIS, 2006) foram desenvolvidas nessa região, que atua como sistema coletor de água e sedimentos aportados pela alta bacia (centro da expansão agropecuária do estado de Goiás) e que são transferidos para o médio curso (FERREIRA et al., 2013). Além disso, a área abrange a primeira estação hidrométrica (estação Aruanã – Figura 1A) operada pela CPRM-ANA no Rio Araguaia, a qual registra a contribuição do alto para o médio curso do rio desde a década de 1970. O Rio Araguaia também desempenha um papel central para o setor econômico do município de Aruanã-GO (Figura 1B) por meio de uma consolidada atividade turística fluvial (pesca esportiva e uso recreativo).

A declividade do vale no segmento corresponde a $0,00017 \text{ m m}^{-1}$. O segmento é marcado pela presença de uma ampla planície aluvial holocênica incidida nos depósitos Quaternários da Formação Araguaia (VALENTE; LATRUBESSE, 2012).

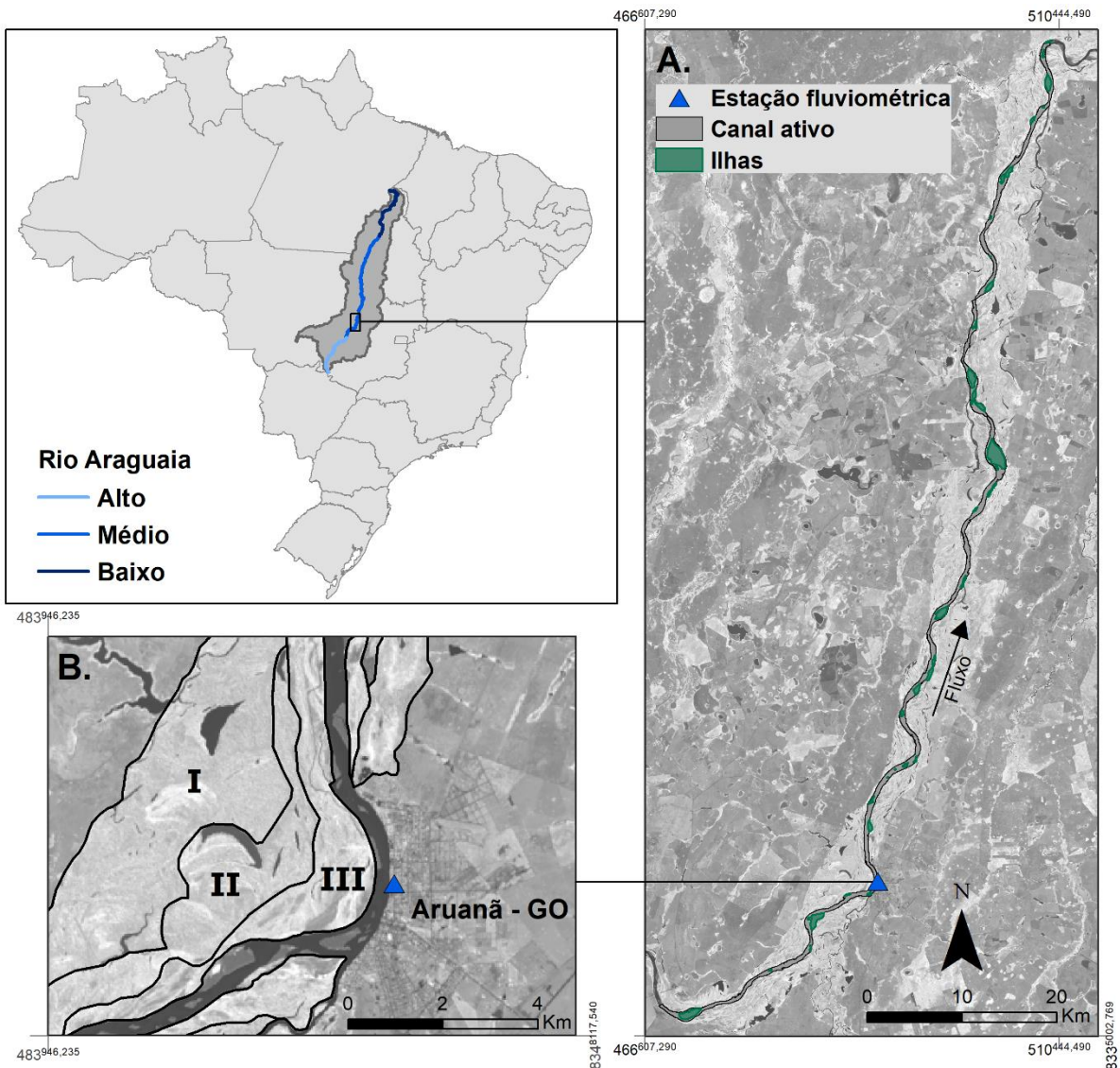


Figura 1. Localização da área de estudo. A. Configuração multicanal (anabanching) da área de estudo no médio-curso superior do Rio Araguaia; B. Detalhamento das unidades morfossedimentares (I, II e III) da planície aluvial próximas ao município de Aruanã – GO (BAYER, 2010). Imagens de fundo: Landsat 8 (25 jul. 2018).

Bayer (2002) e Latrubesse e Stevaux (2002) realizaram a distinção dessa planície aluvial em três grandes unidades morfossedimentares (Figura 1B). A Unidade I é a mais antiga entre as unidades e se constitui de áreas de escoamento impedido que ocupam as porções mais distais e topograficamente inferiores da planície. A Unidade II é a unidade predominante e de maior elevação em relação às demais. Essa unidade, geralmente situada entre as unidades I e III, se caracteriza pela presença de paleomeandros e lagos em meia-lua (*oxbow lakes*). A Unidade III corresponde a um complexo de barras e ilhas derivadas dos processos morfodinâmicos que distinguem o sistema aluvial atual.

As vazões média anual e média anual de inundações nesse segmento (estação Aruanã – Figura 1A) são, respectivamente, 1202,56 e 4777,92 m³/s para a série histórica 1971-2018. A expressiva sazonalidade do clima Tropical Savântico (Aw) (DUBREUIL et al., 2017) reflete na variabilidade dos fluxos, tendo em vista que as descargas máximas podem ser até 13 vezes superiores em relação às mínimas no médio curso do rio (AQUINO; STEVAUX; LATRUBESSE, 2005). As chuvas na região concentram-se entre outubro e abril, com índices pluviométricos que variam de 1850 a 1000 mm no sentido oeste-leste. A estação seca, por sua vez, se estende de maio a setembro (AQUINO; STEVAUX; LATRUBESSE, 2005; LATRUBESSE; STEVAUX, 2002).

O Rio Araguaia possui padrão anabranching (multicanal aluvial) de baixa sinuosidade com tendência ao entrelaçamento (LATRUBESSE, 2008). A ocorrência de canais múltiplos está vinculada às particularidades de seu transporte sedimentar. Estimativas do transporte de sedimento na estação fluviométrica Aruanã (Figura 1A) indicam que os sedimentos arenosos representam até cerca de 57% da carga total transportada pelo rio. A proporção de areia transportada em suspensão, em relação aos sedimentos finos, é muito alta (~55 a 43% da carga suspensa total) (AQUINO; LATRUBESSE; BAYER, 2009) e estima-se que cerca de 93% da carga arenosa do rio seja transportada em suspensão (LATRUBESSE et al., 2009).

2.1.3 Materiais e Métodos

Distintos procedimentos em SIG (Sistema de Informação Geográfica) foram conduzidos visando a quantificação dos elementos morfológicos do sistema fluvial e a análise multitemporal das mudanças do Rio Araguaia nas últimas décadas. Imagens dos sensores TM e OLI dos satélites Landsat 5 e 8 (Tabela 1), disponibilizadas gratuitamente pela USGS (<http://glovis.usgs.gov>), foram utilizadas para a definição das morfologias e o cálculo de suas áreas de superfície (km²). Tais imagens foram selecionadas levando em consideração a similaridade do nível d'água (129-160 cm) na estação Aruanã (Figura 1A) na data de sua aquisição durante o período de vazante (junho a outubro) para capturar, com o maior rigor possível, a exposição das morfologias fluviais relacionadas à carga de fundo (barras arenosas).

Tabela 1. Descrição das imagens de satélite selecionadas para o estudo.

Órbita	Ponto	Data de aquisição	Sensor	Resolução Espacial (m)	Nº de bandas espetrais
223	70	10/07/2001	TM	30	7
223	70	04/09/2004	TM	30	7
223	70	17/08/2009	TM	30	7
223	70	15/08/2014	OLI	30	9
223	70	25/07/2018	OLI	30	9

Após a calibração radiométrica dos dados (conversão para reflectância no topo da atmosfera), seguiu-se a derivação do Índice de Vegetação da Diferença Normalizada (NDVI) no software ENVI 5.3. A fim de automatizar o processo de identificação consistente das feições de canal, foram estabelecidos os seguintes intervalos no âmbito dos valores (-1 a +1) desse índice: máscara d'água (-1 a 0); barras arenosas (0 a 0,2) e; ilhas e planície aluvial (0,2 a 0,8). Regiões de interesse (ROI) das imagens foram determinadas segundo esses limiares dos pixels e convertidas em dados vetoriais (formato shapefile). Por meio da seleção automática do software ArcGIS 10.2.2 e de pequenas correções manuais, realizou-se a qualificação das morfologias em conformidade com as categorias definidas por Morais (2006). Esse autor apresentou em detalhes os valores dos parâmetros morfométricos utilizados por Latrubesse et al. (2009), permitindo o estabelecimento de uma análise comparativa entre os dados obtidos no presente estudo e aqueles referentes aos anos 1965, 1975 e 1998. Dessa forma, as barras arenosas foram classificadas considerando a sua posição no canal – barras laterais, centrais e acrescidas às ilhas e; as ilhas foram definidas com base em sua dimensão areal – ilhas pequenas ($0,01$ a $0,1 \text{ km}^2$), médias ($0,11$ a 1 km^2) e grandes ($1,1$ a 5 km^2) (Figura 2).

As alterações ocorridas no canal entre os anos 2001 e 2018 foram estimadas com a adoção dos procedimentos em SIG descritos por Jana (2019). A autora determinou as novas áreas de erosão e deposição do canal entre cenários subsequentes mediante: (i) a conversão dos referidos dados vetoriais em arquivos raster e; (ii) o cômputo das diferenças entre tais arquivos através do uso da Calculadora Raster do ArcGIS. Tais procedimentos também foram utilizados para avaliar as mudanças a curto prazo (2001-2018) que ocorreram na posição das margens do canal. As áreas das margens erodidas e construídas no cenário mais recente (2018) foram divididas pelo número de anos sob investigação para a definição de uma taxa anual de retrabalhamento das margens (m^2y^{-1}) (KIDOVÁ; LEHOTSKÝ; RUSNÁK, 2016), a qual foi obtida ao longo de 27 segmentos equidistantes (5 km) que abarcaram toda a extensão da área de estudo.

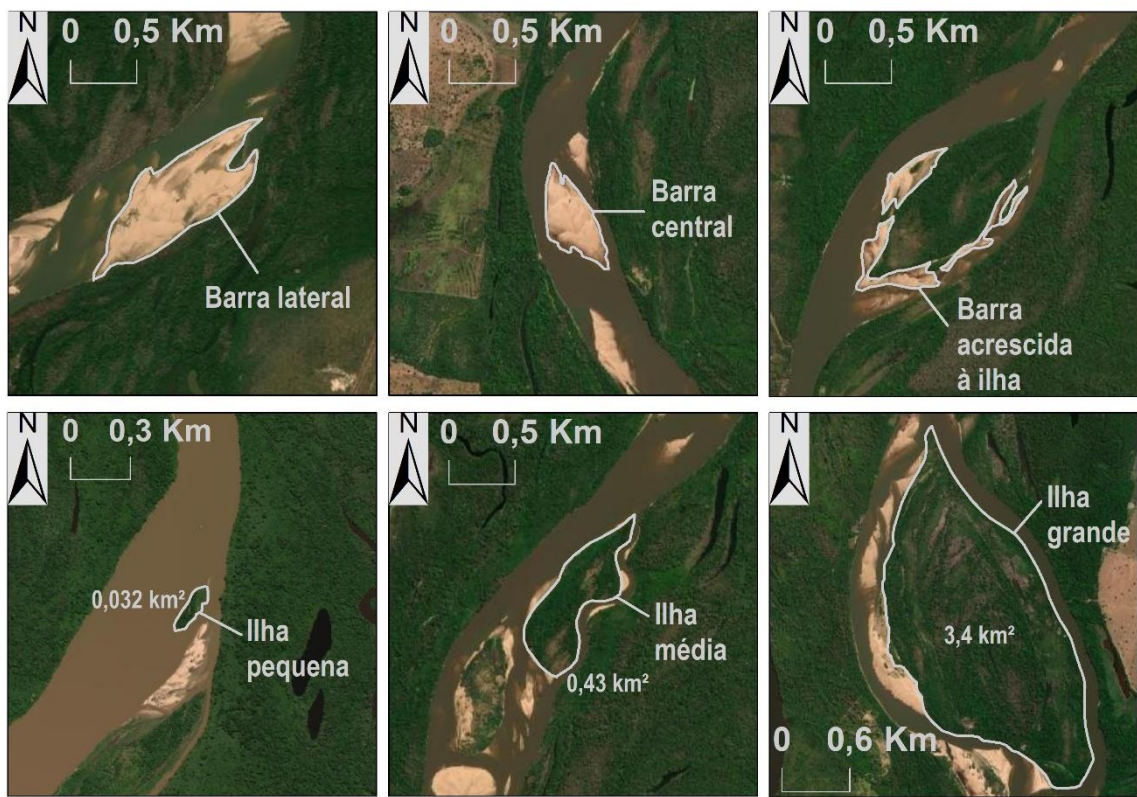


Figura 2. Exemplos das macroformas identificadas na área de estudo segundo as categorias definidas por Morais (2006). Imagens de fundo: Esri® World Imagery Map.

Os dados hidrológicos da estação fluviométrica Aruanã (#25200000) foram adquiridos no Portal HidroWeb (<http://www.snhirh.gov.br/hidroweb>) da Agência Nacional de Águas (ANA). As descargas médias diárias disponíveis para o período 1971-2018 foram avaliadas mensalmente na escala multi-decadal, visando identificar os grandes padrões de mudança dos fluxos nas estações seca e chuvosa.

2.1.4 Resultados

As barras arenosas são morfologias características do Rio Araguaia derivadas dos processos de erosão, transporte e deposição do material de fundo do canal. Ao longo dos 53 anos da série temporal, as barras do médio-curso superior do Rio Araguaia apresentaram, em geral, um aumento em número (Figura 3A). Porém, os distintos tipos de barras se comportaram de forma diferenciada.

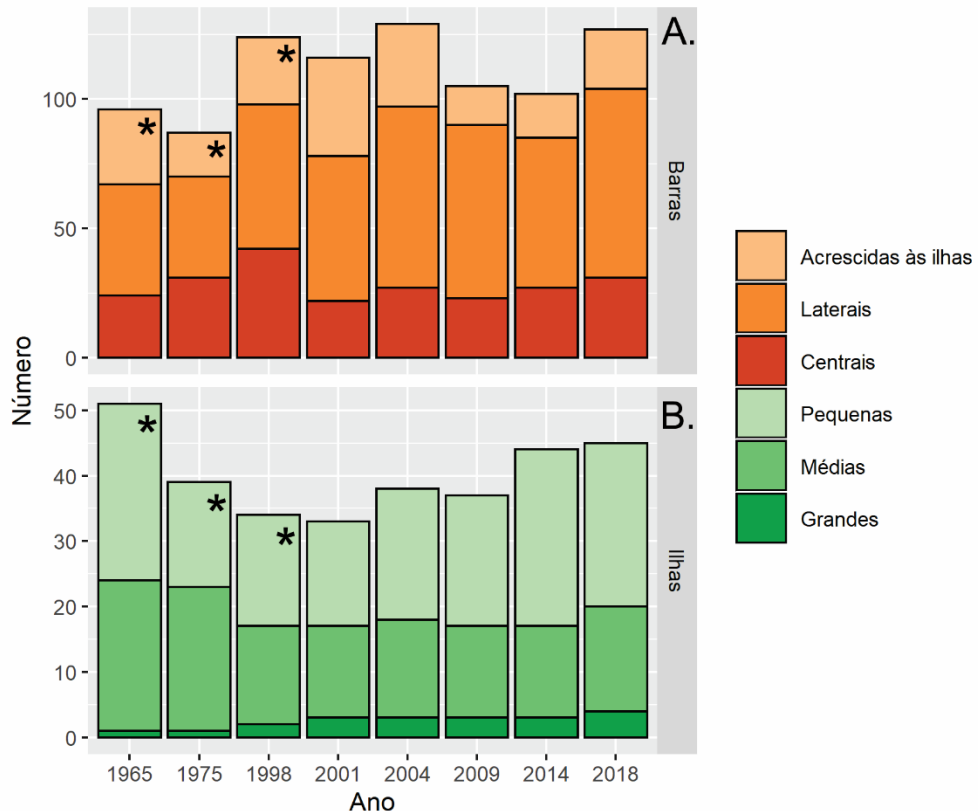


Figura 3. Mudanças no número de morfologias deposicionais ao longo do período 1965-2018. A. Barras. B. Ilhas. *Dados compilados de Morais (2006).

As barras centrais contabilizavam 24 em 1965 e 42 em 1998. A partir de 2001, elas reduziram em média 38%, totalizando 31 feições no ano de 2018. O número de barras laterais passou de 43 para 56 entre 1965 e 1998. Durante o período recente (2001-2018), essas barras apresentaram novo acréscimo, variando de 56 (2001) a 73 (2018). O número de barras acrescidas às ilhas aumentou 35% no período 2001-2004 em relação aos cenários do século XX. Os últimos anos (2009-2018) foram marcados por um decréscimo na quantidade dessas morfologias, atingindo um valor (23), em 2018, próximo daquele verificado (26) em 1998.

O ano de 1965 se destacou pela elevada ocorrência de ilhas (51), principalmente aquelas classificadas como pequenas (27) (Figura 3B). Todavia, nos cenários subsequentes – 1975 e 1998, houve uma redução considerável no número de feições dessa classe (-37%), acompanhada pela queda no número de ilhas de médio porte (-35%). As ilhas grandes se caracterizam por sua natureza relictiva e pela reduzida frequência neste setor do médio curso do Rio Araguaia. Em 1965 e 1975, havia apenas 1 ilha grande; em 1998, haviam 2 e; entre 2001 e 2014, elas eram 3.

O surgimento de uma ilha grande em 2018 foi decorrente da ampliação de morfologia classificada como média nos anos anteriores. O número de ilhas médias não apresentou grandes alterações desde 1998. Em 2001, elas somavam 14, em 2018, 16. A reduzida variação desses valores denota ao equilíbrio entre os processos de eliminação das ilhas médias no sistema, por meio de sua acreção à planície aluvial, e de constituição de novas ilhas nessa classe mediante a expansão e o amalgamento de ilhas de pequeno porte. Nos últimos anos, houve o incremento no número de ilhas pequenas, que alcançaram, em 2018, um número (25) similar ao constatado no cenário inicial de análise – 1965.

Entre 1975 e 1998, as barras passaram por uma fase de grande expansão (+71%) (Figura 4A), equivalente ao aumento de 7,88 km² em sua área total no canal (Tabela 2). No período 1998-2018, verificou-se uma tendência de redução (-19%) dessas morfologias. A taxa anual dos decréscimos em área correspondeu a 0,23 km², sendo as maiores perdas registradas nos intervalos 1998-2001 e 2004-2009 (Tabela 2). As barras acrescidas às ilhas apresentaram um aumento (+23%) entre 2001 e 2004, que foi sucedido por uma diminuição (-31%) no intervalo 2009-2018. A área das barras laterais (11,54 km²) e das barras centrais (3,71 km²) em 1998 reduziram 17% e 46%, respectivamente, entre 2001 e 2018 (Figura 4A).

A área correspondente às ilhas (Figura 4B) exibiu comportamento inverso ao descrito para as barras entre 1965 e 2018. No intervalo 1975-1998 houve a redução (-13%) da área ocupada por essas feições, que sofreram um decréscimo total de 1,6 km² (Tabela 2). O período mais recente (2001-2018) se caracterizou pela tendência de aumento da área insular no canal. Os anos que apresentaram acréscimos são prevalentes (Tabela 2), com uma taxa anual de expansão de 0,15 km². Destaca-se a ampliação da área das ilhas classificadas como pequenas e grandes (Figura 4B), as quais passaram de 5,52 km² e 0,56 km² em 2001 para 7 km² e 1,09 km² em 2018, respectivamente.

As mudanças na morfologia do sistema aluvial atual também foram evidenciadas pela quantificação das áreas de atuação dos processos erosivos e deposicionais entre os anos 2001 e 2018 (Figura 5). Assim como reportado por Latrubblesse et al. (2009), a erosão lateral ainda se constitui no principal mecanismo de erosão do canal, representando 81,4% da área total erodida no período 2001-2018, enquanto que a erosão de ilhas, e a erosão da planície pelo desenvolvimento lateral de ilhas e seus respectivos canais secundários corresponderam a 15,5% e 3,1%, respectivamente. Contudo, tais áreas, em seu conjunto, não superam o desenvolvimento da planície aluvial, o qual compreendeu 43,2% das áreas de deposição, seguido da formação ou ampliação de barras (23,5%), ilhas (23%) e do processo de acreção de ilhas à planície aluvial (10,2%).

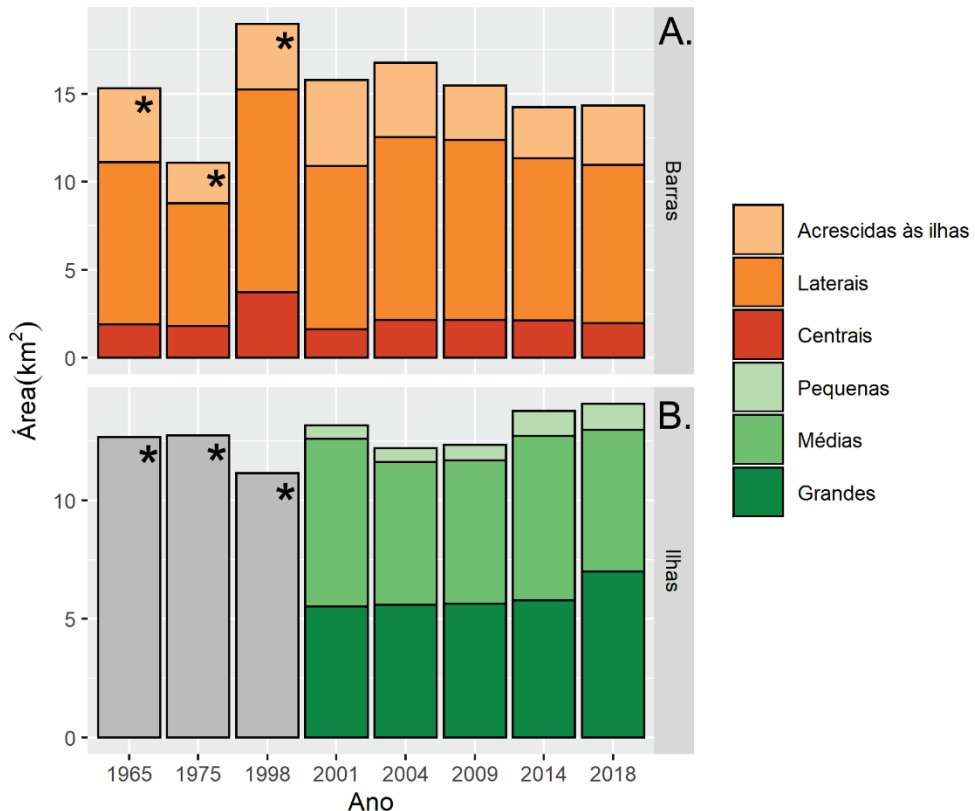


Figura 4. Mudanças na área total (km^2) de morfologias deposicionais ao longo do período 1965-2018. A. Barras. B. Ilhas. *Dados compilados de Morais (2006). As barras em cinza correspondem aos dados não discriminados pelo autor.

Tabela 2. Redução (-) ou aumento (+) em área total (km^2) das morfologias deposicionais entre os sucessivos anos.

Intervalo	Barras	Ilhas
1965 - 1975	-4,24	+0,08
1975 - 1998	+7,88	-1,60
1998 - 2001	-3,18	+2,02
2001 - 2004	+0,97	-0,97
2004 - 2009	-1,28	+0,15
2009 - 2014	-1,22	+1,41
2014 - 2018	+0,09	+0,31

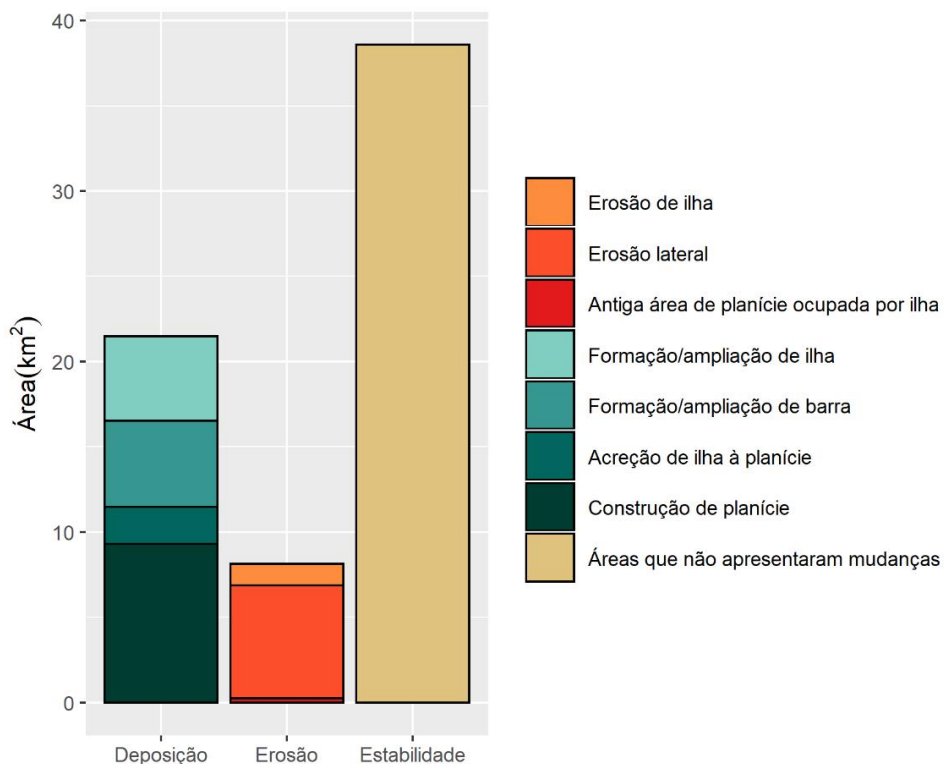


Figura 5. Áreas de deposição, erosão e estabilidade definidas entre 2001 e 2018.

A morfodinâmica mostrou-se bastante elevada nas duas margens da área de estudo entre 2001 e 2018 (Figura 6). A margem direita apresentou taxas anuais de erosão que, em seu conjunto ($310.228,61 \text{ m}^2\text{y}^{-1}$), superam as taxas de deposição ($249.931,31 \text{ m}^2\text{y}^{-1}$). Esse processo de retração da margem direita se torna evidente a partir do segmento 7. Em contrapartida, a margem esquerda se caracterizou pela construção e o avanço lateral. A somatória das taxas anuais de deposição ($422.865,82 \text{ m}^2\text{y}^{-1}$) ao longo da margem esquerda foi 4,5 vezes superior às taxas de erosão ($93.006,01 \text{ m}^2\text{y}^{-1}$). As amplas e novas áreas que se estabeleceram à margem direita dos segmentos 2, 6 e 20 e à margem esquerda dos segmentos 7 e 25 foram decorrentes do processo de acreção de ilhas de médio porte à planície aluvial. De modo geral, as margens na área de estudo não estão sendo construídas e erodidas a uma taxa equivalente. Dessa forma, verificou-se a redução da largura média do canal, que passou de 453,33 para 406,16 m entre 2001 e 2018.

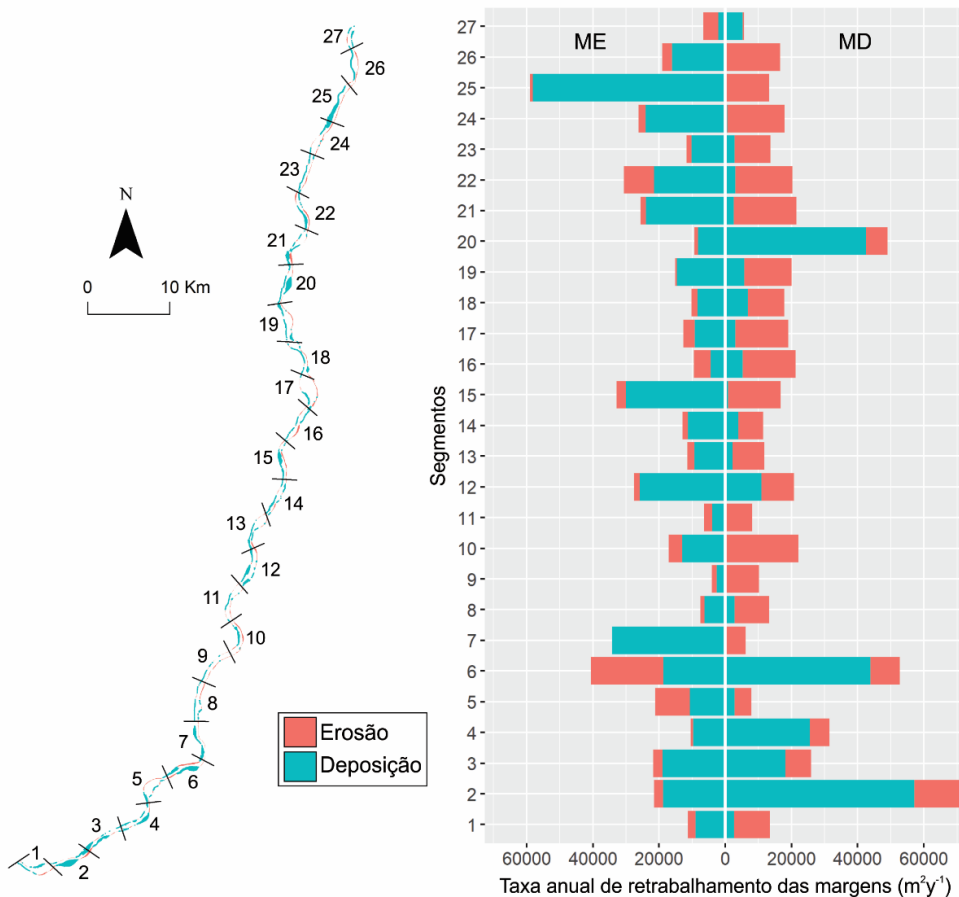


Figura 6. Variabilidade espacial das áreas de erosão e deposição resultantes da migração das margens esquerda (ME) e direta (MD) do canal entre 2001 e 2018. Valores obtidos para 27 segmentos de 5 km de extensão distribuídos ao longo da área de estudo.

Os dados de vazão observados na escala decadal para o período 1971-2018 (Figura 7) revelam o aumento de 21% nas descargas médias mensais do período de inundação (novembro a maio) entre as décadas de 1980 e 2000. Os últimos anos (2010-2018) foram caracterizados pelo decréscimo (-18%) dessas vazões de pico. Após o estágio de elevação (+29%) nos anos 1980, as descargas médias mensais registradas no período de estiagem (junho a setembro) também apresentaram uma redução progressiva que se estendeu até o último intervalo das mensurações. Ao lado disso, constataram-se alterações nos meses de pico do hidrograma. As vazões máximas, usualmente registradas em fevereiro, foram antecipadas em um mês na década de 1990, enquanto no último período houve um atraso em sua ocorrência, sendo identificadas no mês de março.

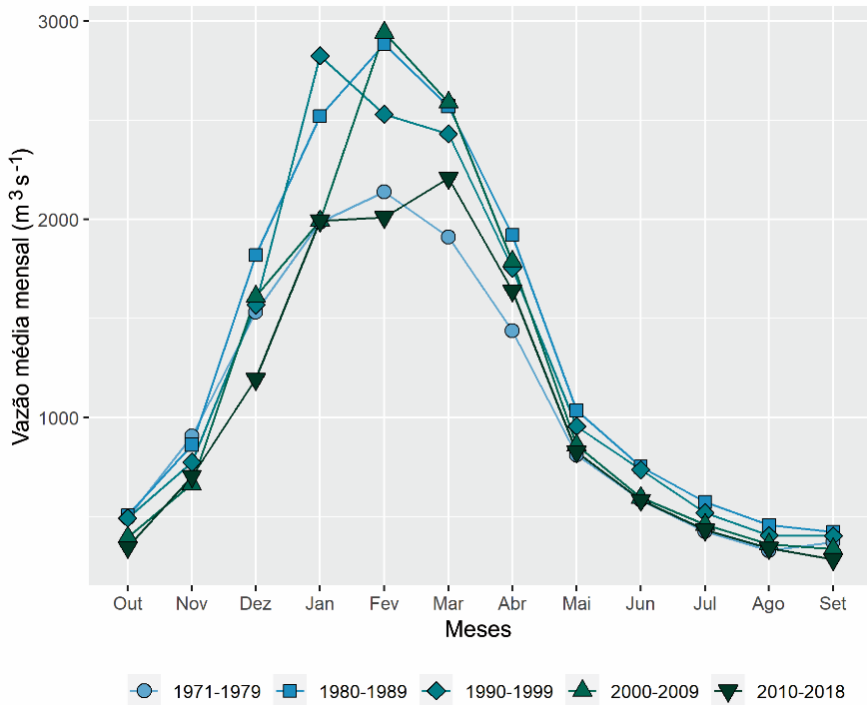


Figura 7. Vazão média mensal do Rio Araguaia na estação Aruanã (#25200000).

2.1.5 Discussão

Latrubblesse et al. (2009) identificaram profundas alterações na carga sedimentar e no padrão de canal do Rio Araguaia em resposta ao intenso desmatamento do Bioma Cerrado entre as décadas de 1970 e 1990. Ao longo desse período, cerca de 232 Mt de sedimentos foram armazenados no canal principal e nas porções proximais da planície aluvial. Ao lado disso, o transporte da carga de fundo aumentou 31% de 1970 (6,7 Mt) para 2000 (8,8 Mt). Como resultado, o rio alterou parcialmente o seu padrão anabanching, ampliando a tendência ao entrelaçamento por meio da: (i) sedimentação de canais secundários; (ii) eliminação de ilhas de menor porte; (iii) ampliação de barras laterais e; (iv) proliferação de barras centrais de caráter transiente.

No entanto, os resultados da análise de imagens de satélite datadas do período 2001-2018 revelam algumas alterações nos mecanismos de ajuste da morfologia do canal nos últimos anos. De modo condizente com o intervalo anterior de análise (1965-1998), as barras laterais ainda possuem grande representatividade no sistema em termos de quantidade (Figura 3A). Todavia, a redução de sua área total a partir de 2001 (Figura 4A) está relacionada à progressiva colonização da vegetação ripária sobre esses depósitos (Figura 8A), levando à conversão de amplas áreas do canal ativo em planície aluvial (Figura 5).

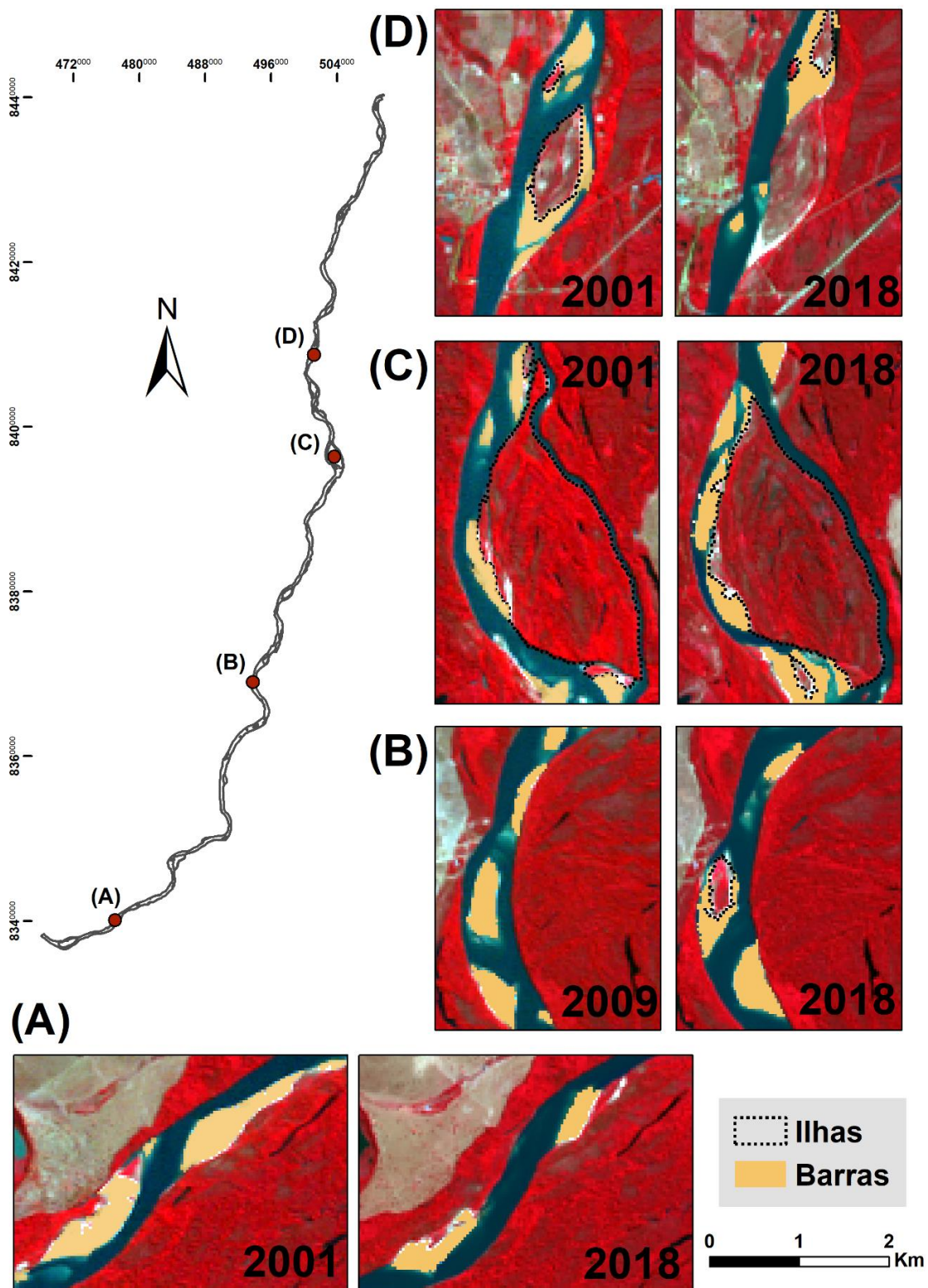


Figura 8. Imagens Landsat 5 e 8 ilustrando exemplos dos principais ajustes da morfologia do canal identificados entre 2001 e 2018. (A) Invasão progressiva da vegetação ripária sobre barras laterais; (B) Formação de ilha pela estabilização de barra central; (C) Expansão de ilha pela anexação de barras laterais e frontais; (D) Anexação de ilha à planície aluvial.

A vegetação ripária relacionada à colonização de ilhas e barras fluviais se enquadra na unidade de vegetação pioneira herbácea definida por Morais (2006). Essa associação vegetal sob influência direta da dinâmica hidrológica do Rio Araguaia caracteriza-se por apresentar plantas de pequeno porte espaçadas entre si, sendo os maiores representantes as gramíneas e ciperáceas, além de ervas (representantes herbáceos) como as amarantáceas, euforbiáceas e onagráceas (ARAÚJO, 2002).

Em relação às barras centrais, uma resposta distinta foi verificada para essas morfologias. Latrubesse et al. (2009) identificaram um crescimento em quantidade (+75%) e área (+95%) das barras centrais entre 1965 e 1998. Porém, houve uma queda nesses valores no período 2001-2018 (Figuras 3A e 4A). O decréscimo das barras centrais ocorreu de forma concomitante ao aumento do número de ilhas, principalmente daquelas de pequeno porte (Figura 3B). Dessa forma, admite-se que tais mudanças estão vinculadas à ampliação da estabilidade geomórfica dessas barras sedimentares, viabilizando o estabelecimento da vegetação pioneira herbácea sobre essas feições (Figura 8B).

A presença de núcleos mais estáveis promove alterações nos padrões de fluxo do canal, culminando na formação de barras que se acrescem lateralmente às ilhas (LATRUBESSE; FRANZINELLI, 2002; LELI; STEVAUX; ASSINE, 2020). Em conjunto com os processos de agradação vertical (LATRUBESSE et al., 2009), tais barras favoreceram a expansão da área das ilhas nos últimos anos (Figura 4B) mediante a colonização da vegetação pioneira herbácea sobre esses depósitos arenosos (Figura 8C).

É importante evidenciar que o desenvolvimento dessas barras no interior de canais subordinados auxilia na aceleração de seu preenchimento e abandono, ocasionando a anexação de ilhas à planície aluvial (Figuras 5 e 8D). A vinculação de amplas barras ao assoreamento de canais secundários, principalmente a partir de 2009, corrobora o decréscimo dessas morfologias nos últimos cenários (Figuras 3A e 4A).

O referido processo de anexação de ilhas (Figura 8D) promove a retenção de amplos depósitos de canal na planície aluvial em ambas as margens (Figura 6) e, juntamente com a expansão da vegetação ripária sobre as barras laterais (Figura 8A), produzem taxas de construção das margens superiores às taxas de erosão (Figura 6). Como resultado, verifica-se uma tendência atual de decréscimo da área da zona ativa do rio.

Um dos controles primários do regime de transporte sedimentar e das características dos depósitos aluviais é o regime de fluxo do rio. Coe et al. (2011) realizaram uma análise dos aspectos hidrológicos da Bacia do Rio Araguaia a montante da área de estudo. Os autores constataram um aumento de 25% na vazão do rio na estação Aruanã (Figura 1A) entre as

décadas de 1970 e 1990, sendo que 2/3 da mudança hidrológica foram atribuídos às mudanças no uso e cobertura da terra na bacia hidrográfica e não às mudanças climáticas, já que as alterações na precipitação foram de apenas 2,5% no mesmo período. Dessa forma, além do impacto direto do desmatamento como fonte de erosão e transporte de sedimentos no sistema, as respostas na morfologia do canal identificadas por Latrubesse et al. (2009) estariam também relacionadas às modificações hidrológicas na bacia hidrográfica derivadas das ações antrópicas.

Os picos de desmatamento na Bacia do Rio Araguaia no final do século passado eram duas vezes maiores que a média (380.000 ha) das taxas registradas a partir de 2000 (Figura 9). Apesar dessa redução, dados do período 2013-2017 revelam uma ampla conversão (51,2%) do Bioma Cerrado em áreas antropizadas na bacia hidrográfica (LATRUBESSE et al., 2019).

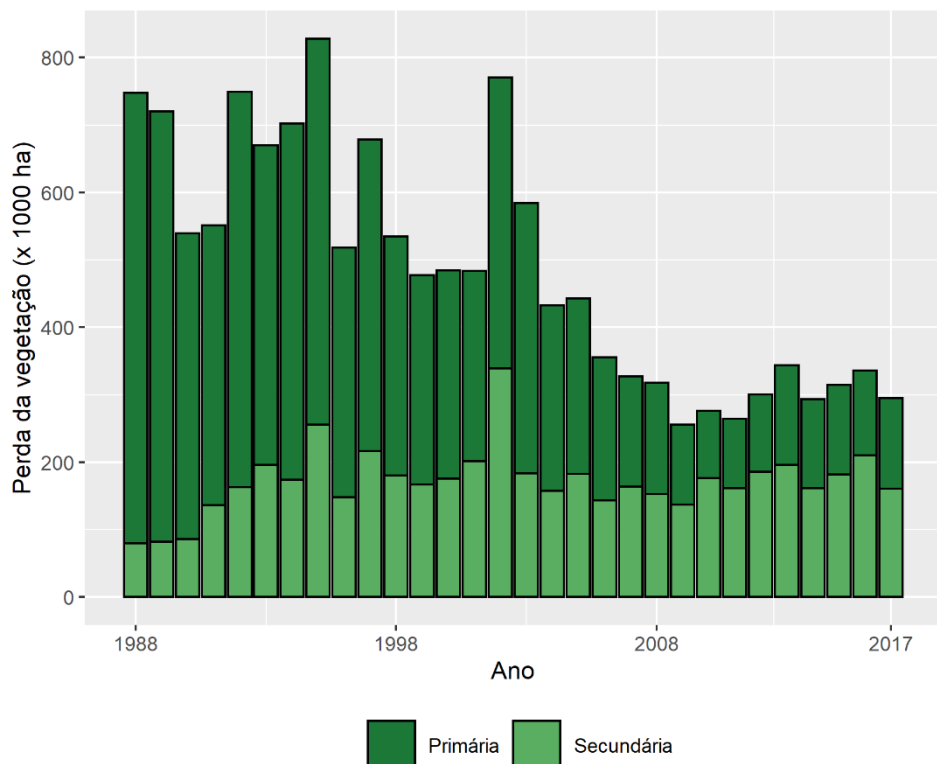


Figura 9. Taxas de desmatamento na Bacia do Rio Araguaia ao longo do período 1988-2017.
Adaptado de MapBiomas (2020).

Diante da manutenção do quadro de transformações no uso e cobertura da terra a partir dos anos 2000, verifica-se a possibilidade de intensificação dos efeitos hidrológicos do desmatamento sobre a vazão do rio descritos por Coe et al. (2011). Lininger e Latrubesse (2016) avaliaram a atenuação dos picos de vazão (sua redução absoluta conforme se movem a jusante) derivada dos mecanismos de transmissão das inundações para a planície aluvial do médio-curso

superior do Rio Araguaia. Os autores não encontraram tendências discerníveis nos padrões de atenuação dos picos que demonstram sua relação com as elevadas taxas de desmatamento na bacia hidrográfica. Não obstante, Lininger e Latrubesse (2016) verificaram a maior probabilidade de ocorrência de vazões mínimas superiores à média após os anos marcados pela atenuação do pico de vazão durante a série histórica 1975-2011. Assim, a água armazenada na planície de inundação durante a estação chuvosa seria gradualmente liberada ao longo da estação seca, aumentando os fluxos de base.

Costa, Botta e Cardille (2003) avaliaram os dados de vazão e precipitação no alto curso da Bacia do Rio Tocantins (adjacente à área de estudo) no período 1949-1998. Assim como Coe et al. (2011), esses autores atribuíram o aumento (+24%) na vazão média anual do rio à expansão das áreas destinadas à agricultura na bacia hidrográfica, pois as mudanças na precipitação não foram estatisticamente significantes. Costa, Botta e Cardille (2003) ainda constataram que os impactos do desmatamento sobre a vazão são evidentes, especialmente, na estação chuvosa, com o incremento de 28% das descargas médias mensais e a antecipação em um mês no pico de vazão sazonal.

Assim como no Alto Tocantins, na área estudo verificou-se o aumento (+21%) das descargas médias mensais na estação chuvosa entre as décadas de 1980 e 2000 e a antecipação em um mês no pico do hidrograma na década de 1990 (Figura 7). Essas alterações condizentes com o decréscimo das taxas de infiltração e o aumento do escoamento superficial em áreas desmatadas (BRUIJNZEEL, 1990) teriam favorecido a erosão das ilhas de pequeno porte (Figura 3B) e o estabelecimento das barras arenosas (Figura 3A), que são formas de maior instabilidade em resposta à evolução do leito nos períodos de inundação.

Todavia, as variações no tempo e na amplitude das vazões nas últimas duas décadas (Figura 7) denotam importantes alterações no regime hidrológico do Rio Araguaia, as quais são condizentes com os ajustes morfológicos observados entre 2001 e 2018. Em um sistema caracterizado pelo elevado suprimento da carga de fundo, a redução da magnitude das inundações e dos fluxos mais baixos na estação seca (Figura 7) auxiliaram na intensificação dos processos agradacionais (Figura 5), na estabilização das formas deposicionais (Figura 8B) e na progressão da vegetação ripária dentro do corredor fluvial (Figura 8A e C).

É válido ressaltar que em grandes rios, os processos responsáveis pelas principais mudanças na morfologia do canal estão relacionados à areia transportada como carga de fundo e em suspensão (LATRUBESSE, 2008). Nesse contexto, pesquisas (AMSLER; RAMONELL; TONILO, 2005; AQUINO, 2007; BIEDENHARN; THORNE, 1994; LATRUBESSE, 2008; THORNE; RUSSEL; ALAM, 1993) revelaram a importância da descarga que maximiza o

transporte da granulometria dominante, denominada vazão efetiva (Q_{ef}), no controle da morfologia dos grandes sistemas fluviais.

Aquino (2007) avaliou as mudanças na vazão efetiva do médio-curso superior do Rio Araguaia ao longo do período 1971-2000. A autora verificou um incremento de 65% no valor dessa vazão entre as décadas de 1970 ($Q_{ef} = 1775 \text{ m}^3/\text{s}$) e 1990 ($Q_{ef} = 2954 \text{ m}^3/\text{s}$), cujo resultado foi o aumento do transporte da carga de fundo e a consequente ampliação da tendência ao entrelaçamento do rio identificados por Latrubesse et al. (2009).

Ao considerar que a variabilidade climática e as mudanças no regime de vazões são as forças motoras dos ajustes que ocorrem na vazão efetiva (AMSLER; RAMONELL; TONILOLO, 2005), as futuras pesquisas devem ter como enfoque o reconhecimento: (i) do papel desses dois grandes controles na configuração da vazão efetiva do Rio Araguaia nas últimas duas décadas e; (ii) das possíveis flutuações recentes dessa vazão e a sua relação com os processos erosivos e deposicionais que culminaram nos ajustes morfológicos do sistema canal-planície aluvial identificados no presente estudo.

2.1.6 Conclusões

As mudanças na morfologia bidimensional do médio-curso superior do Rio Araguaia foram avaliadas durante o período 2001-2018, ampliando para 53 anos a série temporal dos dados sobre a evolução das macroformas desse rio apresentados por Latrubesse et al. (2009). A tendência à agradação do sistema fluvial reportada para os cenários do final do século XX ainda persiste no período atual.

Entre 1965 e 1998, o rio alterou parcialmente o seu padrão *anabranching*, ampliando a tendência ao entrelaçamento por meio da: (i) sedimentação de canais secundários; (ii) eliminação de ilhas de menor porte; (iii) ampliação de barras laterais e; (iv) proliferação de barras centrais de caráter transiente. Todavia, entre 2001 e 2018, foram identificados os seguintes novos mecanismos de ajuste do canal: (i) redução da área total das barras laterais; (ii) decréscimo em número e área total das barras centrais; (iii) aumento em número e área das ilhas pequenas e grandes e; (iv) incremento das barras acrescidas às ilhas.

A atual fase transicional do Rio Araguaia de contração da zona ativa do canal e perda parcial das características de entrelaçamento devido à ampliação da representatividade das ilhas está possivelmente vinculada às alterações no regime hidrossedimentar desse rio nas últimas duas décadas.

O Rio Araguaia é o último grande rio do Cerrado livre de grandes intervenções antrópicas diretas. Diante das ameaças ambientais iminentes às suas funcionalidades hidrogeomorfológica e ecológica, como o avanço da fronteira agrícola e as propostas de construção de quatro grandes barragens ao longo de seu curso, os resultados desta investigação sobre o atual estado de ajuste do sistema canal-planície aluvial deverão ser considerados nos planos de manejo do Rio Araguaia.

Financiamento: Esta pesquisa foi financiada pela Coordenação de Aperfeiçoamento de Pessoal de Nível Superior – Brasil (CAPES) - Código de Financiamento 001.

Agradecimentos: Os autores agradecem os revisores e o editor pelas contribuições que ampliaram a qualidade do manuscrito.

Referências

- AMSLER, M. L.; RAMONELL, C. G.; TONILO, H. A. Morphologic changes in the Paraná River channel (Argentina) in the light of the climate variability during the 20th century. **Geomorphology**, v. 70, n. 3, p. 257-278, 2005. DOI: 10.1016/j.geomorph.2005.02.008.
- AQUINO, S. Mecanismos de Transmissão de Fluxos de Água e Sedimentos em dois Grandes Rios Aluviais Impactados pela Atividade Humana: o Araguaia e o Paraná. Tese (Doutorado em Ciências Ambientais) - Programa de Pós-Graduação em Ecologia de Ambientes Aquáticos Continentais, Universidade Estadual de Maringá, Maringá. 2007. 142p.
- AQUINO, S.; LATRUBESSE, E. M.; BAYER, M. Assessment of wash load transport in the Araguaia River (Aruanã gauge station), central Brazil. **Latin American Journal of Sedimentology and Basin Analysis**, v. 16, n. 2, p. 119–128, 2009.
- AQUINO, S.; STEVAUX, J. C.; LATRUBESSE, E. M. Regime Hidrológico E Aspectos Do Comportamento Morfohidráulico Do Rio Araguaia. **Revista Brasileira de Geomorfologia**, v. 6, n. 2, p. 29–41, 2005. DOI: 10.20502/rbg.v6i2.49.
- ARAÚJO, F. R. **Controles abióticos da vegetação na planície aluvial do rio Araguaia**. Dissertação (Mestrado em Geografia) – Programa de Pós-Graduação em Geografia, Universidade Federal de Goiás, Goiânia. 2002.
- BAYER, M. **Diagnóstico dos processos de erosão/assoreamento na planície aluvial do rio Araguaia: entre Barra do Garças e Cocalinho**. Dissertação (Mestrado em Geografia) – Programa de Pós-Graduação em Geografia, Universidade Federal de Goiás, Goiânia. 2002. 138p.
- BAYER, M. **Dinâmica do transporte, composição e estratigrafia dos sedimentos da planície aluvial do Rio Araguaia**. Tese (Doutorado em Ciências Ambientais) – Programa de Pós-Graduação em Ciências Ambientais, Universidade Federal de Goiás, Goiânia. 2010. 98p.

BIEDENHARN, D. S.; THORNE, C. R. Magnitude-frequency analysis of sediment transport in the lower Mississippi river. **Regul. Rivers: Res. Mgmt.**, v. 9, n. 4, p. 237–251, 1994. DOI: <https://doi.org/10.1002/rrr.3450090405>.

BRANNSTROM, C.; JEPSON, W.; FILIPPI, A. M.; REDO, D.; XU, Z.; GANESH, S. Land change in the Brazilian Savanna (Cerrado), 1986-2002: Comparative analysis and implications for land-use policy. **Land Use Policy**, v. 25, n. 4, p. 579–595, 2008. DOI: 10.1016/j.landusepol.2007.11.008.

BRUIJNZEEL, L. A. **Hydrology of moist tropical forests and effects of conversion: a state of knowledge review**. UNESCO, Paris. 1990. 224p.

COE, M. T.; LATRUBESSE, E. M.; FERREIRA, M. E.; AMSLER, M. L. The effects of deforestation and climate variability on the streamflow of the Araguaia River, Brazil. **Biogeochemistry**, v. 105, n. 1, p. 119–131, 2011. DOI: 10.1007/s10533-011-9582-2.

COLLI, G. R.; VIEIRA, C. R.; DIANESE, J. C. Biodiversity and conservation of the Cerrado: recent advances and old challenges. **Biodiversity and Conservation**, v. 29, n. 5, p. 1465–1475, 2020. DOI: 10.1007/s10531-020-01967-x.

COSTA, M. H.; BOTTA, A; CARDILLE, J. A. Effects of large-scale changes in land cover on the discharge of the Tocantins River, Southeastern Amazonia. **Journal of Hydrology**, v. 283, n. 1, p. 206–217, 2003. DOI: 10.1016/S0022-1694(03)00267-1.

DUBREUIL, V.; FANTE, K. P.; PLANCHON, O.; SANT'ANNA NETO, J. L. Les types de climats annuels au Brésil: une application de la classification de Köppen de 1961 à 2015. **EchoGéo**, v. 41, p. 0–27, 2017. DOI: 10.4000/echogeo.15017.

FERREIRA, M. E.; FERREIRA JR, L. G.; LATRUBESSE, E. M.; MIZIARA, F. Considerations about the land use and conversion trends in the savanna environments of Central Brazil under a geomorphological perspective. **Journal of Land Use Science**, v. 11, n. 1, p. 33–47, 2013. DOI: 10.1080/1747423X.2013.845613.

FURLEY, P. A. The nature and diversity of neotropical savanna vegetation with particular reference to the Brazilian cerrados. **Global Ecology and Biogeography**, v. 8, n. 3-4, p. 223–241, 1999. DOI: 10.1046/j.1365-2699.1999.00142.x.

JANA, L. S. X. **The planform dynamics of the Irrawaddy River, Myanmar between 1990 and 2010**. Trabalho de Conclusão de Curso (Bachelor of Science with Honours in Environmental Earth Systems Science) – Nanyang Technological University, Singapore. 2019. 56p.

KIDOVÁ, A.; LEHOTSKÝ, M.; RUSNÁK, M. Geomorphic diversity in the braided-wandering Belá River, Slovak Carpathians, as a response to flood variability and environmental changes. **Geomorphology**, v. 272, p. 137–149, 2016. DOI: 10.1016/j.geomorph.2016.01.002

LAPOLA, D. M.; MARTINELLI, L. A.; PERES, C. A.; OMETTO, J. P. H. B; FERREIRA, M. E.; NOBRE, C. A.; AGUIAR, A. P. D.; BUSTAMANTE, M. M. C.; CARDOSO, M. F.; COSTA, M. H.; JOLY, C. A.; LEITE, C. C.; MOUTINHO, P.; SAMPAIO, G.;

STRASSBURG, B. B. N.; VIEIRA, I. C. G. Pervasive transition of the Brazilian land-use system. **Nature Climate Change**, v. 4, n. 1, p. 27–35, 2014. DOI: 10.1038/nclimate2056.

LATRUBESSE, E. M. Patterns of anabranching channels: The ultimate end-member adjustment of mega rivers. **Geomorphology**, v. 101, n. 1-2, p. 130–145, 2008. DOI: 10.1016/j.geomorph.2008.05.035.

LATRUBESSE, E. M.; AMSLER, M. L.; MORAIS, R. P. DE; AQUINO, S. The geomorphologic response of a large pristine alluvial river to tremendous deforestation in the South American tropics: The case of the Araguaia River". **Geomorphology**, v. 113, n. 3-4, p. 239–252, 2009. DOI: 10.1016/j.geomorph.2009.03.014.

LATRUBESSE, E. M.; ARIMA, E.; FERREIRA, M. E.; NOGUEIRA, S. H.; WITTMANN, F.; DIAS, M. S.; DAGOSTA, F. C. P.; BAYER, M. Fostering water resource governance and conservation in the Brazilian Cerrado biome. **Conservation Science and Practice**, v. 1, n. 9, p. 1–8, 2019. DOI: 10.1111/csp2.77.

LATRUBESSE, E. M.; FRANZINELLI, E. The Holocene alluvial plain of the middle Amazon River, Brazil. **Geomorphology**, v. 44, n. 3-4, p. 241–257, 2002. DOI: 10.1016/S0169-555X(01)00177-5.

LELI, I. T.; STEVAUX, J. C.; ASSINE, M. L. Origin, evolution, and sedimentary records of islands in large anabranching tropical rivers: The case of the Upper Paraná River, Brazil. **Geomorphology**, v. 358, 2020. DOI: 10.1016/j.geomorph.2020.107118.

LENTHALL, J. C.; BRIDGEWATER, S.; FURLEY, P. A. A phytogeographic analysis of the woody elements of New World savannas. **Edinburgh Journal of Botany**, v. 56, n. 2, p. 293–305, 1999. DOI: 10.1017/s0960428600001153.

LININGER, K. B.; LATRUBESSE, E. M. Flooding hydrology and peak discharge attenuation along the middle Araguaia River in central Brazil. **Catena**, v. 143, p. 90–101, 2016. DOI: 10.1016/j.catena.2016.03.043.

MORAIS, R. P. **A Planície Aluvial do Médio Araguaia: processos geomorfológicos e suas Implicações Ambientais**. Tese (Doutorado em Ciências Ambientais) – Programa de Pós-Graduação em Ciências Ambientais, Universidade Federal de Goiás, Goiânia. 2006. **Projeto MapBiomass** – Coleção 5.0 da Série Anual de Mapas de Cobertura e Uso de Solo do Brasil. Disponível em: <<https://plataforma.mapbiomas.org>>. Acesso em: 19 nov. 2020.

THORNE, C.R.; RUSSEL, A.; ALAM, K. Planform pattern and channel evolution of the Brahmaputra River, Bangladesh. In: BEST, J.L.; BRISTOW, C.S. (Eds.). **Braided Rivers**. London, UK: Geological Society Special Publication, v. 75, 1993, p. 257–276.

VALENTE, C. R.; LATRUBESSE, E. M. Fluvial archive of peculiar avulsive fluvial patterns in the largest Quaternary intracratonic basin of tropical South America: The Bananal Basin, Central-Brazil. **Palaeogeography, Palaeoclimatology, Palaeoecology**, v. 356-357, p. 62–74, 2012. DOI: 10.1016/j.palaeo.2011.10.002.

2.2 Artigo 2 – Geomorphic diversity of the middle Araguaia River, Brazil: a segment-scale classification to support river management²

Abstract

The complex mosaic of geomorphic units that characterizes the fluvial corridor of large rivers poses challenges to effectively describe and discriminate the landforms diversity, and its relationships with the hydrosedimentological dynamics and state of the system. Consequently, the classification of the diverse array of fluvial features into discrete segments can be a systematic and organized approach useful to sustain geomorphically-informed management strategies. Here we propose a methodological approach and characterize the geomorphic diversity of the middle Araguaia River by applying a classification of reaches into segments with a certain consistent level of morphological variability. A GIS framework developed for this purpose relied on the survey, analysis, and statistical treatment of morphological variables derived from remote sensing data. It allowed to differentiate 19 distinct reaches (R1-R19) that were further clustered into five major segments (SI-SV). We investigated the first-order controls of the fluvial style in each of the identified segments and found that changes in valley gradient influence in a major way the segments I, III, and IV, while the entrance of important tributaries and the nature of the valley floor are natural governing factors in segments II and V, respectively. The system exhibits a significant morphological diversity among segments, and it is strongly influenced by the late Holocene avulsion history of the river. Given the increasing pressure of human activities on the hydrological system, the present study can be of use to subsidize sustainable management plans aiming to safeguard the last large free-flowing river of the Cerrado biome, and our methodological proposal is valid for use in other large rivers worldwide.

Keywords: fluvial geomorphology, large rivers, river segmentation, river management.

2.2.1 Introduction

The spatial flows of energy, materials, and organisms that characterizes the three dimensions (longitudinal, lateral, and vertical) of the riverine landscape can be affected by

²Artigo publicado: SUIZU, T. M.; LATRUBESSE, E. M.; BAYER, M. Geomorphic diversity of the middle Araguaia River, Brazil: A segment-scale classification to support river management. **Journal of South American Earth Sciences**, vol. 121, 2023. <https://doi.org/10.1016/j.jsames.2022.104166>.

intricate paths and mechanisms of flow transferences that not only depend on the hydrological regime but on the channels pattern's types and the complex morphology and evolutive history (time as the fourth dimension) of the floodplains mosaic (Latrubblesse and Suizu, 2022; Petts and Amoros, 1996).

This applies particularly in the case of large axial rivers, where the fluvial corridor is subordinate to the basement rocks and tectonic settings of the valley they transcend (Latrubblesse, 2015; Potter, 1978), the climate-driven changes in discharge regimes under which modern and ancient fluvial forms were adjusted (Blum, 2008; Gautier et al., 2021), are still in the process of adjustment through recent geological times (Latrubblesse and Stevaux, 2015; Valente and Latrubblesse, 2012) and, even over the last century because of the long-standing effects of human impacts (Best, 2019; Latrubblesse and Sinha, 2022). As a result, trans-continent sized rivers display marked changes in main-channel, branch, and floodplain styles due to alongstream variations in sediment feeds, bed sediment transfers, and lateral sediment exchanges (Ashworth and Lewin, 2012; Park and Latrubblesse, 2019).

In the face of such complexities, an important step in the study of large alluvial systems is the geomorphic classification of the river into spatially distinct segments. Reach classification frameworks have been traditionally proposed in river science. They can synthesize stream morphologies and processes of specific geomorphic settings (Montgomery and Buffington, 1997) or can intend to be universal by the stratification of rivers into comparable groups using numerically bounded physical metrics (Rosgen, 1994). Reach types can be defined by procedural trees of identification that range from valley setting scale to the bed material texture (Fryirs and Brierley, 2018), and they can also incorporate information about human pressure responses and trajectories of changes in the system (Gurnell et al., 2016). However, despite the reliability and robustness of many available conceptual frameworks for reach classification, they usually constitute hierarchical procedures developed for small to medium-sized river basins. Thus, their taxonomy approach may not be adequate to capture the complexity and the large-scale features of the domains that characterize large axial rivers.

The segmentation of large rivers is a powerful tool for basic and applied research. The subdivision of the river into more manageable study reaches is a systematic and organized approach in strategic and project-related investigations for river management and engineering (Thorne, 2002).

In his framework for geomorphic studies of large rivers, Thorne (2002) presented a reach-scale geomorphic classification of the Paraná–Paraguay system in Argentina based on the criteria of channel stability and human modification, as part of a wider study of flood

defense issues. Classification schemes have been also developed, for example, to assess the changes in channel morphology variables over spatial and temporal scales (Orlowski et al., 1995; Schumm et al., 1994), to verify the distribution and types of bed morphologies in distinct geomorphic zones (Knox and Latrubesse, 2016), to understand the control of different fluvial styles over the hydrology of the river system (Stevaux et al., 2020), and to estimate the reach-wise sediment volume accumulated in the channel belt (Sinha et al., 2022).

Nowadays, complex and habitat-rich ecosystems of large tropical rivers have been threatened by the strongly increasing trend of land-use changes, damming, water extraction, and other unsustainable practices that significantly impact and modify the hydrogeomorphology, sedimentology, and connectivity structures of these systems (Latrubesse and Sinha, 2022; Wittmann et al., 2022). Furthermore, when compared to boreal and temperate regions, the tropics still preserve several of the most fascinating and pristine rivers of the world and offer to geomorphologists a unique opportunity to investigate its natural, self-adjusting processes and the associated range of forms.

The Araguaia River in the central highlands of Brazil is an example of a large tropical free-flowing river that harbors a significant proportion of freshwater biodiversity at the Cerrado-Amazonia ecotone (Latrubesse et al., 2019). Since the end of the last century, the middle section of the river is showing a marked tendency to aggrade and rapid changes in the channel pattern in response to the extensive deforestation and accelerated soil erosion in the drainage basin (Latrubesse et al., 2009). Additionally, the hydropower potential of the Araguaia basin is being planned for exploitation, as 70 dams have already been proposed, including four large ones on the mainstem (Latrubesse et al., 2019).

The increasing pressure of human activities on the hydrological system mandates conservation efforts of the alluvial plains of the Araguaia. A comprehensive geomorphic study of this river by ordering the array of fluvial features into discrete segments can be a fundamental component of integrated and sustainable management plans aiming to safeguard the last and most important unregulated river of the Cerrado biome.

The first general description of the Araguaia River was made by Latrubesse and Stevaux (2002). Based on detailed investigations and fieldworks, these authors subdivided the system into three main landscape units designated upper, middle, and lower Araguaia, with the channel relatively fixed on bedrock in the upper and lower units and the middle section displaying a well-developed and active alluvial belt. After that, a 570-km length reach of the middle Araguaia was also geomorphologically compartmented by Latrubesse et al (2009) to assess a sedimentary budget and morphological changes during the latter part of the twentieth century.

The results reported in our study provide an extension of those previous subdivisions. By developing and applying a new proposed method, we focus on a more systematic approach to characterize the internal geomorphic variability of the middle Araguaia River valley which improve the segmentation. The method characterizes the geodiversity of the middle Araguaia River based on a river classification into geomorphically distinct segments. Thus, the specific aims of this study are: (i) to derive reach units of the river and assess their longitudinal trends by channel and floodplain metrics; (ii) to conduct a cluster analysis to objectively group river reaches of relatively uniform morphological attributes into major segments; and (iii) to identify the main controlling factors of the fluvial style in each of the segment classes.

2.2.2 Study Area

The Tocantins-Araguaia basin, situated in the tropical South America, stands out due to its large drainage area ($767,000 \text{ km}^2$) (Latrubesse and Stevaux, 2002; Pelicice et al., 2021). The basin formed by two similar-sized rivers with similar drainage basins (Tocantins and Araguaia) spreads on two important and large biomes of South America: the Amazon rainforest to the north and the Brazilian savanna (Cerrado) to the south (Latrubesse and Stevaux, 2002; Latrubesse et al., 2019). The Araguaia basin (Figure 1A) covers an area of $\sim 385,000 \text{ km}^2$. The middle section of the mainstem extends from Registro do Araguaia to Conceição do Araguaia, is characterized by a well-developed alluvial plain (Figure 1B) and runs mainly through the lowlands of the Bananal Plain, an intracratonic Quaternary sedimentary basin characterized by the development of a vast aggradational plain Pleistocene formed by a mega-scale anabranching pattern, where a remarkable geomorphic feature is the huge Bananal Island (Figure 1A) (Valente and Latrubesse, 2012). From a geological perspective, the Bananal Plain relates to the Araguaia Formation, a fluvial sequence of clay, silt, and sand conglomeratic sediments of Pleistocene age, although local outcrops of older rocks rise as hills or small ranges (Valente and Latrubesse, 2012).

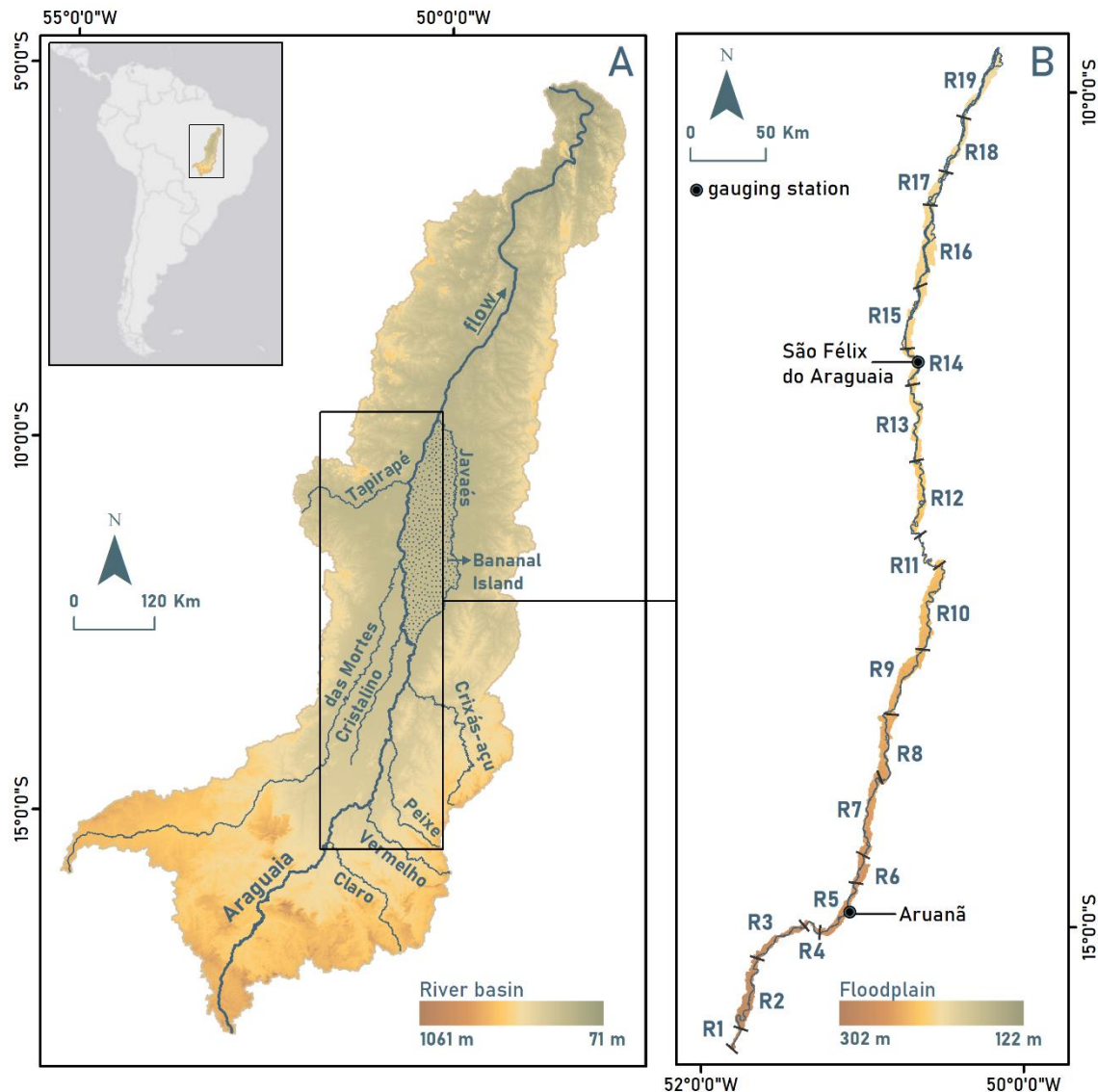


Figure 1. A. Location of the Araguaia basin, mainstream and major tributaries. B. Reaches (R1-R19) of the Middle Araguaia River and floodplain identified in the present study.

The middle Araguaia alluvial plain is incised in the Bananal Plain and consists of a mosaic of younger late Quaternary morpho-sedimentary units, controlled by geological structures in a N-S direction and secondary ENE-WSW and NNW-SSE trends (Latrubblesse and Stevaux, 2002). The modern river displays a variety of anabranching patterns with a tendency to braid that alternates with some sinuous reaches (Latrubblesse, 2008; Suizu et al., 2022).

The entry of significant tributaries in the middle Araguaia River (Figure 1A) increases the drainage area from 36,400 to ~320,290 km² (Latrubblesse and Stevaux, 2002). The Mortes, Javaés, Cristalino and Tapiapé rivers area classified as tributaries draining predominantly the Bananal Plain, while eastern tributaries (Claro, Vermelho, Peixe and Crixás-açu rivers) drain

mainly Precambrian metamorphic and igneous rocks and have their headwaters among structurally controlled hills (Aquino et al., 2009b).

Two gauging stations from Brazil's National Water Agency (Agência Nacional de Águas - ANA) located in the study site (Figure 1B) source historical hydrological data for 1971/74–2019 period. The Araguaia River drains 76,964 and 193,923 km² at the Aruanã (#25200000) and São Félix do Araguaia (#26350000) gauging stations, respectively (Aquino et al., 2005). Mean annual and mean annual flood discharges for the period of record are 1189.84 and 4745.67 m³s⁻¹, respectively, at Aruanã and 2622.43 and 7293.99 m³s⁻¹, respectively, at São Félix do Araguaia.

The interannual variability of the middle Araguaia River flow (Figure 2) reflects the strong seasonality of the tropical savanna climate (Aw). The dry period extends from June to October and the high-water period from November to May. The peak flow usually occurs in February in the upper middle-course and lags approximately one month at São Félix do Araguaia station. On average, annual peak flow is more than 17-times the minimum annual flow (Q_{\max}/Q_{\min}) at Arunã. This number decreases to 10 at the downstream São Félix do Araguaia station. The flows at this second station are highly influenced by the entrance of the most important tributary of the Araguaia River, the Mortes River with an estimated Q_{mean} of 858.41 m³s⁻¹ (Aquino et al., 2009b). Upstream of this confluence, flood transmission through the middle Araguaia is characterized by peculiar peak discharge attenuation (with peak reductions up to 30%), despite receiving tributary inputs, which makes this river distinctive when compared to other large axial tributary alluvial rivers, at least in tropical South America (Lininger and Latrubesse, 2016). Lacustrine geomorphological features of the floodplain (abandoned channel lakes, oxbow lakes, lakes formed on meander scrolls, lakes formed by lateral accretion, blocked valley lakes, and embankment lakes) and their connectivity with the mainstem are the geomorphic mechanisms that cause this peak attenuation, and play an important role for ecological maintenance of the floodplain wetlands (Aquino et al., 2008; Prado de Morais et al., 2005; Lininger and Latrubesse, 2016).

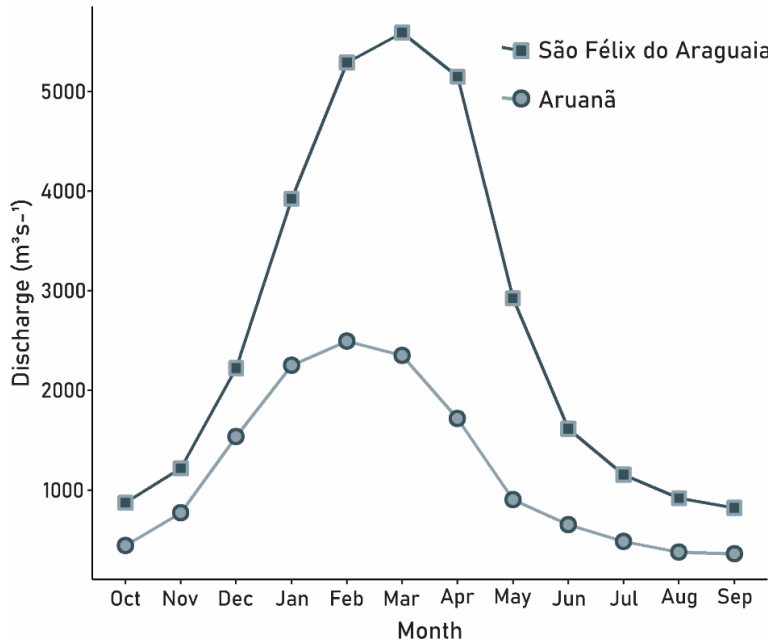


Figure 2. Mean monthly discharge of the middle Araguaia River for the period 1971/74–2019 at Aruanã and São Félix do Araguaia gauging stations.

Another singular aspect of the middle Araguaia, when compared to other large alluvial rivers of South America (e.g., Paraná and a great number of the Amazonian rivers), is the high proportion of sandy load carried by this river (up to ~57% of the total sediment load) compared to wash load, which just represents an average of ~ 43 to 49% of the total sediment load (Aquino et al., 2009a). Suspended sand is a very important component representing up to 93% of the total sand transported by the river (Latrubesse et al., 2009).

In this study, we present geomorphic data for the first 783 km of the middle Araguaia alluvial plain until the confluence with the Javaés River (downstream end of the Bananal Island). The procedures to divide the river into nineteen reaches (Figure 1B), the fundamental units of the river classification into segments, are described further in the next section.

2.2.3 Materials and Methods

A GIS framework was developed to identify the different segments of the middle Araguaia River. It was based on the calculation, statistical treatment and analysis of morphological variables derived from remote sensing data. ENVI 5.3 and ArcGIS 10.6 built-in vector and raster functions were used to extract data from Landsat images (5 TM/Landsat 5, 5 OLI/Landsat 8 scenes) taken on 10-26 July 2001 and 25 July 2018. The imaging selection criteria was the similarity of the water level (129-160 cm) at the Aruanã station (Figure 1B) on

the acquisition date during the low water level period to capture, as accurately as possible, the fluvial forms related to the bed load (sandbars). For each of the images, we performed radiometric calibration by rescaling data to the top of atmosphere (TOA) reflectance.

We applied a Tasseled-cap transformation (TCT) to 2018 Landsat scenes for delineating the floodplain boundaries. The combined components (brightness, greenness, and wetness) of this vegetation index enhance the spectral and textural information of the wetlands, allowing easier manual interpretation.

Active channel features were automatically identified by defining regions of interest (ROIs) on Landsat-derived Normalized Difference Vegetation Index (NDVI). Channel masks were extracted from pixel values ranging from -1 to 0 (water). Fluvial islands and vegetation patches over sandbars were defined where the values ranged from 0.2 to 0.8 (sparsely to densely vegetated surfaces) and channel sandbars in the interval between 0 to 0.2 (bare-earth surfaces). Vector datasets derived from the ROIs were manually checked and corrected and then used to extract planview channel and floodplain metrics.

2.2.3.1 Definition of river reaches

The spatial heterogeneity of a river is primarily controlled by the valley setting (floodplain development, ancient alluvium, and geologic control - lithology and structure) that combined with gradient, sediment supply and water flow determine the functioning and diversity of the modern fluvial forms and the nature and rate of its adjustments.

To divide the Araguaia River into reaches, we considered the important longitudinal variations of these primary controls expressed by the following variables listed in their order of significance for the river subdivision: (i) channel and valley gradient; (ii) presence of structural lineaments along the valley and changes in channel direction as it shifts from one linear element to the other; (iii) entrances of main tributaries as a surrogate for important contributions of discharge and sediment supply; (iv) measurements of the extent of channel confinement and the floodplain degree of development (entrenchment ratio).

Metrics used to distinguish the reaches were sampled at regular 5-km river valley small stretches ($n=156$) based on 2018 Landsat data and the elevation model MERIT Hydro. This 3-arc-second resolution (~90 m at the equator) DEM has been hydrologically adjusted to satisfy the condition 'downstream is not higher than its upstream' while minimizing the required modifications from the original MERIT DEM (Yamazaki et al., 2019). Mean height values of transverse transects crossing the floodplain were considered in the calculation of valley

gradient. Valley gradient was determined by dividing the difference in mean floodplain elevation between the stretches' up-and-down limits by the horizontal distance of the valley centerline. Channel gradient was determined by dividing the difference in elevation between upstream and downstream endpoints (defined by stretches' limits) of the channel centerline by its horizontal distance. Intending to remove “bad” data points but preserving important geomorphic data, we used locally weighted linear regressions (span = 0.05), as suggested by Aiken and Brierley (2013) to smooth data.

Linear features crossing the study area were compiled from the lineament network identified by Valente (2007) for the whole Araguaia basin. We computed orientations of individual lineaments using Coordinate Geometry (COGO) functionalities in ArcGIS 10.6. Results were displayed in a bar plot showing orientations from 0° (right/east) to 180° (left/west).

Channel confinement was calculated by applying Fryirs et al. (2016) as follows:

$$C_c = \left(\frac{\sum_{DS}^{US} CL_{EB} @ C_M}{CL_T} \right) \times 100 \quad (1)$$

where C_c is the channel confinement; $CL_{EB} @ C_M$ is the length of the channel along either bank that is constrained by a valley bottom margin (bedrock valley wall or other confining features such as inactive floodplains); CL_T is the total length of channel. The geologic map of the Araguaia basin presented by Valente (2007) was used to identify the bedrock outcrops that control the river planform. The entrenchment ratio was determined by the ratio of the floodplain width to the channel width (Polvi et al., 2011).

Changes in the morphological pattern of the river along the reaches were assessed by applying the following channel metrics: stability parameter (Kong et al., 2020), lateral migration rate (Giardino and Lee, 2011), sinuosity index (Friend and Sinha, 1993), the total area of sandbars, anabranching index (Kong et al., 2020) and circularity index for islands (Mertes et al., 1996).

Our set of geomorphic data did not meet the assumption of normality per the Shapiro-Wilk test. Therefore, non-parametric Kruskal–Wallis hypothesis test (Table 1) was performed to validate our river subdivision using the RStudio IDE (R Core Team, 2021). Results from this multivariate analysis confirmed the statistically significant differences of the plani-altimetric variables among the sub-reaches ($p < 0.05$). Effect size estimates (eta squared measure using the H -statistic) of the Kruskal-Wallis tests detected large effect sizes for these metrics, save for the moderate effect of the valley gradient, lateral migration rate, and the circularity index for

islands. Spearman's (Sp) rank correlation coefficients (ρ) provided tests for monotonic downstream trends in the variables. Welch's t -test was used to inspect if the means of two groups of the same variable were equal.

	Kruskal Wallis (p)	Effect Size, ETA^2*
Valley gradient	0.008	0.13
Channel gradient	<0.0001	0.28
Channel confinement	<0.0001	0.32
Entrenchment ratio	<0.0001	0.77
Channel stability	0.0004	0.20
Lateral migration rate	0.0066	0.13
Sinuosity index	0.0007	0.19
Total bar area	<0.0001	0.37
Anabranching index	<0.0001	0.33
Circularity index	0.0352	0.08

Table 1. Results of Kruskal Wallis test. * ETA^2 is interpreted as the percentage of the total variance explained by the groups (river reaches). Guidelines for the size of the effects: <0.06 (small); 0.06 - <0.14 (moderate); ≥ 0.14 (large) (Kirk, 2015).

2.2.3.2 River classification into major geomorphic segments

The subdivision of the middle Araguaia River into discrete reaches provided the framework to develop a river classification into major fluvial segments based on an unsupervised approach of the spatial statistics that grouped reaches of relatively uniform morphological attributes. The spatially constrained multivariate clustering of ArcGIS 10.6 (Grouping Analysis tool) identified the potential segments by looking for a solution where all the reaches within each group are as similar as possible, and all the groups themselves are as different as possible (Esri, 2021). Reach similarity was defined by 5 geomorphological variables that can be regarded as independent: (1) valley gradient and (2) entrenchment ratio, and dependent: (3) sinuosity, (4) anabranching index, and (5) stability parameter.

A pseudo F-statistic was used to determine the optimal number of groups. It describes the ratio of between-cluster variance to within-cluster variance (Calinski and Harabasz, 1974). A number of clusters having a large pseudo F value will be very effective at distinguishing the features and variables specified (Esri, 2021). The ratio calculated by the algorithm indicated that five classes of reaches would be a good choice (Figure 3a). A coefficient of determination (R^2) provided a measure of the variance between clusters explained by each geomorphological variable. It implies that the larger the R^2 for a given variable, the more relevant it was for

discriminating among segments (Figure 3b). The standardized values of such variables for the resulting classes were then analyzed to identify the factors driving the singularity of each geomorphic segment.

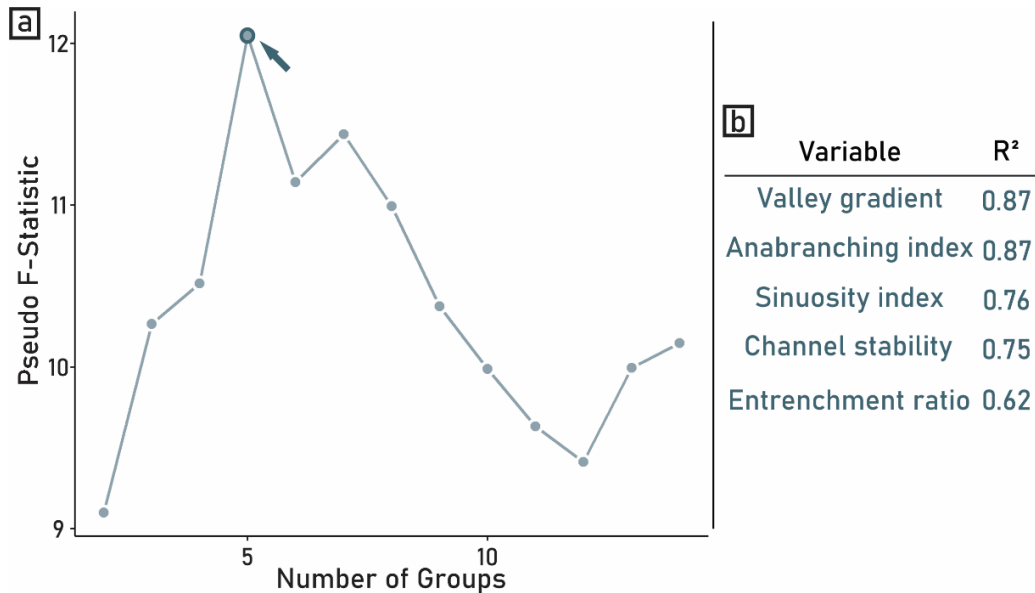


Figure 3. (a) Pseudo F-Statistic Plot. The index was used as a stopping rule for identifying the “optimal” number of groups (segments) as peaks are indicators of greater cluster separation. (b) R² values computed for each geomorphological variable. They showed great potential (>0.6) for discriminating among clusters.

2.2.3.3 Planform dynamics in the river segments

Morphodynamics of the river segments was assessed by comparing the areas of erosion and deposition in the active channel and proximal floodplain between 2001 and 2018. The areal extent of these processes was quantified by adopting GIS procedures described in Jana (2019). The author generates two raster files containing the main fluvial landforms (active channel, sandbars, islands, and floodplains) in two successive years. Using a raster calculator tool, a subtraction raster file is derived from the previous ones, and it express the changes (erosion or deposition) that took place during the time series. In our study, depositional areas resulted from lateral accretion, island accretion to the floodplain, and bar and island formation (creation or expansion) processes. Eroded areas resulted from lateral erosion, and bar and island destruction (surface loss).

Because the two-dimensional mapping of the features does not incorporate differences in elevation, it cannot be translated into a volumetric budget. Even so, the areal data provided

important information on the rates and types of channel adjustments that characterize each segment of the river.

2.2.4 Results and Discussion

2.2.4.1 Spatial patterns of morphological variability at the reach scale

Based on the downstream changes in the variables expressing the primary controls of the river planform – channel and valley gradient (Figure 4A), structural lineaments (Figure 4B), the entrance of main tributaries (Figure 4, upper part), channel confinement (Figure 4C; Figure 5a), and entrenchment ratio (Figure 4D; Figure 5b) – we divided the trunk river into 19 reaches (R1-R19). We assessed morphology and short-term dynamics at the reach scale using lateral migration rate (Figure 5c), channel stability (Figure 5d), sinuosity (Figure 5e), the total area of sandbars (Figure 5f), anabranching index (Figure 5g), and circularity index for islands (Figure 5h).

The Araguaia River occupies a valley of variable longitudinal gradients (Figure 4A). The highest valley gradients mark the beginning of R1 (109 cm km^{-1}) and R11 (80 cm km^{-1}), while the lowest ones occur at R12, R14, R18, and R19, where mean values range between 7-9 cm km^{-1} . Highest channel gradients (39-63 cm km^{-1}) are observed in the following upstream reaches: R5, R6, R8 and R10 (Figure 4A). In the case of R8 and R10, channel steeper slopes in low-sinuous reaches have been established over a relict lower-gradient floodplain. Significant reductions of the channel gradient relative to the valley gradient are associated with the most sinuous reaches – R2, R11, and R12 (Figure 5e), as the channel gradient responds to alongstream changes of the river by adjusting its pattern (Schumm, 1993).

The flow paths of reaches are mainly dictated by NNE–SSW, and N–S dominant regional lineament trends. Except for R11, where the shifting of the main river course is influenced by NW-SE elements (Figure 4B). The presence of lineaments crossing the Araguaia valley controls the river pattern to some extent where they intersect the channel. Note that part of the relevant tributaries joins the mainstream where it drains along or near the lineament traces (Figure 4, upper part). Points of confluence/difluence with the Araguaia River are associated with locations where these lineaments interact and meet.

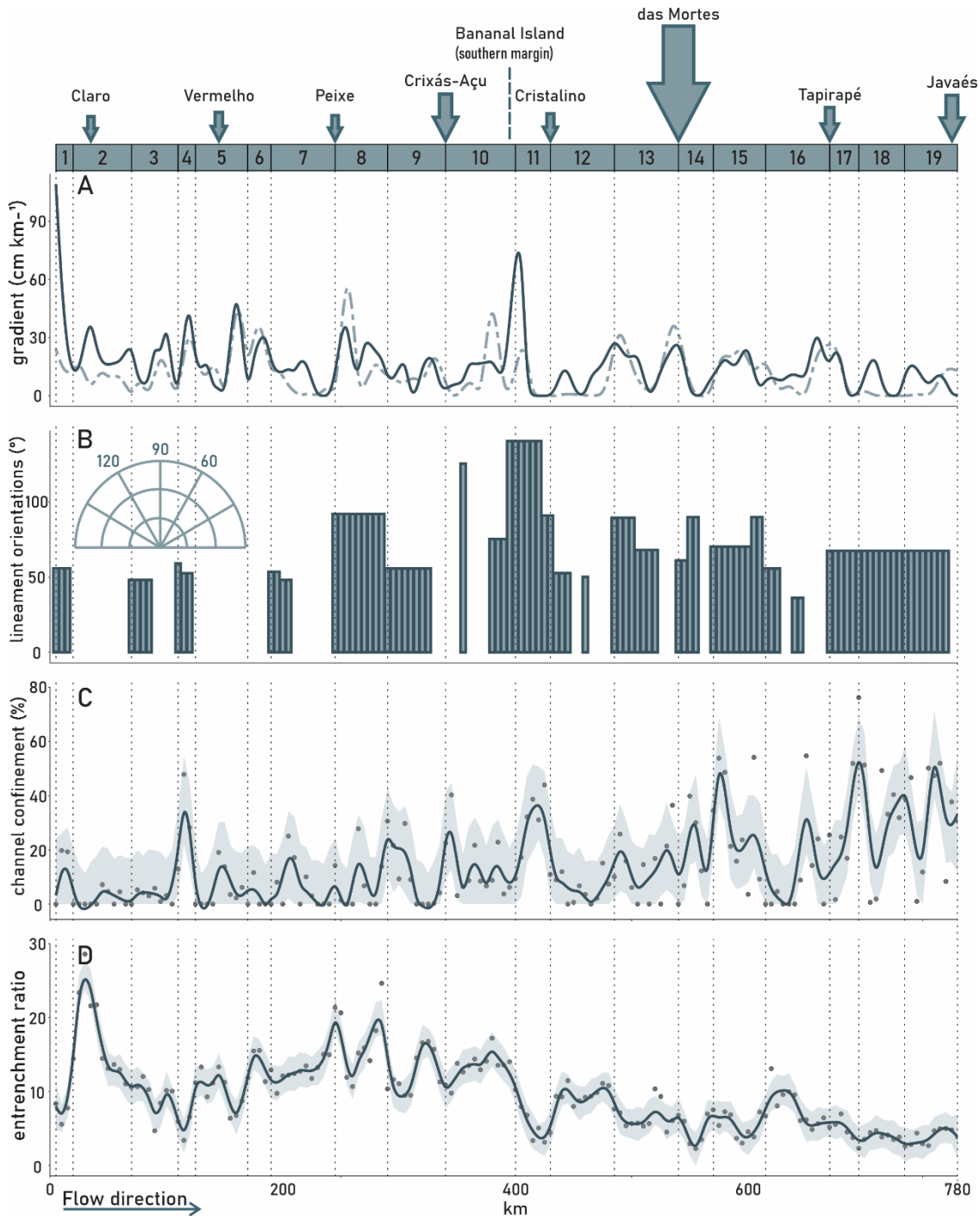


Figure 4. Selected variables for the subdivision of the middle Araguaia River into sub-reaches. Arrows in the upper part of the figure indicate the point where the major tributaries join the mainstream; the size of the arrows is proportional to the mean annual discharge of the tributaries (Aquino et al., 2009). A. Channel (dashed line) and valley (solid line) gradients. B. Orientations of lineaments mapped in the Araguaia River valley (Valente, 2007). Longitudinal trends of (C) channel confinement and (D) entrenchment ratio presented as Loess lines with 95% confidence intervals. The vertical dotted lines represent the spatial limits between the reaches (1-19).

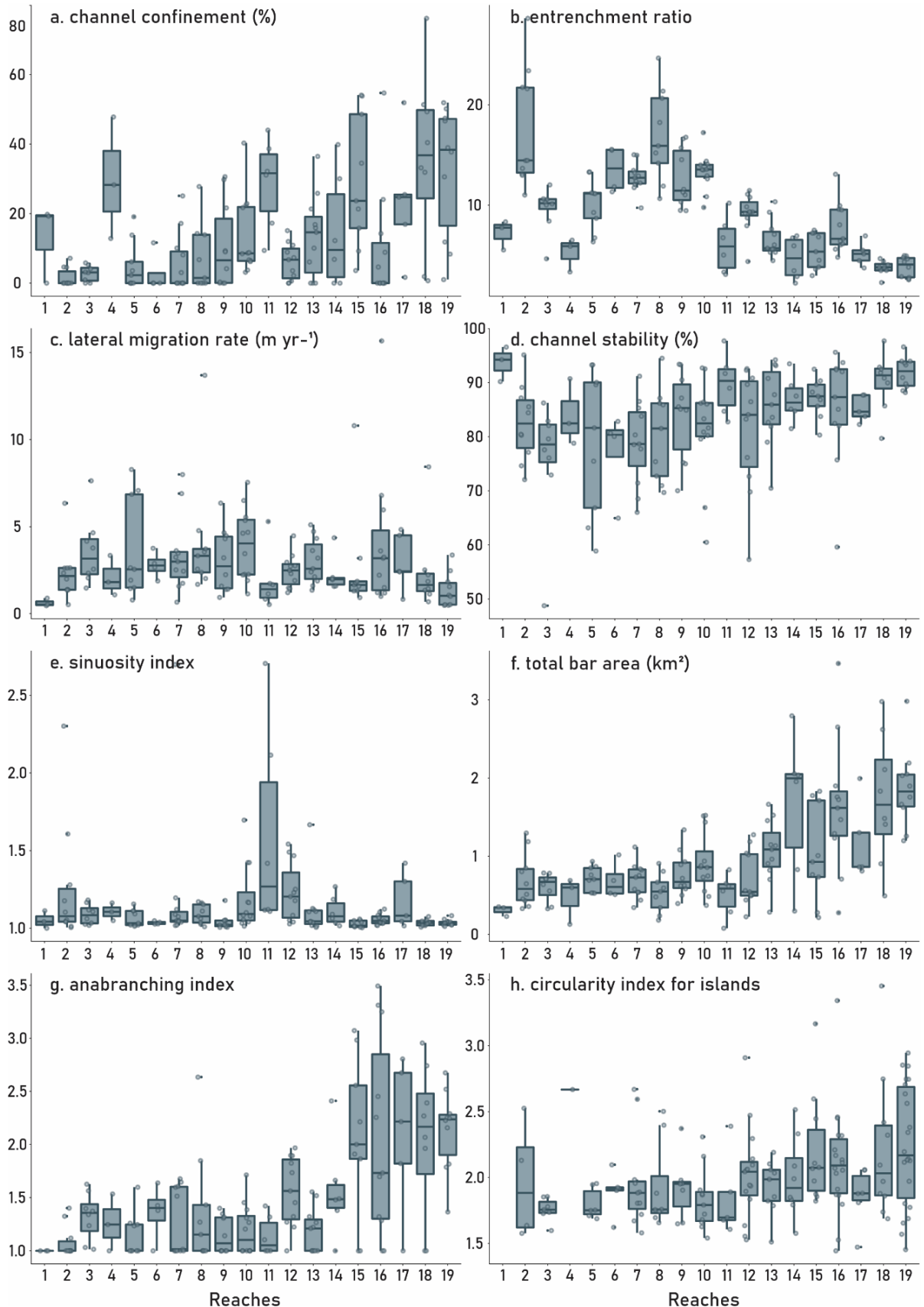


Figure 5. Distribution of channel and floodplain metrics obtained in each river reach.

Morphological changes are usually expected to occur downstream tributary junctions due to changes in sediment supply and water discharge. However, a comparison of metrics obtained along 15 km upstream and downstream confluences showed that the total area of sandbars that form just below the junctions is not significantly different (*t*-test: $p > 0.05$) from the area of these features located upstream. The major variation (*t*-test: $p = 0.1$) was an increase of 168% in the area of sandbars immediately downstream of the entry of the Cristalino River. Stepwise changes of the channel width occur in the majority of confluence zones (*t*-test: $p > 0.05$). The significant increases were observed below the entries of Cristalino (+56%, *t*-test: $p = 0.01$) and Mortes (+53%, *t*-test: $p = 0.07$) rivers.

Channel planform has been partially controlled by varying degrees of confinement (Figures 4C and 5a). Notable lateral constraints (mean value $> 25\%$) occurs at R4, R11, R15 and R17-R19, while the least constrained reaches (mean value $< 10\%$) are R2, R3, R5-R8, R12 and R16 (Figure 5a). The entrenchment ratio is a correlate metric of channel confinement that provides relevant information about the valley geometry and the stages of floodplain development relative to the contemporary river. Broad floodplains characterize R2 and R5-R10, where median entrenchment ranges from 11 (R5) to 16 (R8), and maximum values are attained at R2 (29) and R8 (25) (Figures 4D and 5b). There is a general decreasing tendency for the entrenchment downstream (Sp: $p = 0.003$, $\rho = -0.65$), with floodplain widths just 2-5 orders of magnitude wider than the active channel in the last two reaches.

No spatially consistent trend in the rates of lateral channel shifting was identified (Sp: $p > 0.05$). The highest median values per reach ($3-3.5 \text{ m yr}^{-1}$) were found at R3, R7, R8, R10, and R16, while the lowest ($0.5-1.7 \text{ m yr}^{-1}$) occur at R1, R11, R15, R18, and R19 (Figure 5c). If we extend our examination of lateral stability to the fluvial bed (account for the position of the islands banks) (Figure 5d), we notice a pattern of more unstable planforms in the upper reaches (R2-R10) than in the lower ones (R11-R19) (Sp: $p = 0.02$, $\rho = 0.54$). Nonetheless, the highest proportions (median values $> 90\%$) of the channel that did not experience any planimetric changes from 2001 to 2018 were found at R1, R11, R18, and R19.

Typically straight to gently meandering reaches characterize the main channel planform with median sinuosity values ranging between 1.02 (R15) to 1.2 (R12). The only exception is R11, where unusual highly sinuous bends can be found – median sinuosity: 1.3; max. sinuosity: 2.7 (Figure 5e). The braided style, as indicated by the total area of bars (Sp: $p < 0.0001$, $\rho = 0.87$), and the anabanching character of the river, as pointed by the anabanching index (Sp: $p = 0.0001$, $\rho = 0.77$), increase significantly in the downstream direction (Figures 5f and 5g). The largest extensions of the sandbars take place at R13-R19, where median values are 129% higher

than their upstream counterparts. The upper reaches (R1-R11) evidently have a reduced number of individual channels (median anabranching index: 1-1.4) when compared to the lower ones (R12-R19, median anabranching index: 1.5-2.2). The highest values (2.7-3.5) are reached from R15 to R19.

The plan shape of the islands was expressed by the circularity index, where values near 1 indicate more circular and higher values indicate more elongated features (Mertes et al., 1996). Rounder islands linked to aggradational processes are usually associated with maturity, as stable features tend to become progressively more convex over time due to the lateral accretion process (Hudson et al., 2019). Despite the lack of a consistent alongstream pattern (Sp: $p > 0.05$), the highest median (>2) and maximum (2.9-3.5) values of circularity index are usually observed from R12 to R19 (Figure 5h).

2.2.4.2 Characterization of the middle Araguaia River segments

The previous description of the morphological variables at the reach level revealed significant alongstream variations in the planform characteristics of the middle Araguaia River. Given the regional extent of this system, we can rescale this first subdivision into major geomorphic segments characterized by fairly contiguous patterns in the river's character and the degree of development of the fluvial corridor. A quantitative unsupervised approach of spatially constrained clustering provided an objective classification of the reaches into five segments with a consistent level of morphological variability between them (Figure 6).

The Segment I – *Single-channel reach, planform controlled, restricted floodplain*, has been defined for the first reach (R1) of river. It marks the transition from a narrow V-shaped valley to the broad alluvial plain. The highest valley gradients in this straighter and structurally controlled channel reach result in low rates of lateral migration and minimum planform changes with little sediment storage in the form of a few bars and no islands formation (Figures 6, 7B and 8).

Approximately 15 km downstream from the beginning of the floodplain until the confluence with the Javaés River (R2-R10), we documented the second segment, named *Alluvial anabranching pattern, laterally unconfined, wide, and complex Holocene floodplain*. Along the 375 km of valley's length comprising this segment, the river locally hit outcrops of Precambrian metasedimentary rocks (e.g., R4, Figure 5A) or the valley margin itself (e.g., R10, Figure 5A).

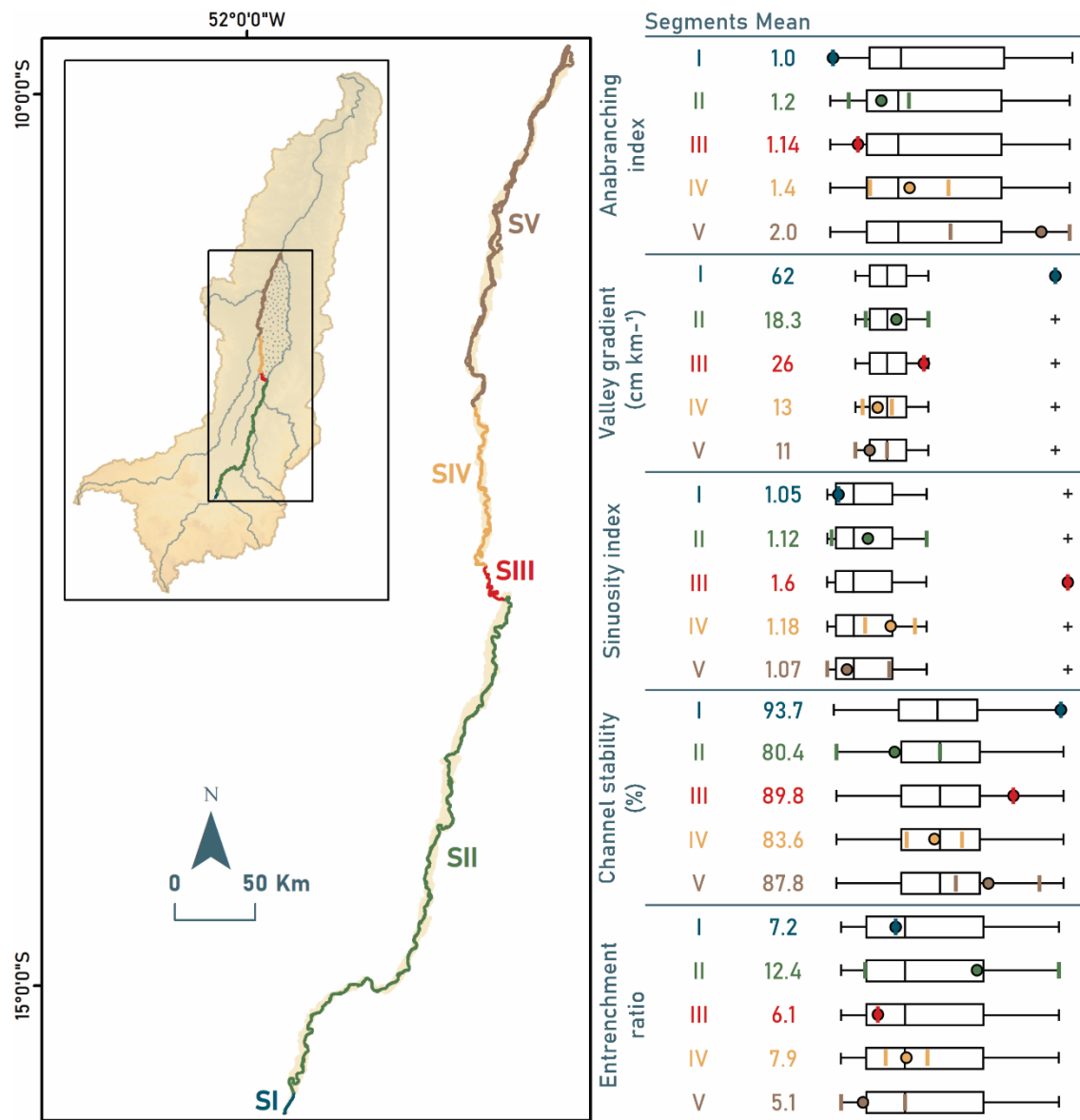


Figure 6. River valley segments (SI-SV) identified for the middle Araguaia River using a GIS-based multivariate clustering algorithm. Boxplots display global ranges of each geomorphic variable employed in the cluster analysis. The colored bold lines and circles represent respectively min-max and mean values attained in a given segment. The crosses represent outliers.

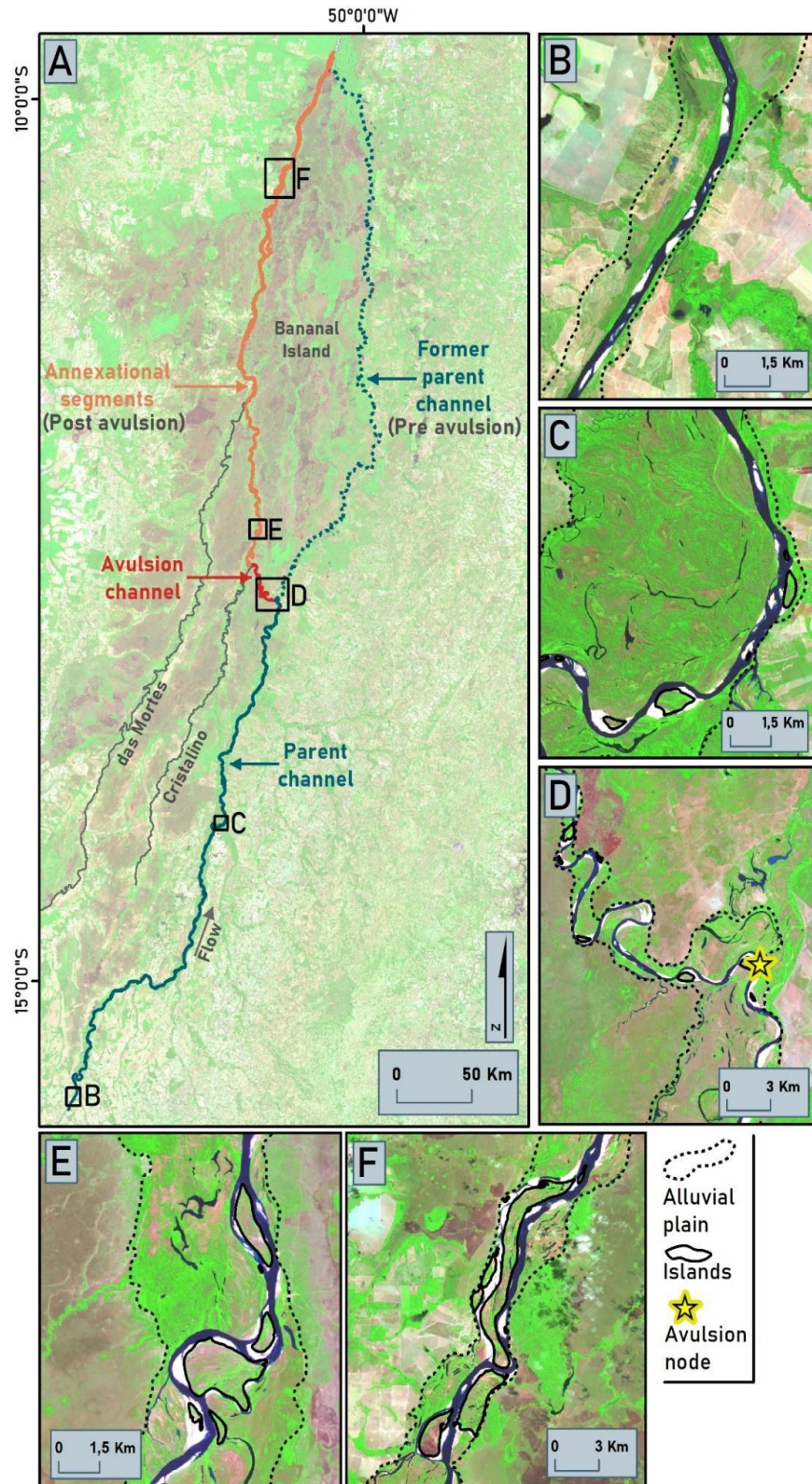


Figure 7. A. The middle Araguaia River avulsion site. Location of the modern channel (dark blue/red/orange solid line) and the parent channel prior to avulsion (dark blue dotted line). B, C, D, E and F are representative sites of segments I, II, III, IV, and V, respectively. Background Sentinel-2 images taken on 13 August 2021 (water level of Aruanã station: 136 cm) and downloaded from Google Earth Engine (GEE) platform.

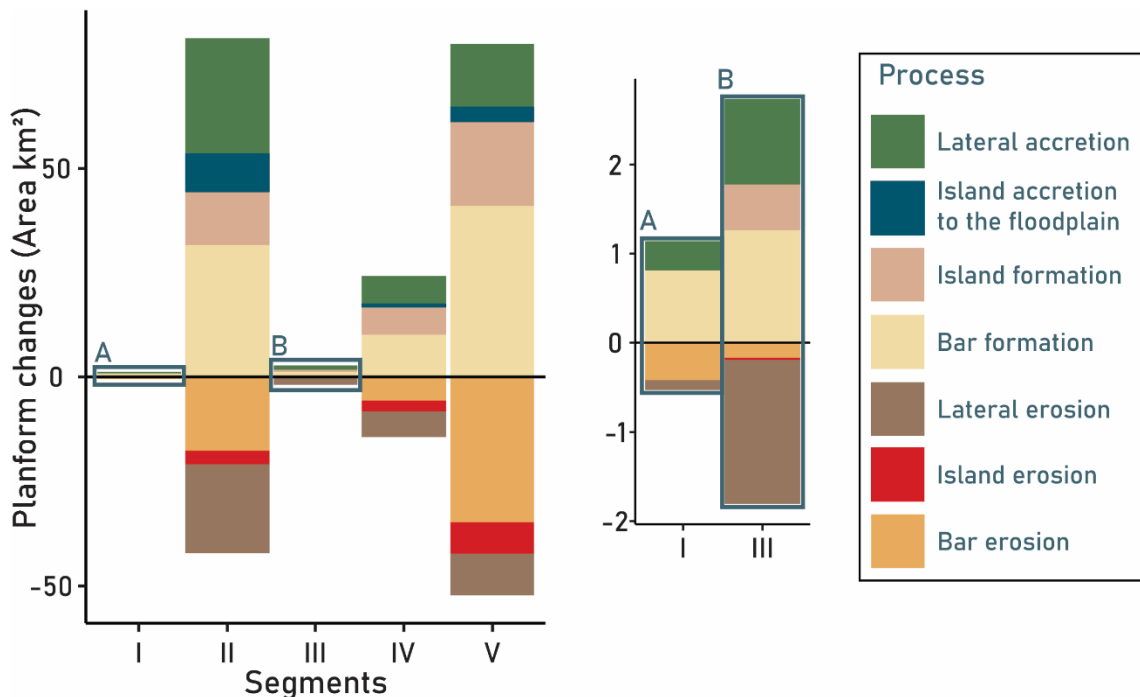


Figure 8. Variability in the rates of deposition and erosion (km^2) in the active channel and proximal floodplain between 2001 and 2018 summed for the five river segments. A and B are zoomed-in versions of bars displaying segments I and III data.

However, the influence of these constrictions is small, and the channel is most capable of reworking its boundaries in the materials of the extensive floodplains that characterize Segment II. Most channel banks are made up of friable Holocene deposits of floodplain units II and III (Latrubblesse and Stevaux (2002)). Unit II is characterized by paleomeanders and oxbow lakes. Coarse to medium sands at the base of the deposit indicate an active channel environment, while a thin layer of sand interspersed with clay and silt (low-energy environment) characterizes the upper part. Unit III is a complex of accreted bars and islands generated by the present flow regime, forming an irregular belt along the active channel. Sediments in this unit are mainly medium and fine sands, with layers of finer materials (Bayer, 2002).

Islands formed by the excision of the floodplain are less commonly found in Segment II, and within-channel islands display more rounded shapes (R2-R10, Figure 5h) due to the intensive aggradational processes associated with the higher channel dynamics. As the low-sinuous thalweg laterally shifts, changes in the position and efficiency of the branches lead to secondary channels atrophy and, consequently, accretion of the islands to the floodplain (Figure 8). Hence, islands have a shorter lifespan and rarely attain a large size (R2-R10, Figures 5g and 7C).

The entrance of the major eastern tributaries flowing from the hilly areas of the Brazilian shield – Claro, Vermelho, Peixe, and Crixás-açu rivers (Figure 1) influences the geomorphic style of the second segment. Their sediment inputs contribute to the overall aggrading character of the Araguaia in Segment II. The alluvial deposits resulting from lateral shifts of the river, bars, and islands formation represent, respectively, 55%, 49%, and 36% of the net storage in the system (Figure 8). Thus, the combination of large sandy loads of sediment, incohesive banks and moderate valley gradient results in a low-sinuous pattern with smaller branches and less stable features (Figure 6).

The reach of the Araguaia between the diffluence with the Javaés River and the confluence with the Cristalino River (R11) corresponds to the Segment III – *Highly sinuous anabranching pattern, partly confined on alluvium, younger meander belt with scrolls*. It is a singular segment comprising an outstanding avulsion channel (Figure 7A) of 54.4 km in length that diverts the flow of the mainstream and forms the southern part of Bananal Island. Once the river turns to NW, it transitions toward the younger belt characterized by incision into the Araguaia Formation, a decrease in the mean entrenchment ratio, and an increase in planform stability (Figure 6).

Nonetheless, we suggest that the high valley gradient is the basic determinant of the river morphology in Segment III. The channel flowing on steeper terrain is found to display a high sinuosity (Figures 6 and 7D) to dissipate more uniformly the excess of energy along the segment but the migration rates are low because the system is incised, and there is moderate development of bar and islands (Figure 8).

The Segment IV – *Anabranching pattern, planform controlled, discontinuous floodplain*, extends from the confluence with the Cristalino River until immediately prior the entrance of the Mortes River (R12 and R13, length of the valley = 106.3 km). The avulsion changes from incisional (construction of a new channel) to annexational (reoccupation of preexisting fluvial system) from this segment as the Araguaia flows join the Cristalino and downstream the Mortes River (Figure 7A).

Currently, the Cristalino is an underfit river on the Bananal plain (Valente and Latrubesse 2012), most active during the rainy season and with a $Q_{mean} \sim 4.3x$ lower than the Mortes outflow. As increments from this modest tributary cannot explain the prominent changes in river morphology that marks this segment, the lower valley gradient is set as the first-order control. It gives rise to a zone of channel widening, bar deposition and development of alluvial islands (Figure 8) that differs to a great extent from the zone of sediment flushing produced by the steep and narrow valley of the segment preceding it.

The river displays some sinuous features in R12 (Figure 5e) as the Araguaia overprints its anabranching character by activating minor channels and depressions of the old meandering-river floodplain of the Cristalino (Figure 7E). In general, the low valley gradient and the moderate entrenchment of the river (Figure 6) are limiting factors for the generation of meanders of greater amplitude. Along Segment IV, discontinuous floodplains occur on alternating sides of the river and, when not constricted by the valley configuration, the low-sinuous pattern has substantial capacity for adjustment (Figure 6).

The downstream reaches (R14-R19) of the middle Araguaia River were classified Segment V – *Complex anabranching pattern, partly confined on alluvium and/or bedrock, underfit floodplain*. It occupies 247.9 km of the valley's length, stretching from the confluence with the Mortes River to the confluence with the Javaés River, where it constitutes the downstream end of Bananal Island.

Segment V lies on the lowest valley gradients of the study site (Figure 6). Thus, the widespread occurrence of large sandbars (R14-R19, Figure 5f) implies a limited capacity of the river to transport the large volume of bed load delivered from upstream segments. In spite of the strong influence of this low energy gradient in the geomorphic style of this segment, we assume it is mainly governed by the nature of the valley floor and the geometry of the floodplain.

Volcanic rocks and granites of the Iriri-Xingu Domain, Central Amazonian province, and Mesoarchean rock associations of the Rio Maria Domain, Carajás Province, outcrop discontinuously along the left bank of R14, R15, and R17 and constitute local lateral constraints to the development of the floodplain. However, the most prevalent confining media of Segment V is not bedrock, but the valley margins composed of the older, well-indurated alluvium of the Araguaia Formation. The discontinuous contact of the active channel with the confining margins allows for the occurrence of a narrow and patchy floodplain, where some lateral change is possible (Figure 8). As the low gradient is not enough to overcome the resistance of the Pleistocene cohesive sediments, very straight reaches (Figure 6) characterize the most downstream segment of the middle Araguaia River.

It is noteworthy the significant increase in the anabranching character of the river from Segment V (Figure 6). This change is related to the presence of large islands (Figure 7F) that displays irregular and more elongated outlines (R14-R19, Figure 5h), complex inner morphology, and both concordant (aligned parallel) and discordant (cut across) margins regarding the current shape and orientation of islands. These singular properties plus the lower channel mobility of the lower reaches reveal that these macroforms have been formed by flow

diversion, relief exploitation, and excision of a portion of the pre-existent floodplain. In this setting of large and permanent islands, the mean entrenchment ratio decreases to 5.1 (Figure 6), meaning that the modern channel belt of Araguaia River is 'overfit' relative to the width of the genetic floodplain.

We can interpret this geomorphic context as a metamorphosis of channel pattern induced by a new flow regime following the river avulsion (Figure 7A). To accommodate the incoming discharge and sediment load from the Araguaia relict system into the ancient paleo-Mortes belt, the river changed from meandering to anabranching. Changes possibly involved a dramatic channel widening and the large-scale reworking of floodplain deposits of the earlier and smaller Mortes River, which led to the islands' development from extra-channel diversion after the avulsion.

Based on OSL and TL age estimates, Valente and Latrubesse (2012) inferred that river avulsions under an aggradational regional regime in the Bananal Basin were intensive in the Lower–Middle Pleniglacial between 70.5 ka and 34.0 ± 4.6 ka (MIS 4 and 3) and in the Upper Pleniglacial between 24.5 ± 3.1 and 17.2 ± 2.3 ka (MIS 2). Meanwhile, radiocarbon dating obtained by the authors in the floodplain of Segment III, where the incisional avulsion took place, provided a modern age, suggesting that the large-scale ongoing diversion of the Araguaia River has been triggered by neotectonic activity in more recent times, during the Holocene.

Thus, it seems reasonable that the Araguaia River disrupted the pre-existing channel geometries of the Cristalino and Mortes rivers, but hasn't had enough time to build a surrounding floodplain compatible with the flow regime and geomorphic processes of the contemporary river. Nowadays, the abundant supply of bed material forms large sandbars subject to high turnover process, and promotes the creation of new islands and the evolution of those complex ones inherited from the ancient fluvial system (Figure 8).

2.2.5 Conclusions

Based on a set of river and floodplain variables derived from a GIS framework we developed a methodology to subset the Middle Araguaia River into 19 distinct reaches (R1-R19). The unsupervised clustering method incorporating spatial constraints objectively grouped the river reaches into five classes of segments. Changes of valley gradient influence in a major way the morphology of segments I, III and IV, while the entrance of important tributaries and the nature of the valley floor are the main controlling factors of the fluvial style in segments II and V, respectively. In a complex geomorphic system like the Araguaia, we also documented

the strong influence of the late Holocene avulsion history over the modern channel character and its adjustments.

This first planform characterization of the middle course of the river complements previous geomorphic studies by providing insights about the morphological diversity of the segments, and the channel's sensitivity to change. We also consider that the river segmentation can lend scientific support to a variety of disciplinary researches, and management plans searching for sustainable management actions and conservation, as well as to impacting projects such as dams, irrigation, and waterways.

Acknowledgments

We are grateful for the financial support of the Coordination for the Improvement of Higher Education Personnel – Brazil (CAPES) - Finance Code 001, and the Brazilian National Council for Scientific and Technological Development (CNPq) - No. 422559/2021-0. We also thank the anonymous reviewers for their insightful comments and suggestions.

References

- Aiken, S.J., Brierley, G.J., 2013. Analysis of longitudinal profiles along the eastern margin of the Qinghai-Tibetan Plateau. *J. Mt. Sci.* 10, 643–657. <https://doi.org/10.1007/s11629-013-2814-2>
- Aquino, S., Latrubesse, E., Bayer, M., 2009a. Assessment of wash load transport in the Araguaia River (Aruanã gauge station), central Brazil. *Lat. Am. J. Sedimentol. Basin Anal.* 16, 119–128.
- Aquino, S., Latrubesse, E.M., de Souza Filho, E.E., 2008. Relações entre o regime hidrológico e os ecossistemas aquáticos da planície aluvial do rio Araguaia. *Acta Sci. - Biol. Sci.* 30, 361–369. <https://doi.org/10.4025/actascibiolsci.v30i4.5866>
- Aquino, S., Latrubesse, E.M., Elias, E., Filho, S., 2009b. Caracterização hidrológica e geomorfológica dos afluentes da Bacia do Rio Araguaia. *Rev. Bras. Geomorfol.* 10, 43–54. <https://doi.org/10.20502/RBG.V10I1.116>
- Aquino, S., Stevaux, J.C., Latrubesse, E.M., 2005. Regime Hidrológico E Aspectos Do Comportamento Morfohidráulico Do Rio Araguaia. *Rev. Bras. Geomorfol.* 6, 29–41. <https://doi.org/10.20502/rbg.v6i2.49>
- Ashworth, P.J., Lewin, J., 2012. How do big rivers come to be different? *Earth-Science Rev.* 114, 84–107. <https://doi.org/10.1016/j.earscirev.2012.05.003>
- Bayer, M. 2002. Diagnóstico dos processos de erosão/assoreamento na planície aluvial do rio Araguaia: entre Barra do Garças e Cocalinho. Master thesis. Universidade Federal de Goiás.

- Best, J., 2019. Anthropogenic stresses on the world's big rivers. *Nat. Geosci.* 12, 7–21. <https://doi.org/10.1038/s41561-018-0262-x>
- Blum, M.D., 2008. Large River Systems and Climate Change. *Large Rivers Geomorphol. Manag.* 627–659. <https://doi.org/10.1002/9780470723722.CH30>
- Caliński, T., Harabasz, J., 1974. A Dendrite Method Foe Cluster Analysis. *Commun. Stat.* 3, 1–27. <https://doi.org/10.1080/03610927408827101>
- Esri, 2021. How Grouping Analysis works—ArcMap | Documentation [WWW Document]. URL <https://desktop.arcgis.com/en/arcmap/latest/tools/spatial-statistics-toolbox/how-grouping-analysis-works.htm> (accessed 8.14.22).
- Ferreira, M.E., Ferreira, L.G., Latrubesse, E.M., Miziara, F., 2008. High resolution remote sensing based quantification of the remnant vegetation cover in the Araguaia river basin, central Brazil. *Int. Geosci. Remote Sens. Symp.* 4, 2008–2010. <https://doi.org/10.1109/IGARSS.2008.4779828>
- Friend, P.F., Sinha, R., 1993. Braiding and meandering parameters. *Geol. Soc. Spec. Publ.* 75, 105–111. <https://doi.org/10.1144/GSL.SP.1993.075.01.05>
- Fryirs, K.A., Brierley, G.J., 2018. What's in a name? A naming convention for geomorphic river types using the river styles framework. *PLoS One* 13, 1–23. <https://doi.org/10.1371/journal.pone.0201909>
- Fryirs, K.A., Wheaton, J.M., Brierley, G.J., 2016. An approach for measuring confinement and assessing the influence of valley setting on river forms and processes. *Earth Surf. Process. Landforms* 41, 701–710. <https://doi.org/10.1002/esp.3893>
- Gautier, E., Dépret, T., Cavero, J., Costard, F., Virmoux, C., Fedorov, A., Konstantinov, P., Jammet, M., Brunstein, D., 2021. Fifty-year dynamics of the Lena River islands (Russia): Spatio-temporal pattern of large periglacial anabranching river and influence of climate change. *Sci. Total Environ.* 783. <https://doi.org/10.1016/j.scitotenv.2021.147020>
- Giardino, J.R., Lee, A.A., 2011. Rates of Channel Migration on the Brazos River: Final Report.
- Gurnell, A.M., Rinaldi, M., Belletti, B., Bizzi, S., Blamauer, B., Braca, G., Buijse, A.D., Bussettini, M., Camenen, B., Comiti, F., Demarchi, L., García de Jalón, D., González del Tánago, M., Grabowski, R.C., Gunn, I.D.M., Habersack, H., Hendriks, D., Henshaw, A.J., Klösch, M., Lastoria, B., Latapie, A., Marcinkowski, P., Martínez-Fernández, V., Mosselman, E., Mountford, J.O., Nardi, L., Okruszko, T., O'Hare, M.T., Palma, M., Percopo, C., Surian, N., van de Bund, W., Weisseiner, C., Ziliani, L., 2016. A multi-scale hierarchical framework for developing understanding of river behaviour to support river management. *Aquat. Sci.* 78, 1–16. <https://doi.org/10.1007/s00027-015-0424-5>
- Hudson, P.F., van der Hout, E., Verdaasdonk, M., 2019. (Re)Development of fluvial islands along the lower Mississippi River over five decades, 1965–2015. *Geomorphology* 331, 78–91. <https://doi.org/10.1016/j.geomorph.2018.11.005>

- Jana, L.S.X., 2019. The planform dynamics of the Irrawaddy River, Myanmar between 1990 and 2010. Nanyang Technological University, Singapore.
- Kirk, R.E., 2015. Effect Size Measures. Wiley StatsRef Stat. Ref. Online 1–13. <https://doi.org/10.1002/9781118445112.stat06242.pub2>
- Knox, R.L., Latrubblesse, E.M., 2016. A geomorphic approach to the analysis of bedload and bed morphology of the Lower Mississippi River near the Old River Control Structure. *Geomorphology* 268, 35–47. <https://doi.org/10.1016/j.geomorph.2016.05.034>
- Kong, D., Latrubblesse, E.M., Miao, C., Zhou, R., 2020. Morphological response of the Lower Yellow River to the operation of Xiaolangdi Dam, China. *Geomorphology* 350. <https://doi.org/10.1016/j.geomorph.2019.106931>
- Latrubblesse, E.M., 2015. Large rivers, megafans and other Quaternary avulsive fluvial systems: A potential “who’s who” in the geological record. *Earth-Science Rev.* 146, 1–30. <https://doi.org/10.1016/j.earscirev.2015.03.004>
- Latrubblesse, E.M., 2008. Patterns of anabranching channels: The ultimate end-member adjustment of mega rivers. *Geomorphology* 101, 130–145. <https://doi.org/10.1016/j.geomorph.2008.05.035>
- Latrubblesse, E.M., Amsler, M.L., de Moraes, R.P., Aquino, S., 2009. The geomorphologic response of a large pristine alluvial river to tremendous deforestation in the South American tropics: The case of the Araguaia River. *Geomorphology* 113, 239–252. <https://doi.org/10.1016/j.geomorph.2009.03.014>
- Latrubblesse, E.M., Arima, E., Ferreira, M.E., Nogueira, S.H., Wittmann, F., Dias, M.S., Dagosta, F.C.P., Bayer, M., 2019. Fostering water resource governance and conservation in the Brazilian Cerrado biome. *Conserv. Sci. Pract.* 1, 1–8. <https://doi.org/10.1111/csp2.77>
- Latrubblesse, E.M., Sinha, R., 2022. Human Impacts on Sediment and Morphodynamics of Large Tropical Rivers, 2nd ed, Treatise on Geomorphology. Elsevier Inc. <https://doi.org/10.1016/b978-0-12-818234-5.00160-7>
- Latrubblesse, E.M., Stevaux, J.C., 2015. The Anavilhanas and Mariuá Archipelagos: Fluvial Wonders from the Negro River, Amazon Basin. *World Geomorphol. Landscapes* 157–169. https://doi.org/10.1007/978-94-017-8023-0_14_COVER
- Latrubblesse, E.M., Stevaux, J.C., 2002. Geomorphology and environmental aspects of the Araguaia fluvial basin, Brazil. *Zeitschrift für Geomorphol.* 129, 109–127.
- Latrubblesse, E.M., Suizu, T.M., 2022. The Geomorphology of River Wetlands, 2nd ed, Encyclopedia of Inland Waters. Elsevier Inc. <https://doi.org/10.1016/b978-0-12-819166-8.00209-7>
- Lininger, K.B., Latrubblesse, E.M., 2016. Flooding hydrology and peak discharge attenuation along the middle Araguaia River in central Brazil. *Catena* 143, 90–101. <https://doi.org/10.1016/j.catena.2016.03.043>

- Mertes, L.A.K., Dunne, T., Martinelli, L.A., 1996. Channel-floodplain geomorphology along the Solimões-Amazon River, Brazil. *Bull. Geol. Soc. Am.* 108, 1089–1107. [https://doi.org/10.1130/0016-7606\(1996\)108<1089:CFGATS>2.3.CO;2](https://doi.org/10.1130/0016-7606(1996)108<1089:CFGATS>2.3.CO;2)
- Montgomery, D.R., Buffington, J.M., 1997. Channel-reach morphology in mountain drainage basins. *Bull. Geol. Soc. Am.* 109, 596–611. [https://doi.org/10.1130/0016-7606\(1997\)109<0596:CRMIMD>2.3.CO;2](https://doi.org/10.1130/0016-7606(1997)109<0596:CRMIMD>2.3.CO;2)
- Orlowski, L.A., Schumm, S.A., Mielke, P.W., 1995. Reach classifications of the lower Mississippi River. *Geomorphology* 14, 221–234. [https://doi.org/10.1016/0169-555X\(95\)00107-G](https://doi.org/10.1016/0169-555X(95)00107-G)
- Park, E., Latrubblesse, E.M., 2019. A geomorphological assessment of wash-load sediment fluxes and floodplain sediment sinks along the lower Amazon River. *Geology* 47, 403–406. <https://doi.org/10.1130/G45769.1>
- Pelicice, F.M., Agostinho, A.A., Akama, A., Andrade Filho, J.D., Azevedo-Santos, V.M., Barbosa, M.V.M., Bini, L.M., Brito, M.F.G., dos Anjos Candeiro, C.R., Caramaschi, É.P., Carvalho, P., de Carvalho, R.A., Castello, L., das Chagas, D.B., Chamom, C.C., Colli, G.R., Daga, V.S., Dias, M.S., Diniz Filho, J.A.F., Fearnside, P., de Melo Ferreira, W., Garcia, D.A.Z., Krolow, T.K., Kruger, R.F., Latrubblesse, E.M., Lima Junior, D.P., de Fátima Lolis, S., Lopes, F.A.C., Loyola, R.D., Magalhães, A.L.B., Malvasio, A., De Marco, P., Martins, P.R., Mazzoni, R., Nabout, J.C., Orsi, M.L., Padial, A.A., Pereira, H.R., Pereira, T.N.A., Perônico, P.B., Petre, M., Pinheiro, R.T., Pires, E.F., Pompeu, P.S., Portelinha, T.C.G., Sano, E.E., dos Santos, V.L.M., Shimabukuro, P.H.F., da Silva, I.G., Souza, L.B. e., Tejerina-Garro, F.L., de Campos Telles, M.P., Teresa, F.B., Thomaz, S.M., Tonella, L.H., Vieira, L.C.G., Vitule, J.R.S., Zuanon, J., 2021. Large-scale Degradation of the Tocantins-Araguaia River Basin. *Environ. Manage.* 68, 445–452. <https://doi.org/10.1007/s00267-021-01513-7>
- Petts, G.E., Amoros, C., 1996. The fluvial hydrosystem. *Fluv. Hydrosystems* 1–12. https://doi.org/10.1007/978-94-009-1491-9_1
- Polvi, L.E., Wohl, E.E., Merritt, D.M., 2011. Geomorphic and process domain controls on riparian zones in the Colorado Front Range. *Geomorphology* 125, 504–516. <https://doi.org/10.1016/j.geomorph.2010.10.012>
- Potter, P.E., 1978. SIGNIFICANCE AND ORIGIN OF BIG RIVERS. *J. Geol.* 86, 13–33.
- Prado de Morais, R., Gonçalves Oliveira, L., Latrubblesse, E.M., Diógenes Pinheiro, R.C., 2005. Morfometria de sistemas lacustres da planície aluvial do médio rio Araguaia. *Acta Sci. Biol. Sci.* 27, 203–213. <https://doi.org/10.4025/actascibiolsci.v27i3.1278>
- R Core Team, 2021. R: A language and environment for statistical computing. R Foundation for Statistical Computing, Vienna, Austria. URL <https://www.R-project.org/>.
- Rosgen, D.L., 1994. A classification of natural rivers. *Catena* 22, 169–199. [https://doi.org/10.1016/0341-8162\(94\)90001-9](https://doi.org/10.1016/0341-8162(94)90001-9)

- Schumm, S., Rutherford, I., Brooks, J., 1994. Pre-cutoff morphology of the lower Mississippi river, in: Schumm, S., Winkley, B. (Eds.), *The Variability of Large Alluvial Rivers*. American Society of Civil Engineers, New York.
- Schumm, S.A., 1993. River Response to Baselevel Change: Implications for Sequence Stratigraphy. *J. Geol.* 101, 279–294. <https://doi.org/10.1086/648221>
- Sinha, R., Singh, S., Mishra, K., Swarnkar, S., 2022. Channel morphodynamics and sediment budget of the Lower Ganga River using a hydrogeomorphological approach. *Earth Surf. Process. Landforms* 1–20. <https://doi.org/10.1002/esp.5325>
- Stevaux, J.C., Macedo, H. de A., Assine, M.L., Silva, A., 2020. Changing fluvial styles and backwater flooding along the Upper Paraguay River plains in the Brazilian Pantanal wetland. *Geomorphology* 350, 106906. <https://doi.org/10.1016/j.geomorph.2019.106906>
- Suizu, T.M., Latrubesse, E.M., Stevaux, J.C., Bayer, M., 2022. Resposta da morfologia do médio-curso superior do Rio Araguaia às mudanças no regime hidrossedimentar no período 2001-2018. *Rev. Bras. Geomorfol.* 23, 1420–1434. <https://doi.org/10.20502/rbg.v23i2.2088>
- Thorne, C.R., 2002. Geomorphic analysis of large alluvial rivers. *Geomorphology* 44, 203–219. [https://doi.org/10.1016/S0169-555X\(01\)00175-1](https://doi.org/10.1016/S0169-555X(01)00175-1)
- Valente, C.R., 2007. Controles Físicos Na Evolução Das Unidades Geoambientais Da Bacia Do Rio Araguaia, Brasil Central. Ph.D. thesis, Universidade Federal de Goiás.
- Valente, C.R., Latrubesse, E.M., 2012. Fluvial archive of peculiar avulsive fluvial patterns in the largest Quaternary intracratonic basin of tropical South America: The Bananal Basin, Central-Brazil. *Palaeogeogr. Palaeoclimatol. Palaeoecol.* 356–357, 62–74. <https://doi.org/10.1016/j.palaeo.2011.10.002>
- Wittmann, F., Schöngart, J., Piedade, M.T.F., Junk, W.J., 2022. Tropical Large River Wetlands. *Encycl. Inl. Waters* 90–104. <https://doi.org/10.1016/B978-0-12-819166-8.00188-2>
- Yamazaki, D., Ikeshima, D., Sosa, J., Bates, P.D., Allen, G.H., Pavelsky, T.M., 2019. MERIT Hydro: A High-Resolution Global Hydrography Map Based on Latest Topography Dataset. *Water Resour. Res.* 55, 5053–5073. <https://doi.org/10.1029/2019WR024873>

2.3 Artigo 3 – The role of geomorphology on flood propagation in a large tropical river: the peculiar case of the Araguaia River, Brazil³

Abstract

In large rivers, floods are affected by the mosaic of geomorphic and geologic settings of the fluvial corridor. Here, we assess the role of geomorphology on the downstream flood dynamics of the Araguaia River, the largest free-flowing river in Central Brazil. The study integrates and advances existing flood-type classifications. We assess the factors that govern flood hydrograph properties and their downstream propagation by using flow time series, conducting statistical analysis, and evaluating geomorphic and flood metrics. Our findings highlight the role of geomorphology in the transmissions of floods. In the upper and lowermost fluvial segments the geological characteristics of the valley are a major factor. In the intermediate section, two main factors modulate the floods. The wide and complex floodplain plays a major role through storage and buffer effect for floods, and water diversion from the main system to a huge abandoned channel by avulsion governs seasonal flow transfers. The Araguaia is the most geodiverse floodplain of the Amazon-Cerrado ecotone, and floods play a fundamental ecological role in the river-floodplain environments. The combination of diverse factors controlling the flood mechanisms has to be considered when implementing conservation plans for the fluvial corridor and effective river management strategies.

Keywords: Large rivers; Flood transmission; Peak attenuation; Hydrology; Geomorphology, Savanna, Brazil.

2.3.1 Introduction

The economic development and population growth of modern societies located in the tropics have fueled the demand for natural and energy resources. Thus, while the tropics still preserve some of the world's most fascinating and pristine rivers, the intense development pressures are adversely affecting major river systems in this global region [1,2].

The Araguaia River, situated in the central highlands of Brazil, serves as a prime illustration of a large tropical system susceptible to degradation by human activities. Over the past century, it has undergone sedimentation, fluvial metamorphism, and hydrological shifts

³Artigo submetido no periódico científico Water (ISSN: 2073-4441). Impact Factor: 3.4 (2022); 5-Year Impact Factor: 3.5 (2022).

due to intensified deforestation in its watershed since the 1970s [3,4]. Excessive water usage for irrigation places further stress on its water resources [5], with large-scale irrigation projects showing expansion prospects [6]. Additionally, there is interest in exploiting its hydroelectric potential, as evidenced by proposals to construct 70 dams in the watershed, including four large ones in the mainstem [7].

Despite the escalating anthropogenic impact, the Araguaia River, the last and most important free-flowing river nestled within the Cerrado-Amazônia biomes ecotone, offers an incomparable opportunity for investigating the hydrogeomorphic functioning of a large tropical system draining cratonic areas in a savanna's dominated environment.

Previous studies adequately addressed the peculiar transmission patterns of floods that characterize this river's middle section. Along a 430-km of the middle reach, Aquino et al. (2008) observed that downstream gauging stations recorded lower peak flows compared to upstream stations as the drainage area increased, a phenomenon known as peak discharge attenuation [8]. To further enhance the understanding of peak discharge attenuation in the middle Araguaia River, a simplified water budget [9] revealed that water lost to the floodplain during peak discharge attenuation typically returns to the channel by the end of the flooding season, resulting in overall net gains of water.

The free-flowing Araguaia River is the main fluvial artery that sustains the most complex and geodiverse floodplains within the Cerrado biome, alongside hosting the highest diversity of fish species [7]. However, despite being one of the least studied large fluvial systems from an ecological standpoint [7], the available research points to the relevance of the influence of the annual flood cycle on the riverine ecosystem's structure and dynamics [10–15]. Furthermore, a recent study has unveiled a longitudinal diversity within the river continuum [16]. Therefore, exploring the distinct hydrological patterns is relevant to increasing the knowledge of flood transmission mechanisms in large tropical rivers and providing scientific support to fluvial science and basin management programs in the Araguaia basin.

We propose a novel approach to classify and assess flood types methods in the middle Araguaia. We also extend the time frame of pre-existing results by analyzing the period from 1975 to 2014 and tracking all flood events along the entire middle course. We also aim to identify and assess each flood type's key attributes and controlling factors. To accomplish this, we thoroughly examine flood hydrograph properties, conduct statistical analyses, and provide insights into the influence of tributaries on peak flow attenuation. Furthermore, we delve into how distinct geomorphic segments shape the downstream propagation of flood waves. Focusing on the dynamic interface between hydrology and geomorphology enhances our understanding

of the fluvial functions operating in this large and intricate system while providing new insights into flood transmission processes and mechanisms in large tropical rivers.

2.3.2 Study area

The Araguaia River catchment (Figure 1A) covers approximately 385,000 km² in the central highlands of Brazil, where it experiences a tropical savanna climate (Aw). Between 1975 and 2014, average annual precipitation across the basin ranged from 1506 to 2024 mm, with a northward increase [17]. Most rainfall (93% on average) occurs between October and April, while the dry season spans from May to September [18].

The middle Araguaia River, depicted in Figure 1B, stretches from Araguaiana to Conceição do Araguaia and has a mean annual discharge of 4761 m³/s. Its drainage area is augmented from 50,120 to approximately 325,740 km² by the entry of major tributaries. Aquino et al. (2009) classified the eastern tributaries such as the Claro, Vermelho, Peixe, and Crixas-ácu (Figure 1A) as rivers that primarily drain Precambrian metamorphic and igneous rocks originating from hills with structural controls [19]. On the other hand, the Cristalino, Mortes, Tapirapé, and Javaés rivers (Figure 1A) are tributaries mostly draining the Bananal Plain, a Quaternary sedimentary basin featuring a vast aggradational plain formed during the Pleistocene [20].

Along its 1100 km length, the middle Araguaia River flows through a late Quaternary alluvial plain, which is composed of three main morpho-sedimentary units [18,21]. The modern channel exhibits a variety of anabranching patterns, often with a tendency to braid, interspersed with reaches of higher sinuosity [16,22].

The Cerrado biome, which once covered the upper and middle basin, has been replaced by unsustainable agricultural practices since the 1970s, leading to widespread landscape fragmentation and soil erosion [23]. Currently, only 38.5% of the total area is preserved, while 61.5% has been impacted by some form of environmental disturbance, including 44.6% of the riverine vegetation [24]. As a response to land-use/land cover changes, significant changes in the middle Araguaia River's anabranching pattern due to an increase in sediment supply from the upper and middle catchment were reported [3].

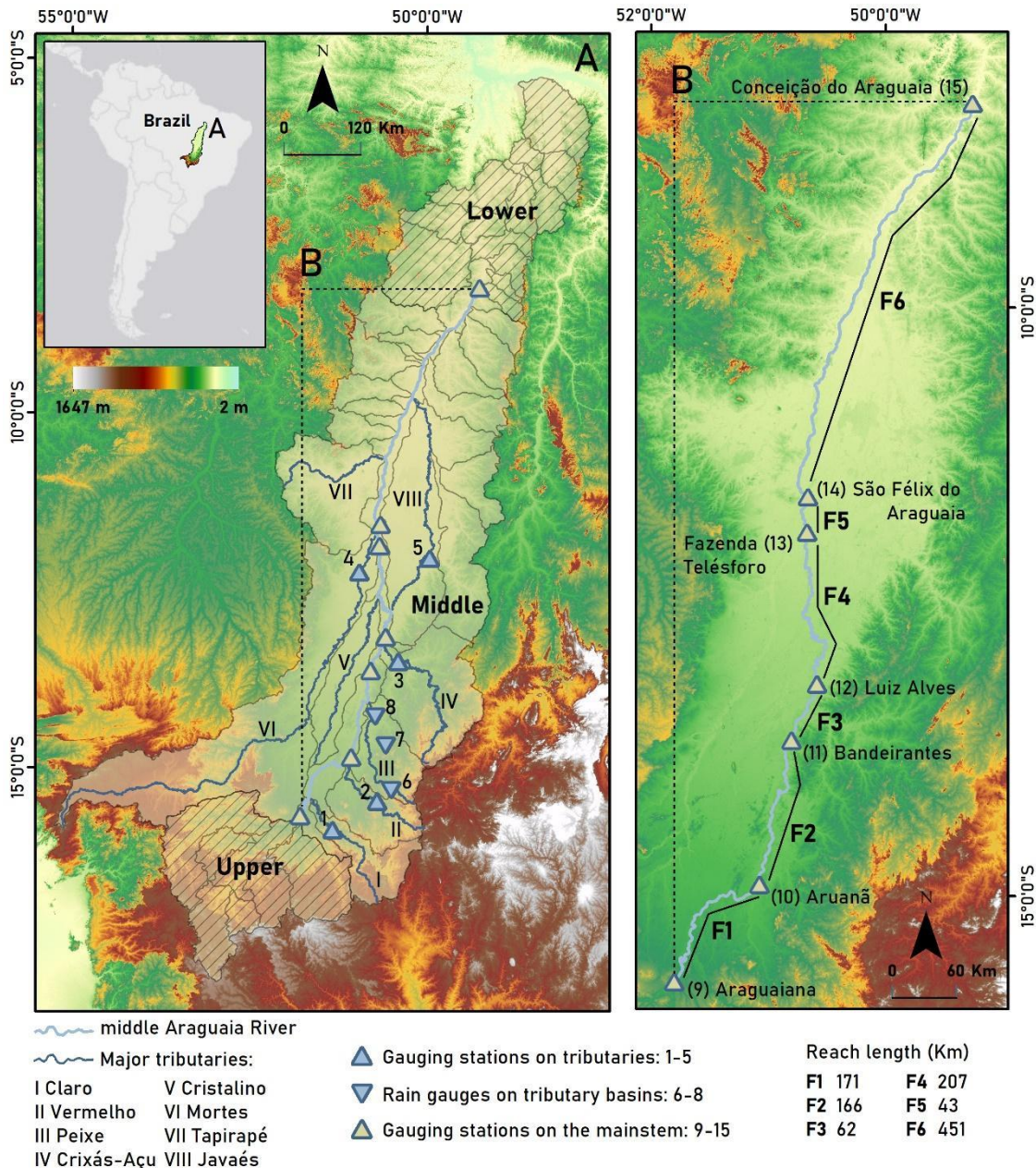


Figure 1. A: Araguaia River basin in central Brazil with major tributaries and selected gauging stations. B: Study reaches (F1-F6) in the middle Araguaia River. Gauge station 1-15 information is provided in Table 1.

2.3.3 Data and methods

2.3.3.1 Hydrological data

Flood events in the middle Araguaia River were analyzed using daily mean discharge time series. The analysis also considered discharge and precipitation data from major tributary watersheds. Gauging station records (Table 1) were obtained from the Brazil's National Water

Agency (Agência Nacional de Águas – ANA). The analysis period spans from October 1975 to September 2014, corresponding to the available discharge measurements for the Luiz Alves station (Figure 1B), which plays a central role in capturing flood patterns influenced by upper-middle basin conditioning factors.

Table 1. River discharge and rain gauge stations with records duration available for analysis.

Number*	Gauging station	Code No.	Upstream catchment area (km ²)	Years of record	Number of missing days
1	Montes Claros de Goiás	24950000	10,100	1975-2014	0
2	Travessão	25130000	5,310	1975-2014	92
3	Jusante do Rio Pintado	25800000	18,300	1980-2014	1411
4	Santo Antônio do Leverger	26300000	59,300	1975-2014	0
5	Barreira do Pequi	26710000	8,150	1987-2014	79
6	Jeroaquara	1550001	-	1975-2014	183
7	Mozarlândia	1450001	-	1975-2014	153
8	Lagoa da Flecha	1450000	-	1975-2014	375
9	Araguaiana	24850000	50,120	1975-2014	0
10	Aruanã	25200000	76,688	1975-2014	0
11	Bandeirantes	25700000	93,027	1975-2014	0
12	Luiz Alves	25950000	117,910	1975-2014	0
13	Fazenda Telésforo	26030000	132,025	1975-1995	1128
14	São Félix do Araguaia	26350000	194,854	1975-2014	61
15	Conceição do Araguaia	27500000	325,740	1975-2014	0

*Numbers 1-15 correspond to the stations' locations as depicted in Figure 1.

Continuous-record gauging stations are present along the mainstem, except for Fazenda Telésforo, which was operational until 1995 and experienced a significant data gap in the early 90s (Table 1). We estimated missing measurements in this gauge using a three-step approach. Firstly, we applied the drainage-area ratio method to estimate the streamflow at the mouth of the Mortes River tributary (Figure 1) based on the available historical data from the Santo Antônio do Leverger station (Table 1). Secondly, we subtracted the estimated outflow of the Mortes River from the São Félix do Araguaia time series (Table 1) to eliminate the influence of this large tributary on the flow measurements at the closest gauging station to Fazenda Telésforo. Lastly, we generated the estimated records using log-log regression equations derived from the relationship between observed discharges at Fazenda Telésforo and the reference downstream flows established in the previous step. To enhance the linearity of the correlation, we derived two regression equations: one for the low-flow period (Jun-Oct) and another for the high-flow period (Nov-May). Both models exhibited high R² values (0.85 and 0.9) and were statistically significant ($p < 0.001$). Hence, we considered this approach valid.

In our analysis of peak discharges in the mainstem, we have considered the significance of bankfull discharge as an important indicator of the initial stages of flood overflows. Field-estimated values of bankfull discharge for Aruanã and Luiz Alves stations were available from Latrubesse (2008) [22]. For the remaining stations in the middle Araguaia where field data was unavailable, we utilized the concept of bankfull discharge as the 1.5-year flood [25] in the annual flood series, employing the Gumbel (extreme value type I) distribution.

In the absence of data directly from the outlets of the tributaries, their relative contribution to the main system was derived from Aquino et al. (2009) [19]. They estimated the average annual discharges of the Araguaia contributing watersheds by establishing a regression relationship between the available gauged data of the tributaries and their corresponding drainage areas, resulting in a high r-squared value of 0.97.

Flood peaks in the middle Araguaia were determined by identifying and extracting the highest flow measurements from the annual hydrographs for each water year (Oct 1 - Sep 30) in the time series. Since multipeak hydrographs are common, we selected the annual maximum daily water discharges at Aruanã (Figure 1B) as the reference flood event to be monitored along the study site. This approach allows us to focus on the most significant floods while disregarding events happening before or significantly later at the subsequent river gauging stations.

2.3.3.2 Flood type classification

An initial flood classification scheme for the middle Araguaia River was proposed by Aquino et al. (2008), categorizing seven typical years into three distinct flood types based on the magnitude of peak discharge in Aruanã gauge and its subsequent progression downstream towards Faz. Telésforo gauge (Figure 1B) [8]. These flood types are as follows:

1. Type A: Very large flood peaks that surpass the channel capacities, such as the floods in 1980 and 1983, resulting in significant peak-transmission losses between Aruanã and Luís Alves (-27%) and even higher losses (-33%) between Aruanã and Faz. Telésforo.
2. Type B: Floods characterized by small magnitudes, showing slight increases up to Luís Alves, followed by relatively consistent levels or modest declines from Luís Alves to Faz. Telésforo. This pattern is evident in the years 1977, 1978, and 1979.
3. Type C: Intermediate floods that exhibit a slight increase in peak flows between Aruanã and Bandeirantes, followed by a trend of losses (-4.5%) between Bandeirantes and Luís

Alves. They may display conservative magnitudes or experience additional decreases in peak discharge between Luís Alves and Faz. Telésforo. This flood type can be observed in the years 1982 and 1985.

This first flood categorization was later revised by Lininger (2013) [26]. Due to the limited availability of continuous gauge data at Faz. Telésforo, the analysis focused on data from Aruanã up to the Luiz Alves gauges. Firstly, a single flood wave tracking approach was adopted, instead of relying solely on the maximum peak discharge recorded at each station. Additionally, it was defined lower and upper limits for peak magnitudes in Aruanã as follows: Type A: 5000 m³/s and above, Type B: below bankfull discharge up to approximately 4000 m³/s, and Type C: predominantly ranging from 4500 to 5500 m³/s [26]. That autor also quantified the downstream rates of change in peak discharge for all the analyzed years (1975-2003) and even proposed two new categories: Types D1 and D2. These types exhibit distinct patterns of peak discharge translation downstream, characterized by marked increases followed by marked decreases and vice versa. This distinguishes them from the other flood types (A, B, and C) that display more monotonic trends along the river. Type D1 floods are characterized by higher peak discharges at Aruanã (average: 4003 m³/s), while Type D2 floods occur below bankfull flows (average: 2929 m³/s), resulting in more significant absolute peak reduction downstream for the former [26].

In this paper, we further refine the flood-type classes previously proposed for the middle Araguaia River. This updated classification is presented in the results section. Some considerations drove our choice to improve the groupings. Firstly, the area coverage of the previous studies was limited to only one thirds of the total length of the middle section of the Araguaia. A thorough hydrogeomorphologic analysis enclosing the whole middle Araguaia River was still pending. Thus, we expanded our analysis to encompass all gauge stations along the middle Araguaia River. Secondly, we recognized that the Brazilian National Water Agency had reviewed historical flow data estimates for the middle Araguaia River and addressed data gaps identified in the previous study [26]. Therefore, we aimed to establish consistent flood types based on the revised flow records and the extended time series from 1975 to 2014. Additionally, we sought to offer further insights into the distinct behaviors of the D1 and D2 flood types concerning the more typical patterns observed in types A, B, and C.

To achieve the scope, we divided our study site into six fluvial reaches (Figure 1B) whose limits correspond to the locations of consecutive gauge stations: F1 (Araguaiana-Aruanã), F2 (Aruanã-Bandeirantes), F3 (Bandeirantes-Luiz Alves), F4 (Luiz Alves-Faz.

Telésforo), F5 (Faz. Telésforo-S.Félix do Araguaia), and F6 (S.Félix do Araguaia-Conceição do Araguaia).

Four hydrological years (1996, 1998, 2004, and 2010), were excluded from our analysis as they exhibited anomalous flood translation patterns that did not align with any of our proposed categories. In 1996, the peak flow in Aruanã ($3099 \text{ m}^3/\text{s}$) was below bankfull discharge, but significant losses (-29%) occurred up to Luiz Alves. Similarly, in 1998, a low flood in Aruanã ($3627 \text{ m}^3/\text{s}$) showed unusual high losses (-47%) in Bandeirantes, followed by substantial gains (+78%) in Luiz Alves. On the other hand, 2004 and 2010 were characterized by high flood flows in Aruanã (7931 and $7438 \text{ m}^3/\text{s}$, respectively). Still, they experienced exceptionally large losses (-50% and -58%) between Aruanã and Bandeirantes, followed by increases in the subsequent station (+12% and +18%). Due to the derivation of flood events from observed discharge values, primarily obtained by applying stage observations to a stage-discharge relationship, it is important to acknowledge the potential influence of observational errors or instrumental inaccuracies on sudden and random shifts in peak discharge. Consequently, additional investigations are warranted to better understand these anomalies within the data series.

2.3.3.3 Geomorphic and flood metrics

The six fluvial reaches (F1-F6) selected for examining the downstream behavior of flood waves in the middle Araguaia encompass the five geomorphic segments defined in a previous article by the authors [16]. These segments were established by statically grouping 19 reaches with relatively uniform morphological attributes, such as channel and valley gradients (measured in cm/km) and the degree of floodplain development, indicated by the entrenchment ratio, a metric derived from the ratio of floodplain width to channel width, as described by Polvi et al. (2011) [27]. Channel planform metrics like sinuosity [28] and anabranching [29] indexes were also incorporated. By considering these elements, we explored the role of channel and floodplain morphology in controlling the translation and attenuation of flood peaks, addressing another crucial research question in our study.

Five flood metrics, namely peak discharge ratio (QpR), slope of the rising limb (S), flood wave celerity (c), water volume (V), and coefficient of overflow hydrograph asymmetry (ν) were employed to characterize the flood events and their corresponding flood types along the study site. The first two metrics, QpR and S, were adapted from Spellman et al. (2019) [30]. QpR quantifies the attenuation or intensification of flood peaks between consecutive reaches as

the ratio of peak discharge observed at the downstream to the upstream stations. The slope of the rising limb (S) in $\text{m}^3\text{s}^{-1}/\text{day}$, represents the average rate of flood rise from overflow to the peak discharge, calculated as the difference between the hydrograph peak (Q_p) and bankfull discharge (Q_{bf}) divided by the number of days (t_1) between them. Flood wave celerity (c), measured in m/s, indicates the speed at which peak flows propagate downstream and is determined by dividing the river reach length (m) by the peak-to-peak travel time (s) between the upstream and downstream stations [31]. Water volume (V) in km^3 was derived using the 'add_daily_volume()' function from the fasstr package, a Flow Analysis Summary Statistics Tool for R [32]. This function converts daily mean discharges into daily volumetric flows. The volume was summarized both annually and monthly to evaluate overall net changes in flow along F4 (For more detailed information on the utilization and interpretation of this metric, please refer to the subsequent sections). Additionally, it was calculated cumulatively to estimate the average total overflows of station hydrographs (V_{ovf}). Finally, the coefficient of overflow hydrograph asymmetry (v) was calculated as the ratio of the duration of the flood overflows in the rising phase (t_1) to the duration of the flood overflows in the recession phase (t_2) [33]. Flood metrics are synthesized in Figure 2.

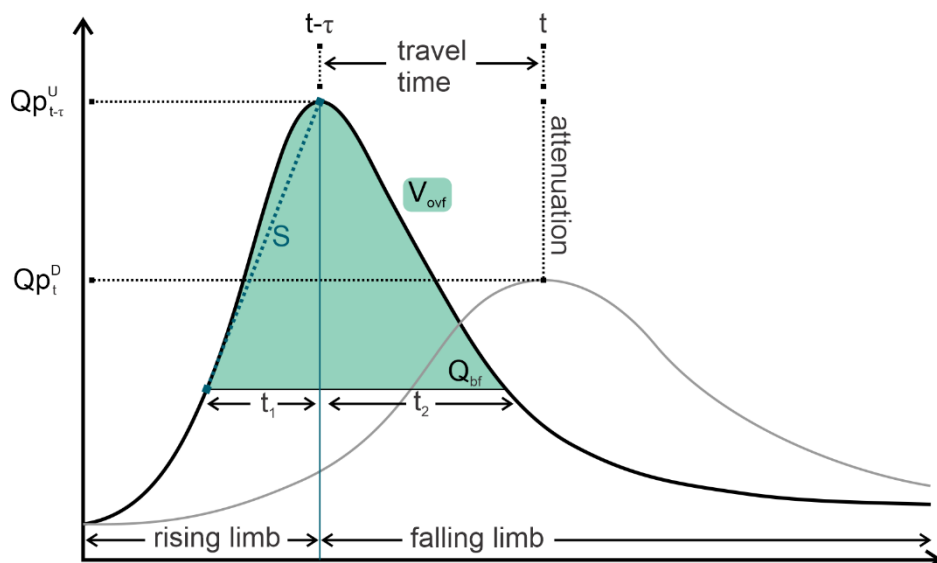


Figure 2. Flood hydrographs showing flood metrics employed in the present study.

2.3.3.4 Statistical analysis

The hydrological data management and its statistical analysis were conducted using the RStudio IDE [34]. Before performing each statistical analysis, we assessed the normality of data distribution using the Shapiro-Wilk test with a significance level of 5%.

To define the significance, strength, and direction of the relationships between QpR values and peak discharges observed at the upstream station, we employed the Spearman Rank correlation method. A significance level of $p < 0.05$ was set, and the Spearman's Rho (ρ) correlation coefficient was categorized as low (<0.39), moderate (0.4-0.59), or strong (0.6-1).

To describe the relationships between the water volume inflows/outflows in F4 and the volume losses to the Javaés River, we performed regression analysis. The overall quality of the fitted model was evaluated using R-squared (R^2), Residual Standard Error (RSE), and the p-value (t-test). A high value of R^2 (ranging from 0 to 1) indicates a good correlation, while a small RSE suggests a well-fitted model. The significance of the predictor on the response variable was set at $p < 0.05$.

The significance of differences among the flood-type groups was assessed by carrying out a one-way analysis of variance (ANOVA). When the results were statistically significant ($p < 0.05$), we conducted Tukey's HSD test for post-hoc pairwise comparisons to identify the specific locations where significant differences ($p < 0.05$) occurred. Additionally, we employed a two-way ANOVA to investigate the hypotheses related to the main factors and potential interactions that influence the notable peak discharge changes observed in F2 and F3.

2.3.4 Results

2.3.4.1 The flood types in the middle Araguaia River

Floods in the middle Araguaia River were characterized based on the magnitude of the maximum annual flood peaks in Aruanã and the modes of downstream flood wave transmission. In our study, we built upon and adapted the classification schemes proposed by previous authors [8,26]. As a result, annual flood events were grouped into 5 distinct flood types (Figure 3).

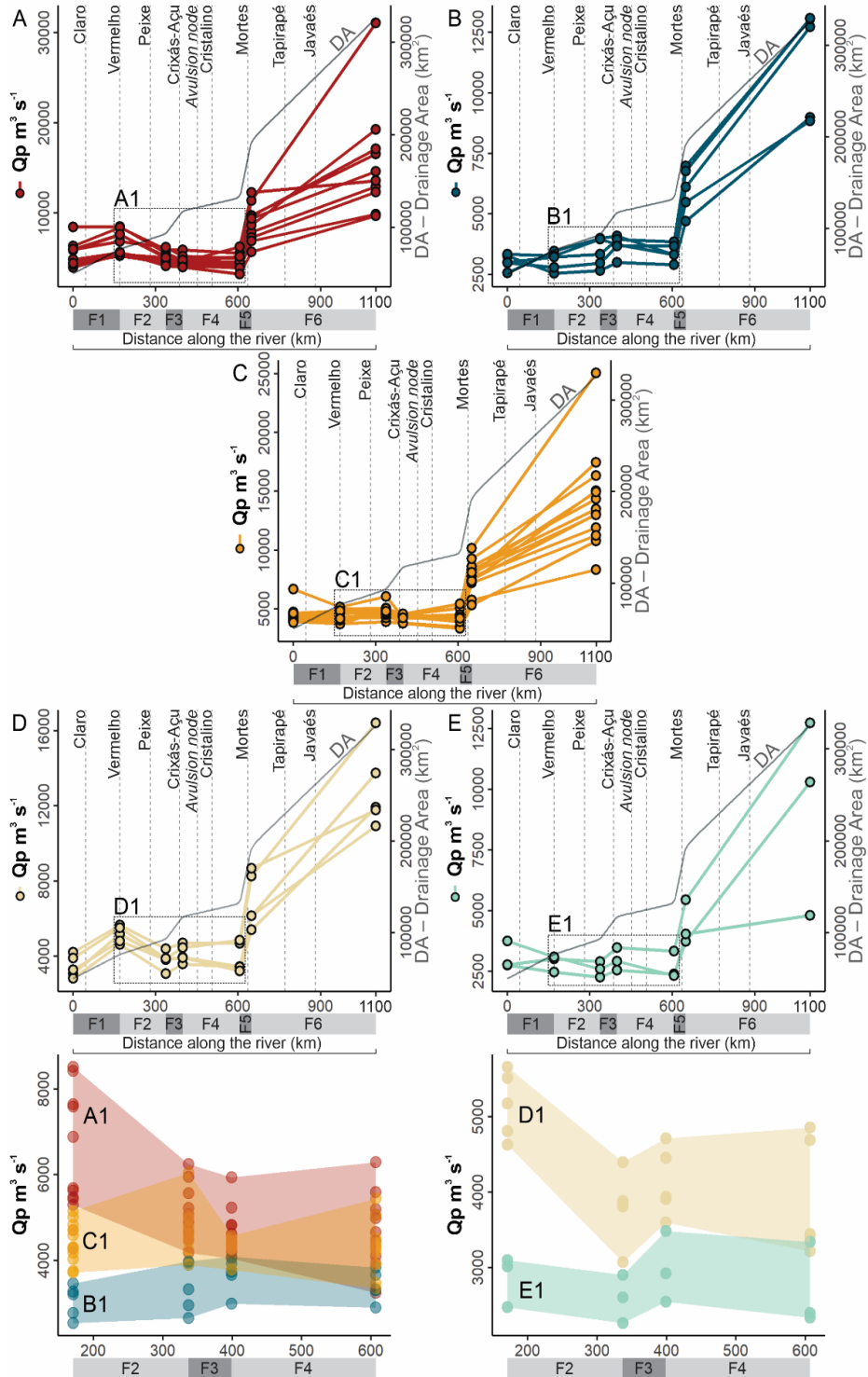


Figure 3. Classification of flood events in the middle Araguaia River between 1975 and 2014. A (Type A), B (Type B), C (Type C), D (Type D1), and E (Type D2) display downstream variations in peak flow (Q_p) and the corresponding increases in drainage area (DA) for the gauging stations located along the study site. The vertical dotted lines indicate the entry points of the major tributaries. F1-F6 refer to the reaches between consecutive gauging stations (Figure 1B), while A1-E1 represent the absolute values of Q_p for each flood type between Aruanã and Faz. Telésforo. The maximum and minimum values are defined by upper and lower envelopes.

Floods classified as type A represent the highest hydrological events in the historical record. These floods exhibit peak values of 5292-8510 m³/s at Aruanã (Figure 3A1), with notable attenuation downstream, resulting in flow losses ranging from 7% to 35% between Aruanã and Bandeirantes. The stretch between Aruanã and Faz. Telésforo experiences even higher losses, reaching up to -43%, except for 1991, which recorded a 12% increase (Figure 4A). It is worth noting that these periods of large flow reductions occur despite the contributions of tributaries to the system and the increase in drainage area. The average discharges of the tributaries are estimated to be 13% (Peixe River, Figure 1A) and 21% (Crixás-Açu River, Figure 1A) of the total flow gain in reaches F2 and F3, respectively. Furthermore, the drainage area increases from 76,688 km² to 132,025 km² between reaches F2 and F4 (Figure 3).

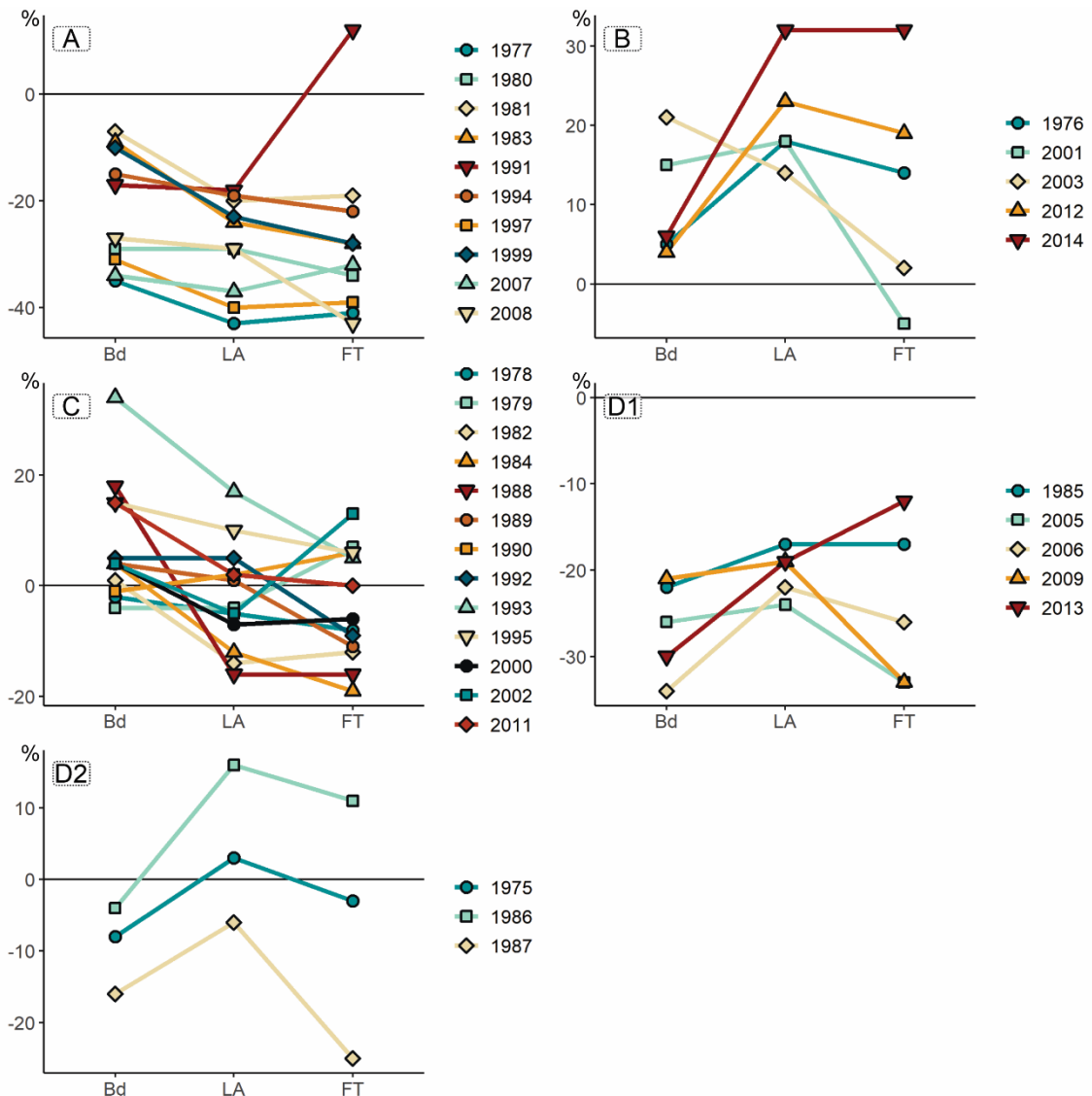


Figure 4. Percentage change rate in downstream peak flows for each flood class (A, B, C, D1, and D2) between 1975 and 2014. The peak flow value in Aruanã was considered the reference to calculate changes in Bandeirantes (Bd), Luiz Alves (LA), and Faz. Telésforo (FT).

Type B flood events are relatively less severe than Type A, with peak flow values (2542-3464 m³/s, Figure 3B1) close to the bankfull discharge (3200 m³/s) at Aruanã and a tendency for increasing peak flow towards Luiz Alves (14-32%, Figure 4B). Maintenance or minor losses in peak flow are observed between Luiz Alves and Fazenda Telésforo (Figure 4B).

Type C encompasses a range of intermediate peak flows (3716-5146 m³/s, Figure 3C1) above the bankfull discharge in Aruanã. These flows demonstrate a general pattern of gains in Bandeirantes (up to 34%), followed by losses in Luiz Alves. In Faz. Telésforo, the changes do not exhibit a consistent trend. Although most years show losses, occasional modest gains (5-13%) are observed between Aruanã and Faz. Telésforo in 1979, 1990, 1993, 1995, and 2002 (Figure 4C).

Flood types D (Figure 3D1 and 3E1) display ranges of flow variability in Aruanã (D1: 4628-5658 m³/s, D2: 2473-3099 m³/s) that overlap with those of types C and B, respectively. However, the main characteristic distinguishing class D from the others is the decrease in peak flow observed in Bandeirantes, followed by increases in Luiz Alves, and a general loss tendency in Faz. Telésforo (Figures 4D1 and 4D2). Type D2 has peak flow values that are lower than the bankfull discharge (3200 m³/s) in Aruanã, resulting in less pronounced peak decreases (average: -9%) in Bandeirantes when compared to type D1 (average: -26%).

2.3.4.2 Propagation of flood waves along the middle Araguaia River

To identify flood propagation patterns along the entire middle Araguaia River, we tracked classified events at stations upstream (Araguaiana) and downstream (São Félix do Araguaia and Conceição do Araguaia) from the reference stations (Aruanã-Bandeirantes-Luiz Alves-Faz.Telésforo) during the study period. Figure 5 presents the values of QpR for consecutive stream gauges and their correlation with the magnitude of peak flow upstream of the flood wave.

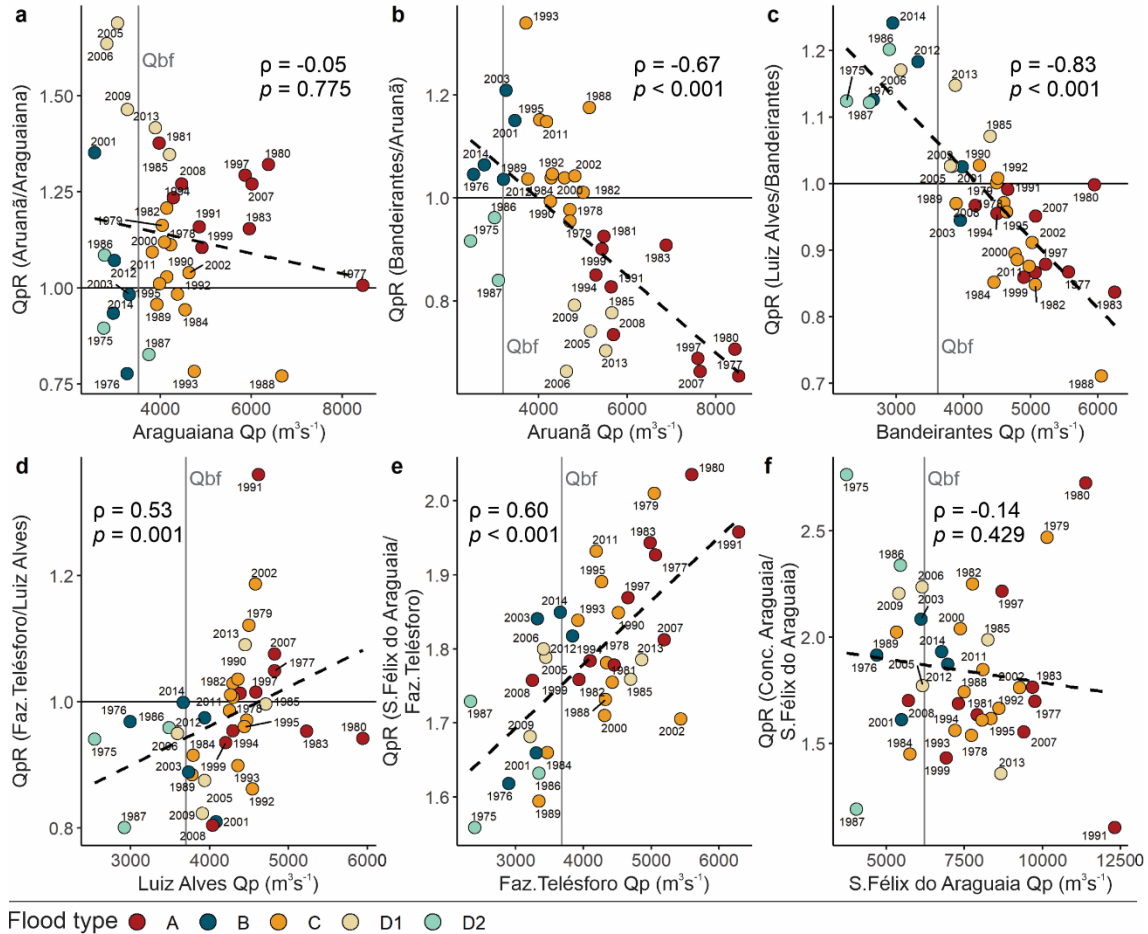


Figure 5. Peak discharge ratio (QpR) plotted against the absolute value of upstream peak flow (Qp) for successive reaches F1 (a), F2 (b), F3 (c), F4 (d), F5 (e), and F6 (f). Qbf: bankfull discharge. The Spearman correlation coefficient (ρ) and the associated p-value (p) provides a measure of correlation significance.

For reach F1 (Araguaiana-Aruanã, Figure 1B), the upstream Qp value did not prove to be significant ($p > 0.05$) in attenuating the downstream flood wave (Figure 5a). Interestingly, we observed attenuations ($\text{QpR} = 0.78-0.98$) in F1 associated with peak flows slightly below or above the bankfull discharge in Araguaiana ($\text{Qbf} = 3528 \text{ m}^3/\text{s}$). It is worth noting that the floods in F1 can also be influenced by two major tributaries - Claro and Vermelho (Figure 1A). The estimated annual average discharge of these tributaries indicates a contribution of 33% to the flow at the downstream station, where the drainage area increases from $50,120 \text{ km}^2$ to $76,688 \text{ km}^2$.

Flood wave attenuation is a prominent feature of the maximum flows recorded in F2 (Aruanã-Bandeirantes, Figure 5b) and F3 (Bandeirantes-Luiz Alves, Figure 5c). The upstream Qp value had a significant impact ($\rho = -0.67$ and -0.85 , $p < 0.05$) in determining the rate of

reduction of peaks transmitted downstream. F2 clearly distinguishes flood-type clusters along this linear relationship (Figure 5b). In F3, the bankfull discharge (Bandeirantes $Q_{bf} = 3621 \text{ m}^3/\text{s}$) constitutes a noticeable threshold for the beginning of attenuations (Figure 5c).

There is a general increasing trend ($\rho = 0.53$, $p < 0.05$, Figure 5d) of downstream peak flows (Faz. Telésforo) in F4 as a function of upstream Q_p magnitude (Luiz Alves). However, this reach exhibits distinctive attenuation patterns. It experiences losses in all events below bankfull discharge (Luiz Alves $Q_{bf} = 3700 \text{ m}^3/\text{s}$), with more significant reductions ($Q_{pR} = 0.8\text{-}0.91$) observed at some flows just above this threshold ($3736\text{-}4085 \text{ m}^3/\text{s}$), and more minor losses ($Q_{pR} = 0.94$ and 0.95) for the two largest events in the Luiz Alves historical series - 1980 and 1983. In F4, the Araguaia River receives the contribution of the Cristalino River (Figure 1A). Unlike the right-bank tributaries (Claro, Vermelho, Peixe, and Crixás-açu) in reaches F1-F3, the Cristalino is currently an underfit system within the abandoned fluvial belt it occupies. It features a narrow channel that becomes more active during the rainy season [20].

The final two reaches of the Middle Araguaia (F5 and F6) are notable for the lack of reduction in peak flows ($Q_{pR} > 1$, Figures 5e and 5f) between gauging stations. The strong and positive relationship observed in F5 ($\rho = 0.60$, $p < 0.05$, Figure 5e) indicates that upstream (Faz. Telésforo) increases in maximum flow lead to larger peak flows downstream at the S. Félix do Araguaia station, even when these exceed the bankfull discharge (Faz. Telésforo $Q_{bf} = 3683 \text{ m}^3/\text{s}$). Q_{pR} values in this reach ranged from 1.56 to 2.04 (Figure 5e), with these increases primarily influenced by the entry of the main Araguaia tributary, the Mortes River (Figure 1A), which expands the contributing drainage area from $132,025 \text{ km}^2$ to $194,854 \text{ km}^2$ and has an annual mean flow equivalent to 32% of the flows measured at the downstream station.

In the F6 reach, the peak upstream (at S. Félix do Araguaia) does not have an explicit control ($p > 0.05$, Figure 5f) over the fluctuation of transmitted peaks downstream (at Conc. Araguaia). Flood flows in this reach reflect the influence of major tributaries, such as the Javaés and Tapirapé, which, together with other smaller basins arranged along the axis of the lower middle valley (Figure 1A), increase the drainage area by 61% and integrate a substantial component of the high flows recorded at Conceição do Araguaia. At this last station, Q_{pR} values ranged from 1.10 to 2.76 (Figure 5f).

2.3.4.3 Impact of tributaries on mainstem flood attenuation

The impact of tributaries on mainstem flood attenuation can be challenging to assess, especially in the case of large rivers with scarce hydrological data, as it depends on a range of

factors, such as tributary size, location, and watershed characteristics, the complex array of floodplain features, and the timing, intensity, and spatial distribution of precipitation. Moreover, the lack of gauged data on tributary outlets further complicates accurate assumptions about tributary contribution to downstream flood magnitude. Nevertheless, we have briefly analyzed discharge records from tributaries that feed into mainstem reaches exhibiting attenuating behaviors (F1-F3). Unfortunately, due to the lack of river flow measurements in the Cristalino River, we could not assess its impact in F4.

Data from two gauges (Figure 1A, stations 1 and 2) located approximately 82% and 37% of the drainage area of the Claro and Vermelho watersheds, respectively, revealed that smaller flood events exhibiting a decline in downstream peak discharge at F1 (i.e., 1975, 1976, 1984, 1987, 1989, 2003, and 2014) also displayed peak magnitudes that were 10-53% (Claro River, Figure 6a) and 15-65% (Vermelho River, Figure 6b) lower than the long-term average of peak events in both contributing watersheds. Except for 1984, when a minor increase (5%) was detected, the mean annual flows for these years were 26-50% (Claro River, Figure 6c) and 5-52% (Vermelho River, Figure 6d) lower than the long-term mean annual flow, suggesting that the subwatersheds experienced more frequent episodes of lower flow during these years.

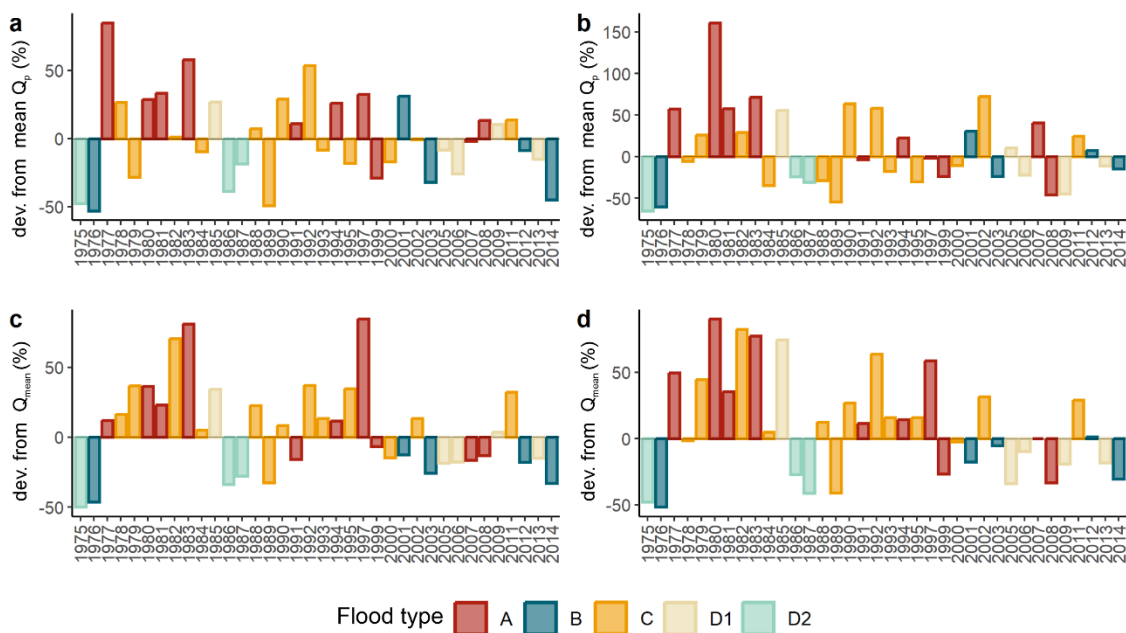


Figure 6. Deviations of Q_p from the long-term average peak flow (1975-2014) expressed as a percentage for the (a) Claro and (b) Vermelho tributaries, as well as the deviations of Q_{mean} from the long-term mean annual flow (1975-2014) expressed as a percentage for the (c) Claro and (d) Vermelho tributaries.

Previous research into the hydrological characteristics of the system revealed that the connection between the river channel and floodplain is established when the river reaches the bar full level, which occurs when the sandbars are entirely submerged, equivalent to 66% of the bankfull stage at the Aruanã station [35]. Thus, it can be inferred that in drought years, anabranches functioning below the bankfull stage may still divert water to the floodplain. In such circumstances, the floodplain lakes and channels experiencing reduced storage and surface-water supply may contribute to discharge losses near bankfull flows (Figure 5a).

The attenuation patterns in reaches F2 and F3 have already been studied, and the geomorphic influence on the flood's transmission mechanisms and the floodplain's water storage capacity was highlighted [8,9]. Since the length of F3 is only 37% of that of F2 (Figure 1), expressing peak discharge gains and losses per unit channel length between these consecutive reaches provides a more accurate comparison of the effectiveness of the reaches in temporarily storing floodwaters (Figure 7a).

The analysis of potential water available for tributary runoff in F2 involved an assessment of the mean annual precipitation of the Peixe basin (Figure 7b), considering the unavailability of in-situ flow data for the main tributary river. To evaluate the input peak flows in F3, we obtained annual peak-discharge data for the Crixás-Açu River (Figure 7c) from a gauge station located within 78% of its total watershed area (Figure 1A, station 3). Our one-way ANOVA reveals a significant difference ($p < 0.05$) in annual rainfall within the Peixe basin (Figure 7b) and peak discharges along the mainstem (Figures 7d and 7e) among certain flood-type categories. However, when it comes to peak discharges in the Crixás-Açu River, there were no distinct patterns of magnitude consistent with the mainstem flood types ($p > 0.05$, Figure 7c), ruling out the requirement for *post-hoc* comparisons.

Despite showing similar peak magnitudes in Aruanã ($p > 0.05$, Tukey *post-hoc* comparisons, Figure 7d), types B and D2 exhibit contrasting behaviors in F2 (Figure 7a). In this reach, type D2 experiences minimal net losses, even below bankfull discharge (Figure 7d), which can be associated with the lowest average annual precipitation values recorded in the Peixe basin (Figure 7b). These drier years, accompanied by reduced flood flows, have also been observed in the preceding reach F1 (Figure 6).

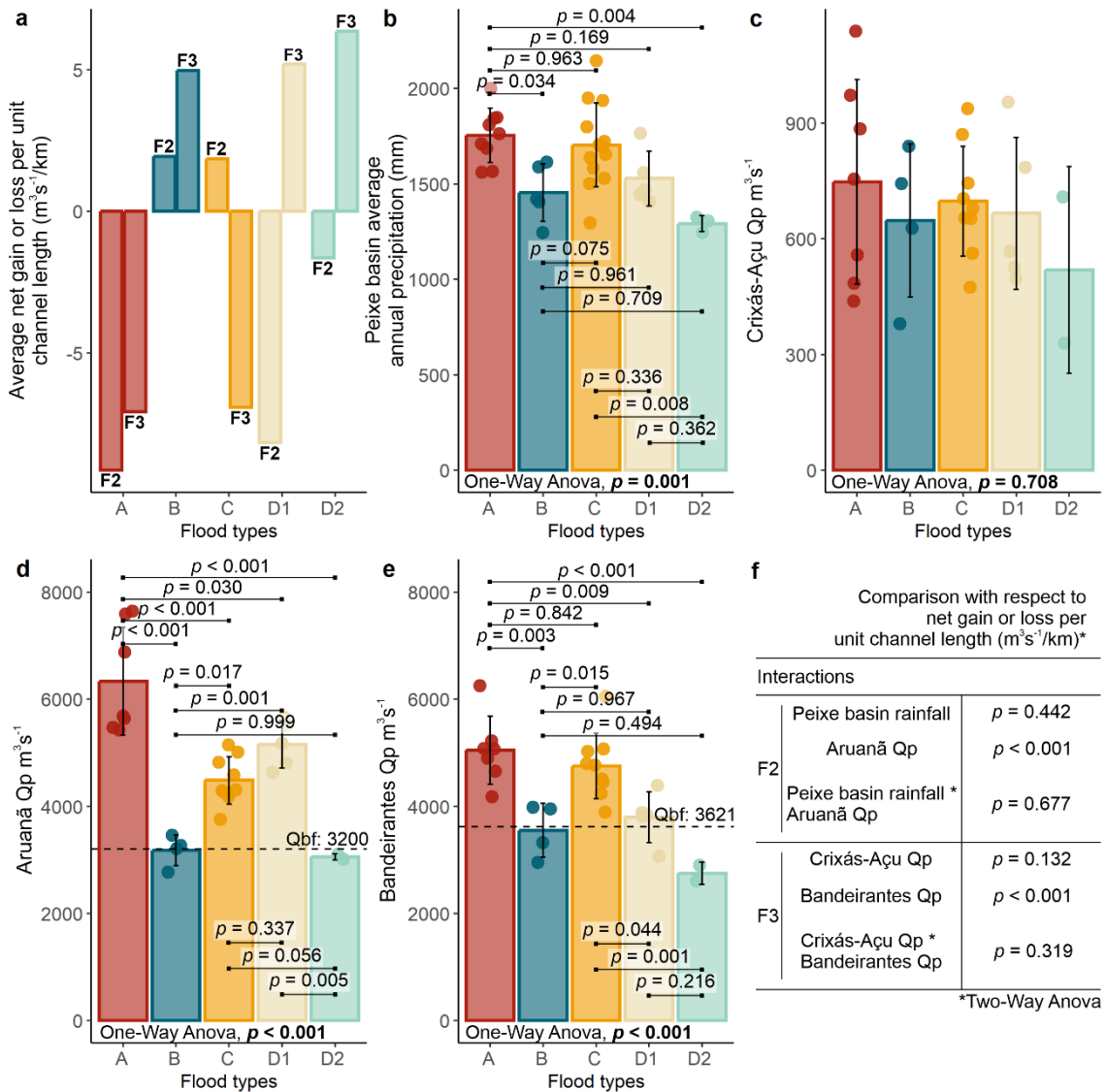


Figure 7. Analysis of peak discharges (Qp) and precipitation patterns in reaches F2 and F3. (a) Net gain or loss in peak flow (m^3/s) per unit channel length (km). (b) Average annual precipitation in the Peixe River basin based on annual rainfall totals from available stations (6, 7, and 8 in Figure 1A). (c) Qp for the lower course of the Crixás-Açu River. (d) Qp for the Aruanã station in the mainstem. (e) Qp for the Bandeirantes station in the mainstem. The colored bars, vertical error bars, and dots represent the mean, standard deviation, and absolute values, respectively, of all yearly measurements associated with a specific flood type in the Araguaia River. The bankfull discharge (Qbf) is indicated on the graphs. Significance levels, represented by p-values, are shown for the one-way ANOVA and Tukey's pairwise comparisons (horizontal lines) in panels (b), (c), (d), and (e). Additionally, the p-values of the two-way ANOVA are provided in panel (f) to identify possible interactions between the net gain or losses in F2 and F3 and the variables depicted in panels (b), (c), (d), and (e).

Tukey *post-hoc* comparisons revealed no significant differences in precipitation patterns of the Peixe basin among flood types A, C, and D1 (Figure 7b). It is interesting to note that type C exhibits average annual precipitation values as high as those observed in the largest type A events. Despite this similarity, type C demonstrates a net gain in F2 that is 5 times smaller than the net loss per unit of channel length estimated for type A (Figure 7a). Conversely, type D1 floods have lower average precipitation values than type C but experience net losses in F2 that are 4.4 times larger than the average gains per unit of channel length observed for type C (Figure 7a).

Such divergent trends observed in intermediate to large flood types can be reasonably explained based on our two-way ANOVA analysis (Figure 7f). The analysis indicates that the magnitude of the peak (Q_p) at the upstream gaging stations Aruanã (Figure 7d) and Bandeirantes (Figure 7e) in the mainstem exerts the primary control ($p < 0.001$) in determining the rates of channel losses and gains along reaches F2 and F3. The statistical analysis reveals that neither tributary precipitation (Figure 7b), tributary peak flow (Figure 7c), nor the interaction effect of these variables with upstream peak discharge show statistical significance ($p > 0.05$) in explaining the absolute peak change per unit channel length along reaches F2 and F3 (Figure 7f). These findings align with the outcomes of our previous correlation analysis (Figures 5b and 5c).

2.3.4.4 Influence of geomorphic variables on the floods

The most striking downstream trends of flood types in the middle Araguaia River cannot be attributed solely to the flow regime; channel and floodplain morphology (Figure 8) also play a crucial role in determining the river's capacity to convey or store floods, with significant implications for associated hydrograph properties (Figure 9).

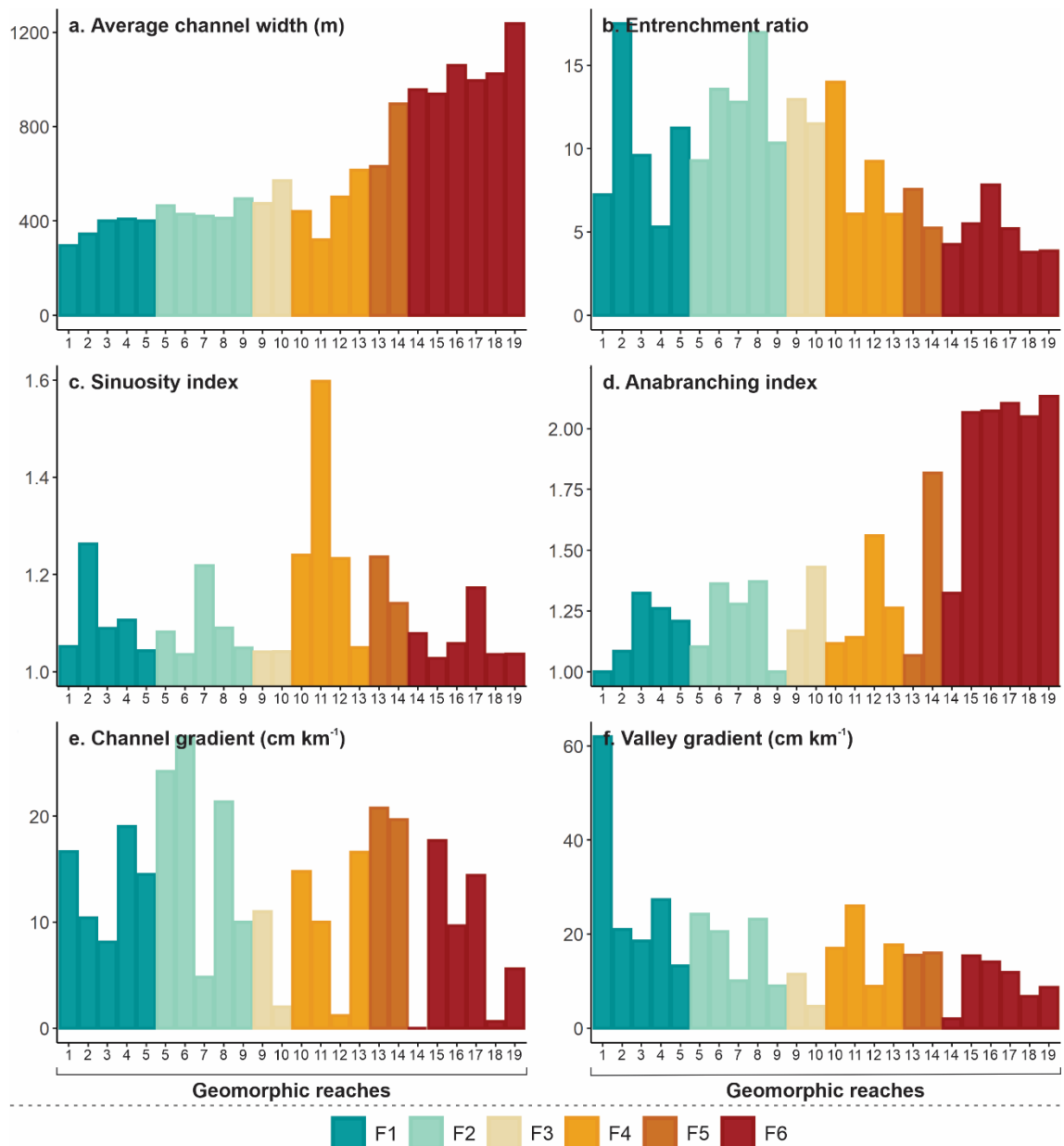


Figure 8. Channel and floodplain metrics of the 19 geomorphic reaches previously defined [16] for the middle Araguaia River. F1-F6 are the reaches between gauging stations (Figure 1B).

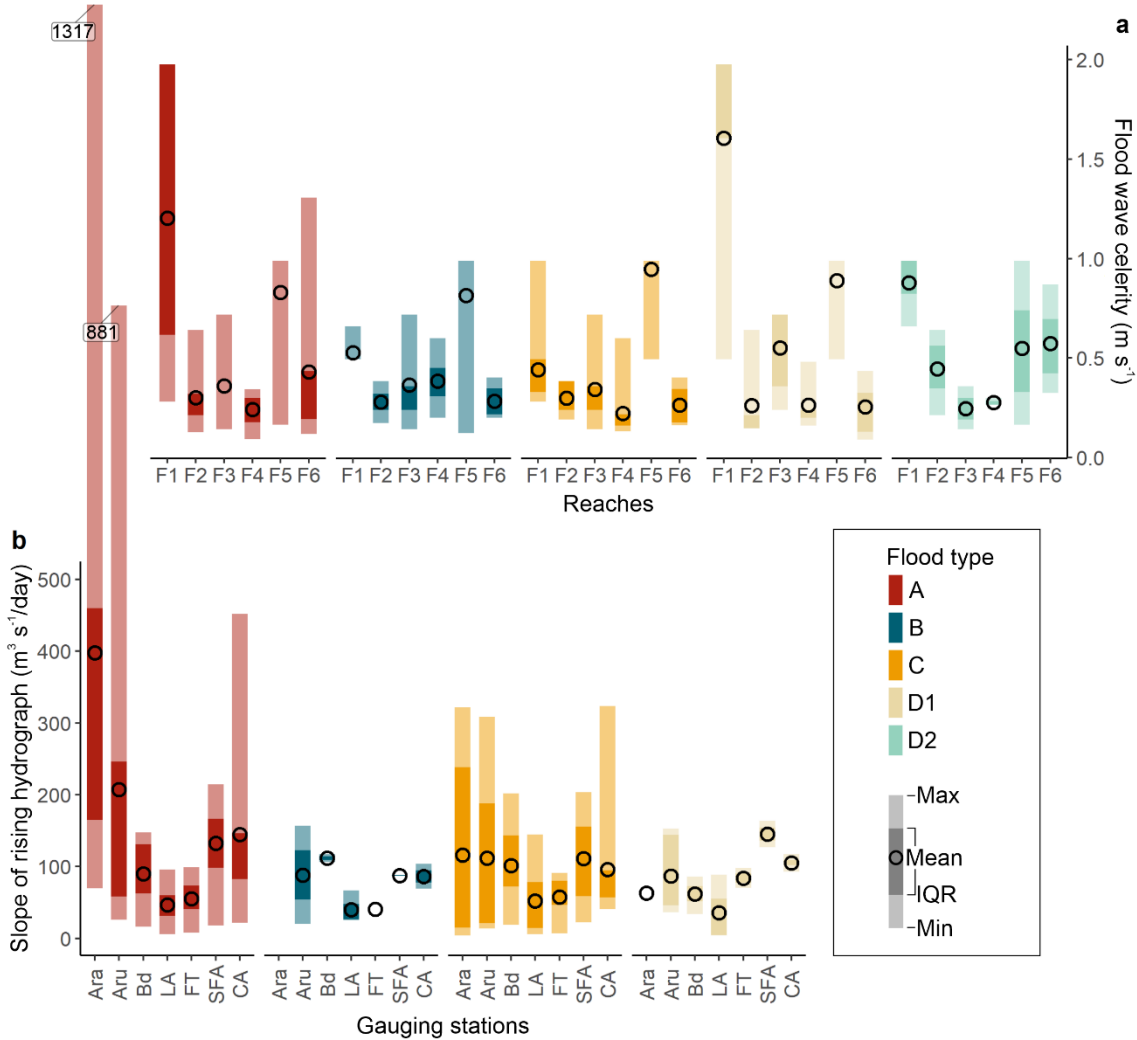


Figure 9. Flood hydrograph properties for each flood type of the middle Araguaia River from 1975 to 2014. (a) Flood wave celerity from peak-to-peak discharges between every river reach monitored (F1-F6). (b) Slope of the rising limb from bankfull to peak discharges for each gauging station (Ara = Araguiana; Aru = Aruanã; Bd = Bandeirantes; LA = Luiz Alves; FT = Faz. Telésforo; SFA = S. Félix do Araguaia; CA = Conc. Araguaia). Gauge stations locations in Figure 1.

F1 is characterized by a low-sinuous channel pattern (sinuosity: 1-1.3, Figure 8c) with narrow channel widths (averaging 296-408 m, Figure 8a). Downstream sections in this reach are less constrained (Figure 8b), typically resulting in the natural attenuation of peak discharges due to the floodplain's increased water storage capacity [31,36]. However, in F1, a combination of moderate channel gradients ($8\text{-}19 \text{ cm km}^{-1}$, Figure 8e) and high valley slopes (13-62 cm/km, Figure 8f) facilitates the rapid conveyance of floodwaters, limiting their contact with the floodplain and impeding the slowing down of large peak flows (Figure 5a). The high wave celerities observed for all flood types in F1 (Figure 9a) evidence this process. The presence of

abrupt rising limbs in the hydrographs of type A floods at consecutive stations in F1 (Figure 9b) further indicates the efficient conveyance of large floods in this reach.

While there were no significant changes in sinuosity (Figure 8c) or anabranching (Figure 8d) indexes between F1 and F2, the modern channel widens by approximately 20% (Figure 8a) in this second reach and flows into an extensive floodplain (entrenchment ratio: 9-17, Figure 8b). The steeper channel gradients at the beginning of F2 ($24\text{-}28 \text{ cm km}^{-1}$, Figure 8e) allow for better conveyance of fast flood waves from F1, producing hydrographs at the Aruanã gauge site with high peak discharge relative to the overall runoff in the rising limb, particularly in the case of large type A floods (Figure 9b). However, as F2 progresses, this channel gradient decreases, and floodwaters inundate the wide floodplain with gentler slopes (Figure 8f). As a result, all flood types in F2 experience a reduction in flood wave velocity (Figure 9a), especially those with considerably smaller peak discharges at the Bandeirantes gauge downstream (i.e., types A, D1, and D2). The lowered and broadened hydrographs of the Bandeirantes station (Figure 9b) support this claim, except for the smallest type B events, indicating that floodplain morphology has little effect on peak discharges close to bankfull. In reach F3, the presence of a gently sloping channel (Figure 8e) in the relatively flat areas of the valley (Figure 8f) allows for the downstream extension of the floodplain's capacity to store (delay) excess floodwater and attenuate flood peaks. This feature may explain the flatter rising limbs of the hydrographs for all flood types at the Luiz Alves station (Figure 9b).

Peak discharge losses in F4 are attributed to water transfer from the main river to its old abandoned river branch, Javaés River [8]. In this reach, it is necessary to note that there is no straightforward relationship between upstream peak magnitude (Figure 10a) and the rate of peak loss (Figure 10b). For instance, we observed that maximum discharges of type A (i.e., 1997 and 2007, Figure 10a) exhibited downstream peak increases (Figure 10b). Conversely, we found that type D2 (e.g., 1987) and B (e.g., 2003), with flows just below to slightly above bankfull discharge (Figure 10a), displayed significant peak reductions (Figure 10b). To address these peculiar transfer patterns, we computed annual net changes (overall gain or loss) in volume (V in km^3) between Luiz Alves and Faz. Telésforo (Figure 10c). Additionally, we estimated the total volume of water discharged into the Javaés River (Figures 10d and 10e) by considering the daily flows recorded in the former channel (Figure 1A, station 5) in the mainstem water balance equation ($V_{\text{Faz. Telésforo}} - (V_{\text{Luiz Alves}} + V_{\text{Javaés}})$).

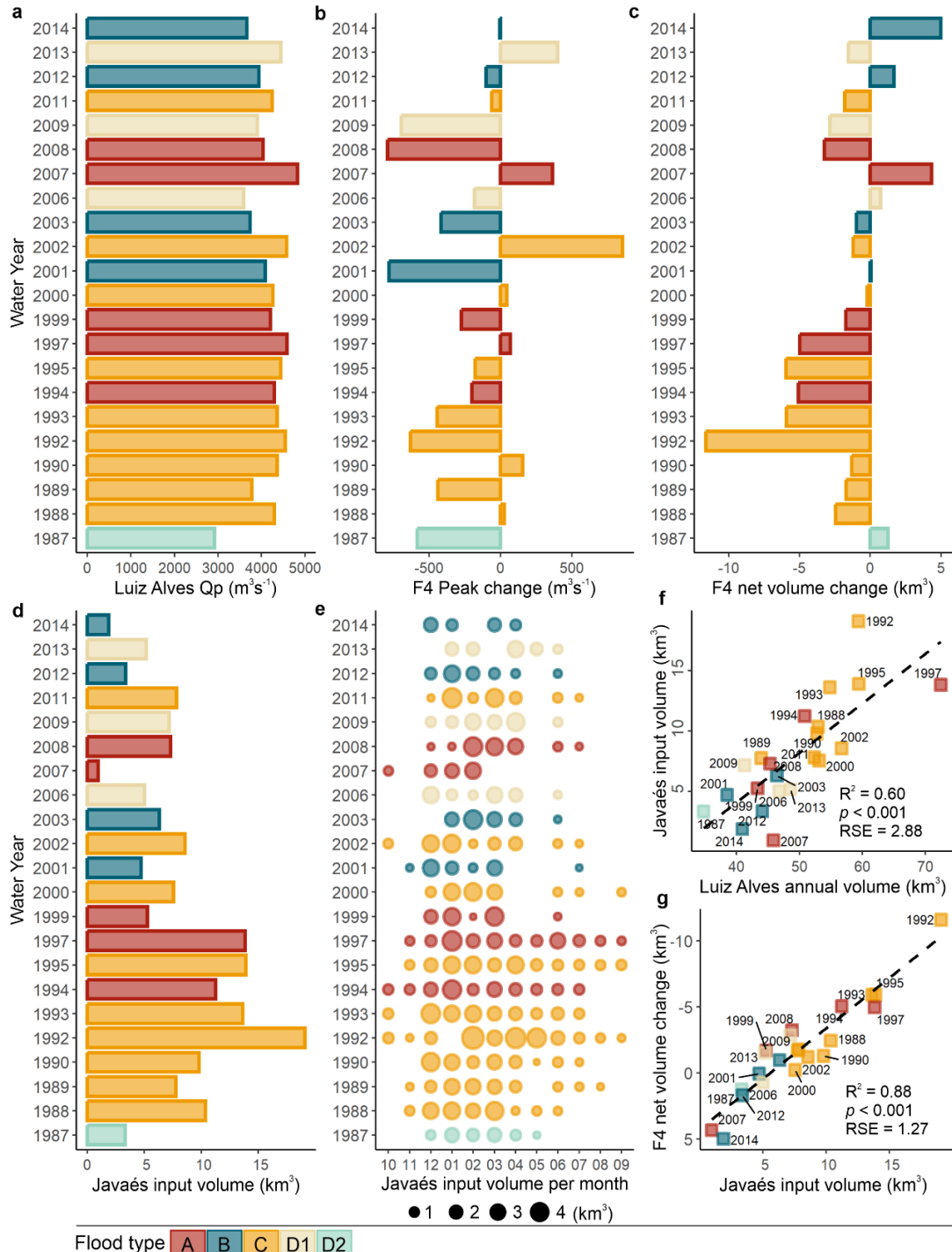


Figure 10. Flood flow dynamics and volume transmission patterns along F4. (a) Peak discharges (Q_p) at Luiz Alves station in the mainstem. (b) Absolute peak change along reach F4 (Luiz Alves to Faz. Telésforo). (c) Net loss (negative values) or gain (positive values) in water volume along F4. (d) Water volume inflow to the Javaés River. (e) Monthly water volume inflow to the Javaés River. (f) Water input to the Javaés River vs. total annual volume at Luiz Alves mainstem station. (g) Net changes in water volume along F4 vs. water input to the Javaés River. (f) and (g) also includes R^2 , RSE, and p-values for assessing significance and strength of relationships.

This estimation of water released into the ancient system is regarded as a valid approach despite our inability to account for the flow contribution of the Cristalino tributary (Figure 1A) to F4 due to the absence of a gauge. Although the drainage area of the Cristalino ($11,427 \text{ km}^2$) is larger than that of the Javaés upstream from its gauged site ($8,150 \text{ km}^2$), the Cristalino basin is primarily located on the vast low-gradient Bananal Plain. In contrast, the Javaés basin contains a source-higher-elevation sub-basins zone in its eastern part, characterized by smaller streams that contribute to a higher hierarchization level than the Cristalino system. These compensatory characteristics of these catchments result in similar outflow (inflow) conditions, allowing us to assume that the discharge yielded by one is equivalent to that transferred to the other, making our previous water balance equation reasonable. The similarity between the mean annual discharge estimated by Aquino et al. (2009) for the Cristalino ($199 \text{ m}^3/\text{s}$) and the calculated mean annual discharge at the Javaés gauge ($168 \text{ m}^3/\text{s}$) supports this assumption [19].

The overall losses and gains of the river along F4 (Figure 10c) exhibit a pattern of higher net volumetric losses during the 1990s, followed by an increasing trend in the frequency of total volumes transmitted downstream in more recent years. Similar patterns are observed in the diversion of volumes to the Javaés branch (Figure 10d), with water inflows in the 1990s approximately double the volumes estimated for the recent decades. The findings of the regression analysis support these observations, demonstrating that water delivered to the Javaés branch has a strong explanatory power ($R^2 = 0.88$; $p < 0.001$, Figure 10g) over the outflows at the Faz. Telésforo station. Furthermore, we can infer the influence of mainstem flow availability (Luiz Alves) on the volume of water flowing into the old river arm, as indicated by the reasonably linear relationship between these variables ($R^2 = 0.60$; $p < 0.001$, Figure 10f).

Figure 11 illustrates distinct patterns of discharge losses to the abandoning bifurcate throughout the year, associated with two type A flood events of similar peak magnitude (1997 and 2007, Figure 10a). In 1997, the hydrograph exhibited multiple peaks (Figure 11a), with discharges exceeding bankfull flows in Luiz Alves ($3700 \text{ m}^3/\text{s}$), lasting nearly four months (Jan-Apr). Discharge losses extended from late November to the first days of September (Figure 11b), resulting in an overall water loss of 13.84 km^3 to the Javaés that year (Figure 10d). In contrast, 2007 experienced a single large peak (Figure 11c), with discharges exceeding bankfull flows for only five weeks (Feb-Mar). Discharge losses extended from October to the first days of March (Figure 11d), resulting in an overall water loss of 0.96 km^3 to the Javaés that year (Figure 10d).

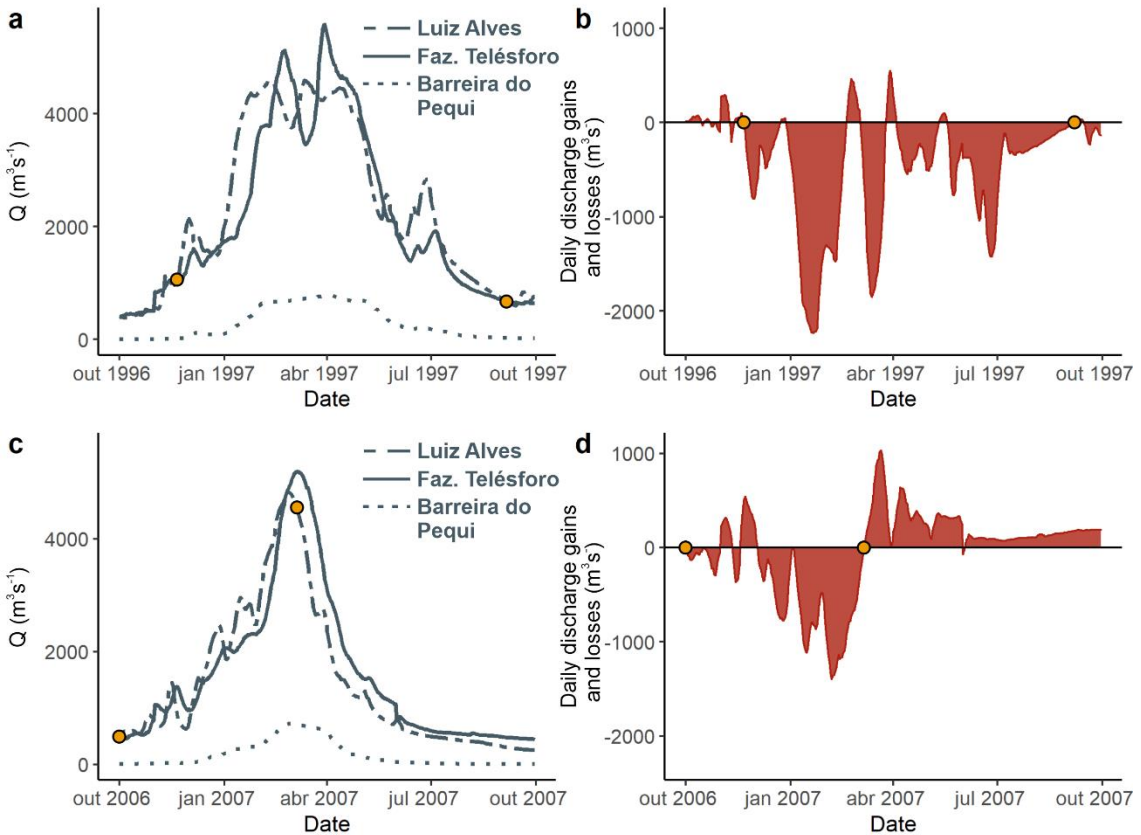


Figure 11. Discharge dynamics and losses to the Javaés River in 1997 and 2007. Hydrographs for (a) 1997 and (c) 2007 water years from Luiz Alves, Faz. Telésforo, and Barreira do Pequi gauge located in the Javaés River (Figure 1A, station 5). Net discharge losses to the Javaés River (negative values) in (b) 1997 and (d) 2007. Yellow-filled circles represent the duration of the period with significant water losses.

In general, F4 exhibits reduced wave propagation velocities and gradual rising limbs for all flood types. This contrasts significantly with the hydrograph properties observed in the downstream reach F5 (Figures 9a and 9b). In F5, the channel gradient experiences an increase (+84% on average, Figure 8e), and the river undergoes substantial channel widening (+63% on average, Figure 8a) due to the entrance of the Mortes River. However, despite these morphological shifts, a wide floodplain has not developed (average entrenchment ratio: 6, Figure 8b). The increased channel capacity to convey flows, coupled with the limited adjacent overbank areas in F5, results in the absence of flood attenuations (Figure 5e), faster propagation of flood waves (Figure 9a), and steeper gradients in the rising limb of downstream hydrographs (Figure 9b).

The main planform changes observed in the F5 are further intensified in F6. These changes encompass a widening of the channel (Figure 8a), an increased anabranching character

of the river (Figure 8d), and the presence of a narrow floodplain (Figure 8b). This configuration allows flood waves to propagate downstream without attenuation (Figure 5f) and contributes to flood hydrographs characterized by steep rising limbs (Figure 9b). Notably, while F5 rapidly translates hydrographs downstream, F6 exhibits a delay in the translation, except for smaller type D2 events that occur within the channel (Figure 9a). The gradual decrease in channel and valley gradients along F6 (Figures 8e and 8f) may reduce peak wave velocities. However, it is important to highlight that F6 spans a length of 451 km (Figure 1) and covers a drainage area of approximately 130,000 square kilometers. Therefore, it is essential to consider this significant physiographic influence when analyzing the generation of high-volume flood events at the downstream station of Conceição do Araguaia. This station experiences a substantial increase of 153% in floodwaters compared to the upstream São Félix do Araguaia station (Figure 12a).

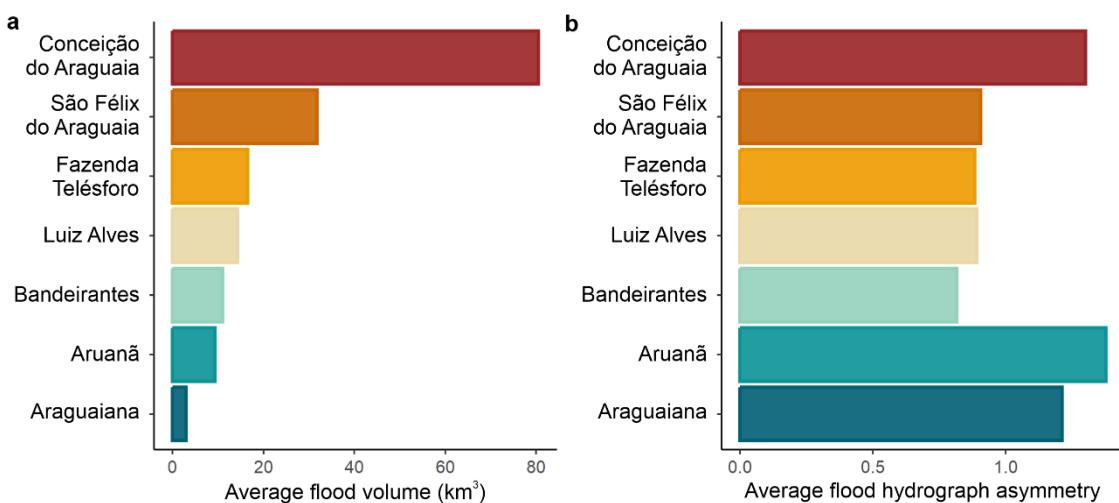


Figure 12. Comparative analysis of flood overflows among gauging stations. (a) Average cumulative overflow water volume for all flood events. (b) Coefficient of overflow hydrograph asymmetry averaged for all flood events.

2.3.5 Discussion: linking flood hydrology in the middle Araguaia River with its major geomorphic segments

Our findings demonstrate that different types of flood in the middle Araguaia River present hydrograph properties (peak magnitude, slope, wave celerity, attenuation, and volume losses) that are ultimately influenced by downstream variations in morphological variables at the reach scale. Suizu et al. (2023), in their geomorphic assessment of the river, identified that the initial subdivision into 19 reaches (Figure 8) could be rescaled into five major geomorphic

segments (SI-SV) [16]. These segments were statistically defined and characterized by consistent trends in the river's character and the degree of development of the fluvial corridor.

By assessing our flood classes in the context of these major fluvial domains, it becomes evident that the complex patterns of flow transmission in the middle Araguaia respond to the regional-scale organization of the system (Figure 13). In the SI – *Single-channel reach, planform controlled, restricted floodplain*, the Araguaia emerges from a relatively narrow, wide V-shaped geologically controlled valley into reaches with a well-developed and broad Quaternary fluvial belt containing the active floodplain. The upstream high valley gradient in this structurally controlled channel reach is the dominant driver behind the efficient conveyance of high floodwaters in F1.

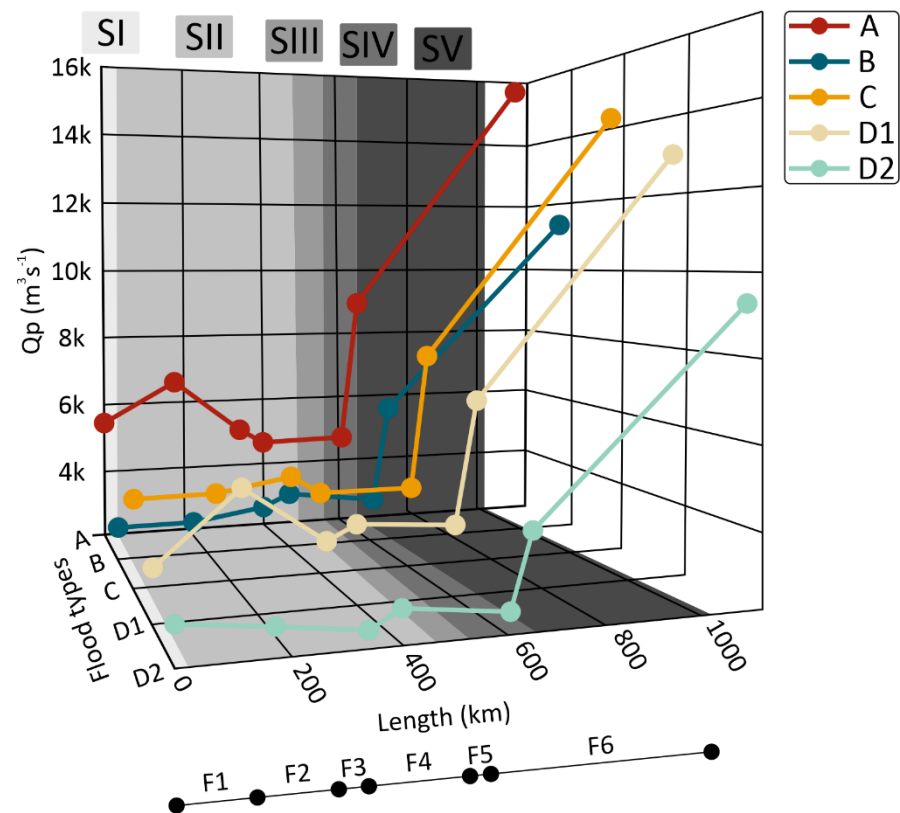


Figure 13. Schematic diagram illustrating flood wave transmission for each flood type along the middle Araguaia River, influenced by major geomorphic segments (SI-SV, [16]). Q_p values (in m^3/s) were averaged by gauging station.

F2 and F3 reaches are entirely situated within the SII – *Alluvial anabranching pattern, laterally unconfined, wide, and complex Holocene floodplain* (Figure 13). Previous research has demonstrated the primary mechanisms responsible for peak attenuation along these reaches, F2 and F3 [8,9,37]. Building upon these findings, we acknowledge the significant potential of

the wide floodplain to act as storage areas and attenuate flood peaks in such reaches. However, we believe that the slope of the trunk stream and the valley may also play a critical role in this process. Additionally, an earlier examination of stream gains and losses (Figure 7a) suggests that, in general, F2 is more prone to discharge loss (or less likely to gain) than F3. This may be partly attributed to the sharp-peaked and rapidly translated hydrographs from the upper basin that reach F2. Floods with quick rises have a higher potential for attenuation, as the crest of the flood wave carries a relatively small volume of water that is unlikely to exceed the capacity of overbank storage areas and can significantly reduce peak discharge [38].

Reach F4 is mainly influenced by SIII – *Highly sinuous anabranching pattern, partly confined on alluvium, younger meander belt with scrolls* (Figure 13). This segment (see geomorphic sub-reach 11, Figure 8) features a remarkable avulsion channel that diverts the mainstem flow to the northwest, forming the southern portion of Bananal Island [20]. It can be inferred that the presence of sufficient gradient (current valley gradient: 26 cm km^{-1} , Figure 8f) facilitated the erosion of the older, well-indurated alluvium of the Bananal Plain, leading to the development of a sinuous channel (sinuosity: 1.6, Figure 8c) to effectively dissipate excess energy along this short segment [16]. Although the lateral mobility of this avulsion channel is currently reduced [16], it has created a partially confined setting (entrenchment ratio: 6, Figure 8b) by a younger meander belt with incised scrolls in the Araguaia Formation. Additionally, the modern channel in this reach is sufficiently large (average width: 321 m, Figure 8a) to accommodate almost the entire discharge of the mainstem.

Aquino et al. (2008) have previously highlighted the significance of discharge loss to the abandoned channel of the Araguaia River as the primary mechanism for attenuating peak discharge along F4 [8]. The study authors observed water transfer from the main river to the old river arm during both small-scale (type B) and large-scale (type A) flood events, with peak discharge losses reaching up to 8%. Based on these previous findings, we have also observed significant reductions in peak flow (up to 20%) between Luiz Alves and Faz. Telésforo associated with different flood types (Figures 5d and 10b). However, the distinctive transmission patterns observed during flood events highlight that while annual peak discharges have been a valuable indicator of discharge losses in F4, they represent isolated occurrences in the time series and may not capture the full range of mainstem flows that allow connections with the abandoning bifurcate.

The connection between the Araguaia and Javaés rivers extends beyond high flood flows. It typically starts on discharges near the average annual mean in Luiz Alves ($1565 \text{ m}^3/\text{s}$) in the early stages of the wet period (December), and it continues until the beginning of the

falling limbs in April, with occasional extensions to July (Figure 10e). Besides, the flow dynamics showed a consistent trend of higher net volumetric losses during the 1990s, followed by an increasing frequency of total volumes transmitted downstream in recent years. Therefore, further research is necessary to comprehend the influence of temporal shifts in flow patterns on the geometry, equilibrium, and maintenance of the abandoning channel within the system.

Segments IV – *Anabranching pattern, planform controlled, discontinuous floodplain*, and V – *Complex anabranching pattern, partly confined on alluvium and/or bedrock, underfit floodplain*, encompass reaches F5 and F6, respectively (Figure 13). These segments have undergone morphological changes due to alterations in the flow regime resulting from river avulsion [16]. SIV and SV represent annexational segments, incorporating sections of the preexisting Cristalino River and the lower portion of the Mortes River. Following the incisional process described earlier in F4, it is presumed that these segments have not had sufficient time to develop a floodplain compatible with the contemporary river's flow regime and geomorphic processes [16]. Consequently, SIV and SV are characterized by a discontinuous floodplain on alternating sides of the river, with intermittent contact with confining margins. The modern system, which is somewhat "overfit" with limited overbank storage areas, exerts a dominant influence over flood flows in F5 and F6, facilitating efficient conveyance downstream.

This observation is further supported by the coefficient of overflow hydrograph asymmetry (v) shown in Figure 12b. The analysis of v reveals similar asymmetries between the upper (Araguaiana and Aruanã) and lowermost (Conceição do Araguaia) stations, indicating a longer duration of flood overflows in the rising phase compared to the recession phase. This suggests a higher conveyance capacity rather than significant flood storage in these areas. In contrast, the intermediate section of the river (Bandeirantes, Luiz Alves, and Faz. Telésforo) exhibits relatively lower values of v , indicating a more abrupt rising phase compared to a longer duration of flood overflows in the recession phase. This implies a more significant potential for flood storage (or loss in the case of Faz. Telésforo) and attenuation in this section.

Our finding regarding the role of the complex morphology of the fluvial corridor as a foundational element in understanding flood properties and hydrological connectivity patterns is in accordance with results from other studies on large rivers [39–43]. In the context of the Solimões-Amazon River, Meade et al. (1991) observed that apart from the shifted timing of tributary inputs, the subdued extremes of discharge, differing only by a factor of 2 or 3 throughout the year, reflects the seasonal storage of substantial water volumes within the intervening floodplain during rising stages [44]. This water then gradually returns to the river channel as the stages recede. Richey et al. (1989) estimated that up to 30% of the Amazon

River's discharge could experience temporary storage within the floodplain during flooding events [45]. Montero and Latrubesse (2013) have also recorded distinct water stage dynamics across geomorphic reaches of the Negro River [46]. They observed that stage oscillations tend to manifest later upstream than in the downstream reaches. This behavior was partly attributed to the reservoir effect induced by a large tectonic block and the presence of the Mariuá archipelago within the intermediate section of the river.

Peak discharge attenuation driven by distinctive fluvial styles has also been observed by Stevaux et al. (2020) in the Upper Paraguay River [47]. Their research revealed that areas of constricted plains serve as bottlenecks for flood runoff, leading to backwater effects that slow down floodwave transmission. This phenomenon creates extensive water bodies upstream that store floodwater, ultimately impacting the duration and magnitude of floods. According to Assine and Silva (2009), there is a substantial loss of water, exceeding 50%, as the Upper Paraguay River enters the Pantanal wetland due to its transition into a depositional mega-fan system [48]. Despite being situated in a similar wet-dry seasonal climate, the Araguaia exhibit distinct geomorphic characteristics from the Upper Paraguay. The Araguaia River is a large axial tributary system [49], with water flow and sediment deposition largely confined to its genetic floodplain. Nevertheless, our study reveals that during large-scale (type A) flood events, the Araguaia River experiences peak discharge attenuation of up to -43% at the Fazenda Telésforo station. This reduction stems from temporary storage within its well-developed floodplain and water diversion toward the abandoned river branch. This unique combination of characteristics differentiates the Araguaia River from other large axial tributary rivers in tropical South America.

2.3.6 Conclusions

The Araguaia River is a large tropical system characterized by a longitudinal geomorphic variability, significantly shaped by late Holocene avulsion events and subsequent adjustments of the modern channel [16]. Previous studies have already highlighted the role of geomorphology in understanding the progression of floods in this river, leading to the identification of distinct flood types [8,26].

Our approach in this study offers a refined perspective on classifying flood events in this river. We found that small-scale floods (types B and D2) exhibit distinct attenuation patterns, with type D2 being associated with drier-than-usual years and low-level water diversion. In contrast, the attenuation of intermediate (Types C and D1) and large-scale (type

A) floods is primarily influenced by the peak magnitude at the upstream gauging station, with no statistical significance observed for the influence of tributaries on absolute peak changes. Flood properties such as wave celerity and slope of the rising limb show limited discernible distinctions between flood types but appear to respond to the regional geomorphological organization of the system. By considering the geomorphically distinct segments, we have observed that the nature of the valley floor plays a central role in facilitating the efficient conveyance of floods in the upper (SI) and the lowermost (SIV and SV) segments. The presence of a wide and complex floodplain significantly influences the storage capacity, allowing for the gradual dissipation of excess floodwater and the attenuation of flood peaks in SII. Additionally, water diversion to the ancient system (Javaés River) does not directly impact peak flows; however, it exhibits unique transfer patterns across a range of flow conditions, resulting in overall annual losses or gains in SIII.

In the Araguaia River, the distinctive hydrogeomorphic transmission of floodwaters plays a crucial role in maintaining the ecological integrity of its highly diverse floodplain at the Cerrado-Amazonia ecotone. Therefore, it is essential for sustainable management practices to consider the outcomes highlighted in this study.

Our findings regarding the propagation patterns of flow across different geomorphic segments can provide insights for studying the spatial dynamics of nutrients and sediments within the system. These insights extend to understanding their effects on the diversity and functioning of aquatic and riparian ecosystems, thereby aiding in identifying areas more prone to vulnerabilities. Our research also holds the potential to be integrated with studies dedicated to evaluating the environmental impacts of potential hydroelectric installations. In particular, examining the downstream hydrophysical repercussions of dam construction is imperative by assessing how the regulation of flows and the decrease of flooding regimes could potentially impact the unique hydrogeomorphic transmission of flood waves in the middle Araguaia River. These impacts carry direct implications for the ecological preservation of the river corridor.

Moreover, paying greater awareness to the partially abandoned branch of the Araguaia River is recommended. Our research demonstrates that Javaés River is a functioning part of the active system across varying flows throughout the year, thereby emphasizing its ecological importance for riverine ecosystems. Additionally, this subsidiary system has been facing progressively severe water crises in recent years, leading to substantial environmental problems affecting indigenous communities and triggering conflicts between rural producers and environmentalists. Consequently, protective management measures and plans for water management are necessary.

References

1. Latrubblesse, E.M.; Sinha, R. *Human Impacts on Sediment and Morphodynamics of Large Tropical Rivers*; 2nd ed.; Elsevier Inc., 2022.
2. Wohl, E.; Barros, A.; Brunsell, N.; Chappell, N.A.; Coe, M.; Giambelluca, T.; Goldsmith, S.; Harmon, R.; Hendrickx, J.M.H.; Juvik, J.; et al. The Hydrology of the Humid Tropics. *Nat. Clim. Chang.* **2012**, *2*, 655–662, doi:10.1038/nclimate1556.
3. Latrubblesse, E.M.; Amsler, M.L.; de Moraes, R.P.; Aquino, S. The Geomorphologic Response of a Large Pristine Alluvial River to Tremendous Deforestation in the South American Tropics: The Case of the Araguaia River. *Geomorphology* **2009**, *113*, 239–252, doi:10.1016/j.geomorph.2009.03.014.
4. Coe, M.T.; Latrubblesse, E.M.; Ferreira, M.E.; Amsler, M.L. The Effects of Deforestation and Climate Variability on the Streamflow of the Araguaia River, Brazil. *Biogeochemistry* **2011**, *105*, 119–131, doi:10.1007/s10533-011-9582-2.
5. Guimarães, D.P.; Landau, E.C. Georreferenciamento Dos Pivôs Centrais de Irrigação No Brasil: Ano-Base 2020. *Bol. Pesqui. e Desenvolv.* **2020**, *64*.
6. COMPANHIA DE DESENVOLVIMENTO DOS VALES DO SÃO FRANCISCO E DO PARNAÍBA - CODEVASF. Codevasf anuncia investimentos federais no Projeto de Irrigação de Luiz Alves Do Araguaia, em Goiás Available online: <https://www.codevasf.gov.br/noticias/2020/codevasf-anuncia-investimentos-federais-no-projeto-de-irrigacao-de-luiz-alves-do-araguaia-em-goias> (accessed on 12 July 2023).
7. Latrubblesse, E.M.; Arima, E.; Ferreira, M.E.; Nogueira, S.H.; Wittmann, F.; Dias, M.S.; Dagosta, F.C.P.; Bayer, M. Fostering Water Resource Governance and Conservation in the Brazilian Cerrado Biome. *Conserv. Sci. Pract.* **2019**, *1*, 1–8, doi:10.1111/csp2.77.
8. Aquino, S.; Latrubblesse, E.M.; de Souza Filho, E.E. Relações Entre o Regime Hidrológico e Os Ecossistemas Aquáticos Da Planície Aluvial Do Rio Araguaia. *Acta Sci. - Biol. Sci.* **2008**, *30*, 361–369, doi:10.4025/actascibiolsci.v30i4.5866.
9. Lininger, K.B.; Latrubblesse, E.M. Flooding Hydrology and Peak Discharge Attenuation along the Middle Araguaia River in Central Brazil. *Catena* **2016**, *143*, 90–101, doi:10.1016/j.catena.2016.03.043.
10. de Moraes, R.P.; Aquino, S.; Latrubblesse, E.M. Controles Hidrogeomorfológicos Nas Unidades Vegetacionais Da Planície Aluvial Do Rio Araguaia, Brasil. *Acta Sci. - Biol. Sci.* **2008**, *30*, 411–421, doi:10.4025/actascibiolsci.v30i4.5871.
11. Ferreira, P.D.; Castro, P. de T. A. Nest Placement of the Giant Amazon River Turtle, *Podocnemis expansa*, in the Araguaia River, Goiás State, Brazil. *Ambio* **2005**, *34*, 212–217, doi:10.1579/0044-7447-34.3.212.
12. Kurzatkowski, D.; Leuschner, C.; Homeier, J. Effects of Flooding on Trees in the Semi-Deciduous Transition Forests of the Araguaia Floodplain, Brazil. *Acta Oecologica* **2015**, *69*, 21–30, doi:10.1016/j.actao.2015.08.002.
13. Nabout, J.C.; Nogueira, I.S.; Oliveira, L.G. Phytoplankton Community of Floodplain Lakes of the Araguaia River, Brazil, in the Rainy and Dry Seasons. *J. Plankton Res.* **2006**, *28*, 181–193, doi:10.1093/plankt/fbi111.

14. Rocha, R.G.; Ferreira, E.; Fonseca, C.; Justino, J.; Leite, Y.L.R.; Costa, L.P. Seasonal Flooding Regime and Ecological Traits Influence Genetic Structure of Two Small Rodents. *Ecol. Evol.* **2014**, *4*, 4598–4608, doi:10.1002/ece3.1336.
15. Tejerina-garro, F.L.; Fortin, R.; Rodríguez, M.A. Tejerina-Garro et Al 1998 Fish Communities Middle Rio Araguaia.Pdf. *Environ. Biol. Fishes* **1998**, *51*, 399–410.
16. Suizu, T.M.; Latrubesse, E.M.; Bayer, M. Geomorphic Diversity of the Middle Araguaia River, Brazil: A Segment-Scale Classification to Support River Management. *J. South Am. Earth Sci.* **2023**, *121*, doi:10.1016/j.jsames.2022.104166.
17. Climate Engine. *Desert Res. Inst. Univ. Idaho* 2023.
18. Latrubesse, E.M.; Stevaux, J.C. Geomorphology and Environmental Aspects of the Araguaia Fluvial Basin, Brazil. *Zeitschrift für Geomorphol.* **2002**, *129*, 109–127.
19. Aquino, S.; Latrubesse, E.M.; de Souza Filho, E.E. Caracterização Hidrológica e Geomorfológica Dos Afluentes Da Bacia Do Rio Araguaia. *Rev. Bras. Geomorfol.* **2009**, *10*, 43–54, doi:10.20502/RBG.V10I1.116.
20. Valente, C.R.; Latrubesse, E.M. Fluvial Archive of Peculiar Avulsive Fluvial Patterns in the Largest Quaternary Intracratonic Basin of Tropical South America: The Bananal Basin, Central-Brazil. *Palaeogeogr. Palaeoclimatol. Palaeoecol.* **2012**, *356–357*, 62–74, doi:10.1016/j.palaeo.2011.10.002.
21. Bayer, M. Diagnóstico Dos Processos de Erosão/Assoreamento Na Planície Aluvial Do Rio Araguaia: Entre Barra Do Garças e Cocalinho, Universidade Federal de Goiás (UFG), 2002.
22. Latrubesse, E.M. Patterns of Anabranching Channels: The Ultimate End-Member Adjustment of Mega Rivers. *Geomorphology* **2008**, *101*, 130–145, doi:10.1016/j.geomorph.2008.05.035.
23. Marinho, G. V.; de Castro, S.S.; de Campos, A.B. Hydrology and Gully Processes in the Upper Araguaia River Basin, Central Brazil. *Zeitschrift für Geomorphol. Suppl.* **2006**, *145*, 119–145.
24. Ferreira, M.E.; Ferreira, L.G.; Latrubesse, E.M.; Miziara, F. High Resolution Remote Sensing Based Quantification of the Remnant Vegetation Cover in the Araguaia River Basin, Central Brazil. *Int. Geosci. Remote Sens. Symp.* **2008**, *4*, 2008–2010, doi:10.1109/IGARSS.2008.4779828.
25. Dunne, T.; Leopold, L.B. *Water in Environmental Planning*; Macmillan, 1978.
26. Lininger, K.B. The Hydro-Geomorphology of the Middle Araguaia River: Floodplain Dynamics of the Largest Fluvial System Draining the Brazilian Cerrado, The University of Texas at Austin, 2013.
27. Polvi, L.E.; Wohl, E.E.; Merritt, D.M. Geomorphic and Process Domain Controls on Riparian Zones in the Colorado Front Range. *Geomorphology* **2011**, *125*, 504–516, doi:10.1016/j.geomorph.2010.10.012.
28. Friend, P.F.; Sinha, R. Braiding and Meandering Parameters. *Geol. Soc. Spec. Publ.* **1993**, *75*, 105–111, doi:10.1144/GSL.SP.1993.075.01.05.
29. Kong, D.; Latrubesse, E.M.; Miao, C.; Zhou, R. Morphological Response of the Lower Yellow River to the Operation of Xiaolangdi Dam, China. *Geomorphology* **2020**, *350*,

- doi:10.1016/j.geomorph.2019.106931.
30. Spellman, P.; Gulley, J.; Martin, J.B.; Loucks, J. The Role of Antecedent Groundwater Heads in Controlling Transient Aquifer Storage and Flood Peak Attenuation in Karst Watersheds. *Earth Surf. Process. Landforms* **2019**, *44*, 77–87, doi:10.1002/esp.4481.
 31. Wolff, C.G.; Burges, S.J. An Analysis of the Influence of River Channel Properties on Flood Frequency. *J. Hydrol.* **1994**, *153*, 317–337, doi:10.1016/0022-1694(94)90197-X.
 32. Goetz, J.; Schwarz, C. Fasstr: Analyze, Summarize, and Visualize Daily Streamflow Data 2023.
 33. Mandych, A.F. Classification of Floods. In *Encyclopedia of Life Support. Natural Disasters Vol. II*; Kotlyakov, W.M., Ed.; UNESCO, Eolss Pbl. Co., 2010; pp. 63–88.
 34. Posit team RStudio: Integrated Development Environment for R 2023.
 35. Aquino, S. Mecanismos de Transmissão de Fluxos de Água e Sedimentos Em Dois Grandes Rios Aluviais Impactados Pela Atividade Humana: O Araguaia e o Paraná, Universidade Estadual de Maringá (UEM), 2007.
 36. Bhowmik, N.G.; Stall, J.B. Hydraulic Geometry and Carrying Capacity of Floodplains. *Res. Rep. - Univ. Illinois Urbana-Champaign, Water Resour. Cent.* **1979**.
 37. de Moraes, R.P.; Oliveira, L.G.; Latrubesse, E.M.; Pinheiro, R.C.D. Morfometria de Sistemas Lacustres Da Planície Aluvial Do Médio Rio Araguaia. *Acta Sci. Biol. Sci.* **2005**, *27*, 203–213, doi:10.4025/actascibiolsci.v27i3.1278.
 38. Woltemade, C.J.; Potter, K.W. A Watershed Modeling Analysis of Fluvial Geomorphologic Influences on Flood Peak Attenuation. *Water Resour. Res.* **1994**, *30*, 1933–1942, doi:10.1029/94WR00323.
 39. Ang, W.J.; Park, E.; Yang, X. Geomorphic Control on Stage-Area Hysteresis in Three of the Largest Floodplain Lakes. *J. Hydrol.* **2022**, *614*, 128574, doi:10.1016/j.jhydrol.2022.128574.
 40. Hudson, P.F.; Colditz, R.R. Flood Delineation in a Large and Complex Alluvial Valley, Lower Pánuco Basin, Mexico. *J. Hydrol.* **2003**, *280*, 229–245, doi:10.1016/S0022-1694(03)00227-0.
 41. Marchetti, Z.Y.; Latrubesse, E.M.; Pereira, M.S.; Ramonell, C.G. Vegetation and Its Relationship with Geomorphologic Units in the Parana River Floodplain, Argentina. *J. South Am. Earth Sci.* **2013**, *46*, 122–136, doi:10.1016/j.jsames.2013.03.010.
 42. Marinho, R.R.; Zanin, P.R.; Filizola Junior, N.P. The Negro River in the Anavilhanas Archipelago: Streamflow and Geomorphology of a Complex Anabranching System in the Amazon. *Earth Surf. Process. Landforms* **2022**, *47*, 1108–1123, doi:10.1002/esp.5306.
 43. Park, E.; Latrubesse, E.M. The Hydro-Geomorphologic Complexity of the Lower Amazon River Floodplain and Hydrological Connectivity Assessed by Remote Sensing and Field Control. *Remote Sens. Environ.* **2017**, *198*, 321–332, doi:10.1016/j.rse.2017.06.021.
 44. Meade, R.H.; Rayol, J.M.; da Conceição, S.C.; Natividade, J.R.G. Backwater Effects in the Amazon River Basin of Brazil. *Environ. Geol. Water Sci.* **1991**, *18*, 105–114, doi:10.1007/BF01704664.

45. Richey, J.E.; Mertes, L.A.K.; Dunne, T.; Victoria, R.L.; Forsberg, B.R.; Tancredi, A.C.N.S.; Oliveira, E. Sources and Routing of the Amazon River Flood Wave. *Global Biogeochem. Cycles* **1989**, *3*, 191–204, doi:10.1029/GB003i003p00191.
46. Montero, J.C.; Latrubesse, E.M. The Igapó of the Negro River in Central Amazonia: Linking Late-Successional Inundation Forest with Fluvial Geomorphology. *J. South Am. Earth Sci.* **2013**, *46*, 137–149, doi:10.1016/j.jsames.2013.05.009.
47. Stevaux, J.C.; Macedo, H. de A.; Assine, M.L.; Silva, A. Changing Fluvial Styles and Backwater Flooding along the Upper Paraguay River Plains in the Brazilian Pantanal Wetland. *Geomorphology* **2020**, *350*, 106906, doi:10.1016/j.geomorph.2019.106906.
48. Assine, M.L.; Silva, A. Contrasting Fluvial Styles of the Paraguay River in the Northwestern Border of the Pantanal Wetland, Brazil. *Geomorphology* **2009**, *113*, 189–199, doi:10.1016/j.geomorph.2009.03.012.
49. Latrubesse, E.M. Large Rivers, Megafans and Other Quaternary Avulsive Fluvial Systems: A Potential “Who’s Who” in the Geological Record. *Earth-Science Rev.* **2015**, *146*, 1–30, doi:10.1016/j.earscirev.2015.03.004.

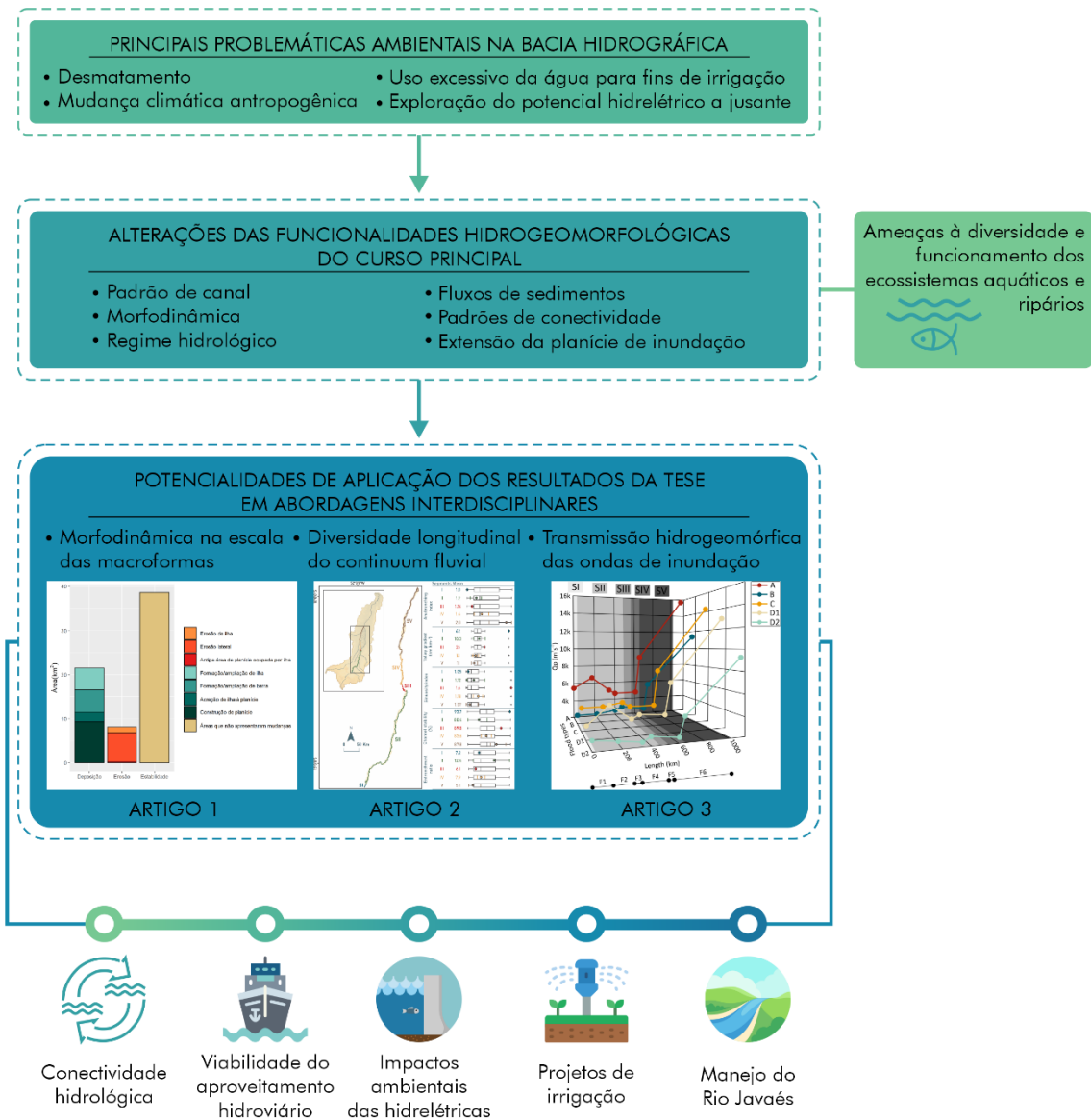
3 CONCLUSÃO E RECOMENDAÇÕES

O Rio Araguaia continua sendo o último e mais importante rio de fluxo livre situado no ecótono Cerrado-Amazônia, abrangendo as áreas úmidas mais geodiversas do bioma Cerrado (LATRUBESSE et al., 2019). No entanto, a biodiversidade única desse sistema contrasta com uma longa história de políticas e iniciativas que têm causado extensa degradação ambiental (PELICICE et al., 2021). A crescente influência humana sobre o sistema fluvial representa uma ameaça iminente à segurança hídrica, assim como às funcionalidades hidrogeomorfológicas e ecológicas desse sistema (LATRUBESSE et al., 2019), tornando essencial a produção do conhecimento sobre a estrutura física e função do Rio Araguaia, enquanto base para a ocorrência de porção significativa da biodiversidade do bioma Cerrado.

Diante do quadro de problemáticas ambientais que se manifestam na Bacia do Araguaia, esta tese não apenas oferece uma contribuição aos campos da Geomorfologia e Hidrologia de grandes rios tropicais, mas também traz novas descobertas que enriquecem o corpo de pesquisa existente sobre esse sistema. As metodologias e os conhecimentos disciplinares básicos gerados nos estudos que desenvolvemos têm o potencial de subsidiar abordagens interdisciplinares, desempenhando um papel essencial no manejo sustentável desse sistema de grande relevância e notável vulnerabilidade (Figura 1).

Ampliamos a série temporal dos dados sobre a evolução das macroformas do rio apresentados por Latrubblesse et al. (2009) para um período de 53 anos (Artigo 1) e identificamos alterações nos mecanismos de ajuste do canal nas últimas décadas (2001–2018), relacionadas às mudanças no regime hidrológico. Aportamos um novo entendimento da integralidade longitudinal do sistema a partir de uma classificação objetiva do médio Araguaia em grandes segmentos fluviais (Artigo 2), complementando estudos geomorfológicos anteriores (LATRUBESSE et al., 2009; LATRUBESSE; STEVAUX, 2002) e revelando uma diversidade longitudinal do continuum fluvial até então desconhecida. Apresentamos também uma nova abordagem em relação às classificações existentes na literatura (AQUINO; LATRUBESSE; SOUZA FILHO, 2008; LININGER, 2013) dos eventos de inundação no médio Araguaia (Artigo 3), demonstrando que as características dos tipos de inundação e sua transmissão atípica a jusante são fortemente influenciadas pela organização geomorfológica regional do sistema (Artigo 2).

Figura 1 – Síntese das contribuições da tese na abordagem das questões ambientais do Rio Araguaia: uma visão integrada para a conservação do corredor fluvial e a gestão efetiva dos recursos hídricos.



Nossos resultados podem ser integrados aos estudos sobre conectividade hidrológica, contribuindo para um aprofundamento do entendimento da diversidade do mosaico ambiental presente em toda a extensão da planície ao longo do médio Rio Araguaia. A análise dos padrões de propagação dos fluxos em diferentes segmentos geomórficos do rio pode fornecer informações aos estudos da dinâmica espacial dos nutrientes e sedimentos no sistema atual, assim como sua influência na diversidade e funcionamento dos ecossistemas aquáticos e ripários, permitindo a identificação de áreas de maior fragilidade e a adoção de estratégias de

manejo adequadas para garantir a sustentabilidade do complexo de habitats do sistema rio-planície de inundação.

A proposta de implementação da hidrovia Tocantins–Araguaia, apresentada na década de 1990, foi interrompida devido a uma série de omissões e à falta de dados geomorfológicos adequados, bem como às preocupações levantadas por especialistas sobre os impactos vindouros desse empreendimento nas comunidades ribeirinhas, no turismo e no funcionamento do sistema fluvial. Nesse sentido, nossas pesquisas sobre a hidrologia do sistema, a morfodinâmica na escala das macroformas do rio e a sua variabilidade geomórfica longitudinal podem fornecer uma base sólida para potenciais estudos de viabilidade econômico-ambiental relacionados ao aproveitamento hidroviário do Rio Araguaia.

A nossa investigação também tem o potencial para integrar estudos de avaliação dos impactos ambientais associados às hidrelétricas que possam vir a ser instaladas. A respeito das barragens, é imprescindível direcionar uma atenção minuciosa aos impactos hidrofísicos que ocorrerão a jusante no sistema, avaliando como a regulação dos fluxos e o decréscimo do regime de inundações poderá impactar a transmissão hidrogeomórfica atípica das ondas de inundação do médio Rio Araguaia, com implicações diretas na manutenção ecológica do corredor fluvial.

Em relação ainda à caracterização da dinâmica dos fluxos, ela poderá auxiliar no planejamento da gestão de água em grandes projetos de irrigação, permitindo a utilização eficiente dos recursos hídricos disponíveis ao longo do ano. Além disso, os nossos resultados fornecem *insights* para o manejo do sistema subsidiário, o Rio Javaés, que enfrenta crises hídricas cada vez mais graves, resultando em danos ambientais significativos que afetam a subsistência das comunidades indígenas e geram tensões entre os produtores rurais e os ambientalistas.

Esta pesquisa também abre novas perspectivas para futuros trabalhos, com o objetivo de preencher lacunas ainda existentes e fornecer um entendimento ainda mais sólido e abrangente do sistema Araguaia. A fim de aprofundar a compreensão dos ajustes morfológicos do sistema canal-planície aluvial (Artigo 1), é recomendável uma investigação mais detalhada das possíveis flutuações recentes na vazão efetiva (Q_{ef}) do médio Araguaia enquanto parâmetro crítico para o desenvolvimento de seu padrão *anabranching*. Essa análise permitiria examinar o papel da variabilidade climática e das mudanças no regime de vazões como fatores impulsionadores dos ajustes observados na vazão efetiva (AMSLER; RAMONELL; TONILO, 2005), além de explorar a relação dessa vazão com as tendências erosivas e deposicionais atuais desse sistema.

A variação espacial no estilo fluvial do médio Araguaia (Artigo 2) também nos proporcionou uma compreensão da existência de uma variabilidade longitudinal na forma, dinâmica e formação das barras e ilhas fluviais. Portanto, seguindo a linha de pesquisa conduzida por Pereira (2016) no médio Paraná, a classificação das tipologias de barras e o estabelecimento de modelos morfodinâmicos para as ilhas fluviais, explorando os mecanismos e fatores de controle da sua gênese e evolução, seriam uma valiosa contribuição para o conhecimento dos grandes sistemas fluviais com padrão *anabranching*.

A compreensão da transmissão distinta das inundações no médio Araguaia (Artigo 3) pode ser aprimorada por meio da modelagem das interações entre a planície e o canal durante a passagem da onda de inundação em cada segmento fluvial. Ademais, a inclusão da modelagem das contribuições totais de cada afluente permitiria uma melhor estimativa das taxas efetivas de perdas de vazão para diferentes tipos de inundação. Além das mudanças sedimentares conhecidas no canal e na planície proximal, decorrentes das alterações no uso e cobertura da terra (LATRUBESSE et al., 2009), é importante que pesquisas futuras se concentrem na compreensão do impacto dessas mudanças no transporte de sedimentos em suspensão para a planície. Por fim, é crucial ampliar o conhecimento sobre o funcionamento do braço parcialmente abandonado do Rio Araguaia – o Rio Javaés. Nossa pesquisa evidenciou que esse braço é uma parte funcional e significativa do sistema ativo, desempenhando um papel importante na transmissão de uma variedade de fluxos ao longo do ano, o que denota sua relevância ecológica para os ecossistemas fluviais locais. Portanto, pesquisas adicionais são necessárias para compreender como as mudanças temporais nos padrões de fluxo e transporte sedimentar afetam a geometria, o equilíbrio e a manutenção desse canal abandonado dentro do sistema Araguaia.

REFERÊNCIAS

- AMSLER, M. L.; RAMONELL, C. G.; TONILO, H. A. Morphologic changes in the Paraná River channel (Argentina) in the light of the climate variability during the 20th century. **Geomorphology**, vol. 70, no. 3-4 SPEC. ISS., p. 257–278, 2005. <https://doi.org/10.1016/j.geomorph.2005.02.008>.
- AQUINO, S.; LATRUBESSE, E. M.; SOUZA FILHO, E. E. Relações entre o regime hidrológico e os ecossistemas aquáticos da planície aluvial do rio Araguaia. **Acta Scientiarum - Biological Sciences**, vol. 30, no. 4, p. 361–369, 2008. <https://doi.org/10.4025/actascibiolsci.v30i4.5866>.
- LATRUBESSE, E. M.; AMSLER, M. L.; MORAIS, R. P.; AQUINO, S. The geomorphologic response of a large pristine alluvial river to tremendous deforestation in the South American tropics: The case of the Araguaia River. **Geomorphology**, vol. 113, no. 3–4, p. 239–252, 2009. DOI 10.1016/j.geomorph.2009.03.014.
- LATRUBESSE, E. M.; ARIMA, E.; FERREIRA, M. E.; NOGUEIRA, S. H.; WITTMANN, F.; DIAS, M. S.; DAGOSTA, F. C. P.; BAYER, M. Fostering water resource governance and conservation in the Brazilian Cerrado biome. **Conservation Science and Practice**, vol. 1, no. 9, p. 1–8, 2019. <https://doi.org/10.1111/csp2.77>.
- LATRUBESSE, E. M.; STEVAUX, J. C. Geomorphology and environmental aspects of the Araguaia fluvial basin, Brazil. **Zeitschrift für Geomorphologie**, vol. 129, p. 109–127, 2002.
- LININGER, K. B. **The hydro-geomorphology of the middle Araguaia River: floodplain dynamics of the largest fluvial system draining the Brazilian Cerrado**. 2013. 150 f. The University of Texas at Austin, 2013.
- PELICICE, F. M.; AGOSTINHO, A. A.; AKAMA, A.; ANDRADE FILHO, J. D.; AZEVEDO-SANTOS, V. M.; BARBOSA, M. V. M.; BINI, L. M.; BRITO, M. F. G.; DOS ANJOS CANDEIRO, C. R.; CARAMASCHI, É. P.; CARVALHO, P.; DE CARVALHO, R. A.; CASTELLO, L.; DAS CHAGAS, D. B.; CHAMON, C. C.; COLLI, G. R.; DAGA, V. S.; DIAS, M. S.; DINIZ FILHO, J. A. F.; ... ZUANON, J. Large-scale Degradation of the Tocantins-Araguaia River Basin. **Environmental Management**, vol. 68, no. 4, p. 445–452, 2021. DOI 10.1007/s00267-021-01513-7.
- PEREIRA, M. S. **El Río Paraná: geomorfología y morfodinámica de barras e islas en un gran río anabanching**. 2016. 363 f. Universidad Nacional de La Plata, 2016.